FACULDADE DE ENGENHARIA DA UNIVERSIDADE DO PORTO

Fracture energy assessment of polyurethane adhesives

The influence of mode mixity, loading rate, and temperature

Maria José Pires Ribas



Master Degree in Mechanical Engineering
Specialization in Materials and Technological Processes

Supervisor: Alireza Akhavan-Safar

Co-Supervisor: Ricardo João Camilo Carbas

Co-Supervisor: Lucas Filipe Martins da Silva

September 25, 2023

© Maria Ribas, 2023

Fracture energy assessment of polyurethane adhesives
The influence of mode mixity, loading rate, and temperature

Maria José Pires Ribas

Master Degree in Mechanical Engineering
Specialization in Materials and Technological Processes

September 25, 2023

Abstract

Adhesive bonding has developed in recent years and is becoming increasingly important in various industries. Adhesives offer the advantage of a more uniform stress distribution and lighter structures, unlike joining methods such as riveting, which creates areas of stress concentration near holes, and welding, which makes it difficult to join dissimilar materials. Due to their exceptional properties and strong bonding capacity, polyurethanes are a popular family of adhesives in the automotive industry.

The current study seeks to investigate the relationship between the mechanical characteristics of polyurethane adhesives and loading rate and temperature. This was achieved by defining strength and the envelope of fracture toughness. Additional research was conducted to determine the variation of strain rate within the bondline under differing conditions.

Strength properties were determined using bulk tensile tests and thick adherend shear tests (TAST) at a quasi-static rate of 1 mm/min. The materials were also tested at three different temperatures (-30 ºC, 23 ºC, and 60 ºC) to provide a complete understanding of their performance.

The fracture envelope was defined through mode I and mixed mode tests conducted under varying conditions including quasi-static, intermediate and high strain rates at 0.2 mm/min, 200 mm/min and 6000 mm/min, respectively. The fracture toughness of the material was assessed by conducting double cantilever beam (DCB) tests for mode I and mixed-mode using a mixed-mode apparatus that was specifically developed. The critical strain energy release rate was found to be highly sensitive to operating temperature. The loading rate also significantly affects this parameter, depending on the specimen's temperature.

In addition to the effects of loading rate and temperature on adhesive properties, it is important to investigate the variation in strain rate during testing for different test conditions. Therefore, a comprehensive study was conducted to enhance understanding of this subject. Investigating the variations in strain rate under different test scenarios (varied loading rates and temperatures) yielded valuable insights into the material's behaviour under diverse loading conditions. The specimens underwent testing at a temperature of 23 ºC in a quasi-static condition, as well as at -30ºC and 23 ºC with a loading rate of 200 mm/min. It was discovered that despite maintaining a consistent loading rate during testing, there are variations in the strain rate, demonstrating its inability to remain constant throughout the entire process. The study highlighted the essentiality of maintaining uniform strain rate control during testing. The strain-rate variation for a particular condition increased with the loading rate, suggesting that the strain-rate variation is significant, especially at high test speeds. When the specimen is exposed to low temperatures, the rate of strain does not experience considerable fluctuation.

Keywords: polyurethanes, fracture energy, loading mode, loading rate, temperature and strain rate.

Resumo

As ligações adesivas tem vindo a desenvolver-se nos últimos anos e estão a tornar-se cada vez mais importante em várias indústrias. Os adesivos oferecem a vantagem de uma distribuição uniforme de tensões e estruturas mais leves, ao contrário de métodos de ligação como a rebitagem, que cria áreas de concentração de tensão junto aos furos, e a soldadura, que dificulta a união de materiais diferentes. Devido às suas propriedades excecionais e capacidade de aderência, os poliuretanos são uma família popular de adesivos na indústria automóvel.

O presente estudo visa investigar a relação entre as características mecânicas dos adesivos poliuretanos e a taxa de carga e a temperatura. Isto foi conseguido ao definir os envelopes de tenacidade à fratura. Realizou-se também uma investigação adicional para determinar a variação da taxa de deformação na camada adesiva sob diferentes condições.

As propriedades de resistência foram determinadas através de ensaios de tração bulk e ensaios de corte (TAST) a uma taxa quase-estática de 1 mm/min. Os materiais foram também testados a três temperaturas diferentes (-30 ºC, 23 ºC e 60 ºC) para proporcionar uma compreensão completa do seu desempenho sob diversas condições.

O envelope de fratura foi definido através de ensaios de modo I e modo misto realizados sob condições variadas, incluindo taxas de deformação quase-estáticas, intermédias e elevadas de 0.2 mm/min, 200 mm/min e 6000 mm/min, respetivamente. A tenacidade à fratura do material foi avaliada através de ensaios double cantilever beam (DCB) para modo I e modo misto, utilizando um dispositivo especificamente desenvolvido para testar modo misto. A taxa crítica de libertação de energia de deformação mostrou-se altamente sensível à temperatura de funcionamento. A taxa de carga também afeta significativamente este parâmetro, dependendo da temperatura do espécime.

Para além dos efeitos da taxa de carga e da temperatura nas propriedades do adesivo, é importante investigar a variação da taxa de deformação durante os ensaios em diferentes condições de teste. Portanto, foi realizado um estudo abrangente para melhorar a compreensão deste tema. A investigação das variações na taxa de deformação sob diferentes cenários de teste (taxas de carga e temperaturas variadas) proporcionou informações valiosas sobre o comportamento do material sob diversas condições de carga. Os espécimes foram submetidos a testes a uma temperatura de 23 ºC em condições quase-estáticas, bem como a -30ºC e 23 ºC com uma taxa de carga de 200 mm/min. Descobriu-se que, apesar de manter uma taxa de carga constante durante os ensaios, há variações na taxa de deformação, demonstrando a sua incapacidade de permanecer constante durante todo o processo. O estudo destacou a importância de manter um controlo uniforme da taxa de deformação durante os ensaios. A variação da taxa de deformação para uma determinada condição aumentou com a taxa de carga, sugerindo que a variação da taxa de deformação é significativa, especialmente em velocidades de teste elevadas. Quando o espécime é exposto a baixas temperaturas, a taxa de deformação não sofre flutuações consideráveis.

Acknowledgements

Firstly, I would like to express my gratitude to Professor Lucas da Silva for sharing his knowledge, for the advice given and for the opportunity to develop this thesis. I would also like to thank my supervisor Alireza Akhavan-Safar for his continuous guidance throughout the development of this thesis, for the long hours of work, constant availability and patience to help me.

I would like to give a special thanks to Ricardo Carbas and Eduardo Marques for all the knowledge, experience shared and advice given. To all the members of the Advanced Joining Processes Unit, AJPU, I would like to express my appreciation and gratitude for the support and help needed during the laboratory work. And a special thank you to Vasco Rodrigues for our friendship, for the company and the laughs during the long hours of laboratory work and for helping me to overcome some obstacles that would come up in my personal life. I would also like to express my gratitude towards Beatriz and Catarina for their invaluable assistance during my time of need. Their shared experiences brought me a sense of tranquillity.

To all of my friends who journeyed with me over the past five years and made me realize that no obstacle is insurmountable, thank you for your unwavering support and love. And to Beatriz, the one who has always stood by my side, thank you for the remarkable friendship we have developed through the years and for being the sister I needed. Thank you for being who you are.

To my family, I extend my heartfelt gratitude. My brother, thank you for your unwavering belief in me and for instilling confidence in me. To my parents, who bestowed upon me opportunities they never had, thank you for being my rock. Without your sacrifices, my journey to this point would have been hard. Thank you for all the values you have passed on to me and for making me who I am. Your values and guidance have shaped me to be the person I am today.

Maria José Pires Ribas

"The past can hurt.
But from the way I see it, you can either run from it or learn from it."

Rafiki

Contents

1 Introduction **1**
- 1.1 Background and motivation . . . 1
- 1.2 Objectives . . . 2
- 1.3 Research methodology . . . 2
- 1.4 Thesis outline . . . 2

2 State of the art **3**
- 2.1 Adhesive bonding . . . 3
  - 2.1.1 Classification of adhesives . . . 5
  - 2.1.2 Failure mode and joint design . . . 7
- 2.2 Effect of strain rate and temperature . . . 9

3 Experimental procedure **12**
- 3.1 Materials . . . 12
- 3.2 Manufacturing of specimens . . . 13
  - 3.2.1 Bulk test . . . 13
  - 3.2.2 Thick adherend shear test . . . 14
  - 3.2.3 Double cantilever beam . . . 16
- 3.3 Testing procedure . . . 17
  - 3.3.1 Bulk test . . . 17
  - 3.3.2 Thick adherend shear test . . . 19
  - 3.3.3 Mode I fracture test . . . 19
  - 3.3.4 Mixed mode fracture test . . . 19
- 3.4 Data reduction approach . . . 23

4 Results and discussions **27**
- 4.1 Strength tests . . . 27
- 4.2 Fracture energy: Effect of loading rate and temperature . . . 30
  - 4.2.1 Adhesive A . . . 30
  - 4.2.2 Adhesive B . . . 33
  - 4.2.3 Adhesive C . . . 36
- 4.3 Strain rate study in DCB joints . . . 40
  - 4.3.1 Effect of adhesive thickness on strain rate and fracture energy . . . 44

5 Summary of the appended documents **47**
- 5.1 Paper A . . . 47
- 5.2 Paper B . . . 48

6 Conclusion **50**

7 Future work **54**

A Paper A **56**

B Paper B **73**

References **56**

List of Figures

2.1 Stress distribution for different joining methods [?]. 4
2.2 Failure modes of adhesively bonded joints. 8
2.3 Types of adhesive loading conditions. Adapted from [?]. 9
2.4 Types of joints used in adhesive bonding. 9

3.1 Exploded view of the mould to produce plate specimens under hydrostatic pressure [?]. 13
3.2 Tensile specimen geometry, dimensions in mm. 14
3.3 Bulk specimen with speckle for DIC analysis. 14
3.4 TAST specimen geometry, dimensions in mm [?]. 15
3.5 TAST specimen with speckle for DIC analysis. 16
3.6 DCB specimen. 16
3.7 DCB specimens with respective surface treatments. 17
3.8 Thermal chamber for DCB and mixed mode testing. 18
3.9 Setup to test bulk specimens at room temperature. 18
3.10 DCB setup. 19
3.11 Apparatus used for mixed mode testing. 20
3.12 Schematic representation of the apparatus used for mixed mode testing [?]. . . . 20
3.13 Mixed mode loading conditions [?]. 21
3.14 Schematic representation of FPZ and equivalent crack length concepts [?] 23
3.15 Laser beam method for guaranteeing perpendicularity between the DCB joint and the camera. 26

4.1 Tensile strength results for all adhesives under 1 mm/min at 23 ºC. 27
4.2 Bulk test results for adhesive C under quasi-static loading rate. 29
4.3 TAST results for adhesive C under quasi-static loading rate. 29
4.4 Fracture surface of adhesive A after testing at 23 ºC for different loading rates under pure mode I. 30
4.5 Effects of loading rate on the fracture energy mode I - adhesive A 31
4.6 Fracture envelope of adhesive A. 32
4.7 Effects of loading rate on the fracture energy mode I - adhesive B. 34
4.8 Fracture energy as a function of loading rate for adhesive B, mixed mode. 34
4.9 Fracture surface of adhesive B after testing at 23 ºC for different loading rates under pure mode I. 35
4.10 Fracture envelope of adhesive B. 36
4.11 Fracture envelope of adhesive C. 37
4.12 Fracture energy as a function of loading rate for adhesive C, mixed mode. 37

4.13 Fracture surface of adhesive C after testing at 23 ºC for different loading rates under pure mode I. 38
4.14 Effects of loading rate on the fracture energy in mode I - adhesive C 39
4.15 Fracture energy as a function of temperature for adhesive C, mixed mode. 39
4.16 Fracture energy as a function of loading rate in mode I, comparison between adhesives A, B and C. 40
4.17 True and engineering strains and strain rates over time for various points across the overlap (adhesive A under quasi-static conditions at 23 °C): (a) strain values as a function of time (b) true strain rate as a function of time (c) engineering strain rate as a function of time. 41
4.18 True strains and strain rates over time for various points across the overlap (adhesive C under quasi-static conditions at 23 °C): (a) strain values as a function of time (b) true strain rate as a function of time. 42
4.19 True and engineering strains and strain rates over time for various points across the overlap (adhesive A under 200 mm/min loading rate at 23°C): (a) strain values as a function of time (b) true strain rate as a function of time (c) engineering strain rate as a function of time. 42
4.20 True strains and strain rates over time for various points across the overlap (adhesive C under 200 mm/min at 23 °C): (a) strain values as a function of time (b) true strain rate as a function of time. 43
4.21 True strains and strain rates over time for various points across the overlap (adhesive A under 200 mm/min at -30 °C): (a) strain values as a function of time (b) true and engineering strain rate as a function of time. 43
4.22 True strains and strain rates over time for various points across the overlap (adhesive C under 200 mm/min at -30 °C): (a) strain values as a function of time (b) true strain rate as a function of time. 43
4.23 Fracture energy as a function of thickness of adhesive A. 45
4.24 Crack size as a function of time of adhesive A, different thicknesses. 45
4.25 Investigation into the influence of thickness on the strain rate of adhesive A under testing Conditions of 200 mm/min at a temperature of 23 ºC: (a) Utilizing an adhesive thickness of 4 mm, (b) employing an adhesive thickness of 0.5 mm." . . . 46

List of Tables

2.1 Failure mode as an inference to bond quality. Adapted from [**?**] 7

3.1 Adhesives specifications. 12
3.2 Adhesives mechanical and physical properties. 12
3.3 Substrate mechanical properties. 12
3.4 Summary of test conditions, Fracture test. 22

4.1 Strain rate analysis, testing conditions. 41

Abreviations

1k	One-part component
2k	Two-part component
ADCB	Asymmetric double cantilever beam
AF	Adhesion failure
CBBM	Compliance-based beam method
CERR	Critical energy release rate
CF	Cohesive failure
CFRP	Carbon fibre reinforced polymer
DCB	Double-cantilever beam
DIC	Digital image correlation
ENF	End-notched flexure
FPZ	Fracture process zone
HSR	High strain rate
HT	High temperature
ISR	Intermediate strain rate
LEFM	Linear elastic fracture mechanics
LT	Low temperature
LVDT	Linear variable differential transformer
MMB	Mixed mode bending
NDT	Non-destructive technique
QS	Quasi-static
RT	Room temperature
TAST	Thick adherent shear test

Symbols

a	Crack length
a_0	Initial crack length
a_{eq}	Equivalent length of the crack
a_{eq_I}	Equivalent crack length for mode I in the mixed-mode test
$a_{eq_{II}}$	Equivalent crack length for mode II in the mixed-mode test
a_{FPZ}	Length of the crack FPZ
B	Width of the DCB substrate
c	Half of the thickness of DCB substrate
C	Experimental compliance in the CBBM
C_0	Initial compliance
δ	Displacement for the DCB
Δ	Crack length correction in the CBBM
E	Young's modulus
E_f	Corrected flexural modulus
Φ	Mixed-mode phase angle
G	Shear modulus
G_c	Critical energy release rate
G_{I_c}	Critical energy release rate in mode I
G_{II_c}	Critical energy release rate in mode II
G_{xz}	Shear modulus of DCB substrate
M_f	DCB substrate bending moment
P	Load for the DCB
σ_f	Tensile strength
σ_R	Remote stress applied
t	DCB substrate thickness
t_{TAST}	Adhesive thickness in TAST specimens
T_g	Glass transition temperature
ν	Poisson's ratio
τ_f	Shear strength

Chapter 1

Introduction

1.1 Background and motivation

With the development of the automotive industry, the use of adhesives in automotive applications is increasing and becoming more widespread [**?**, **?**, **?**]. Consequently, there is an ongoing quest for safer, more operative, and environmentally friendly vehicles.

Adhesives are used due to their unique benefits when compared to traditional mechanical joining techniques. These advantages include a more uniform distribution of stress, resulting in good resistance to dynamic fatigue, higher stiffness and load transmission, as well as the ability to bond materials that differ and thin sheets of material. Adhesives also allow for process automation, design flexibility, and regular contours [**?**].

A strengthened and high-performing adhesive can offer exceptional durability while expediting the creation of lightweight structures, hence, boosting the safety and efficiency of vehicles [**?**]. Within the automotive industry, polyurethane adhesives are increasingly favoured for their impressive properties and strong adhesion. Considering that polyurethanes are currently used in the automotive industry, it is important to address the conventional challenges related to the use of these adhesives. These include design limitations resulting from high strain rate crashes and environmental factors. Furthermore, passenger safety must be a top priority. It is crucial to characterise the performance of bonded connections in high-loading and impact conditions, particularly as adhesives are polymers and have viscoelastic and viscoplastic properties [**?**].

There have been many studies on how temperature and strain rate affect adhesive behaviour. However, the majority of these studies have focused on epoxy adhesives rather than polyurethanes, and in most instances, the loading rate has been analysed, whereas for design purposes the strain rate is the key. Consequently, there is a significant research gap when it comes to understanding how polyurethane adhesives behave under varying temperature and strain rate conditions, and even how strain rate varies under these conditions.

1.2 Objectives

The present study fulfils three primary objectives. Firstly, it entails the mechanical characterization of three polyurethane adhesives, whereby their tensile, shear, and fracture properties are evaluated. Secondly, the investigation aims to comprehensively comprehend the variations in adhesive properties under diverse loading rates and temperatures. Lastly, the study aims to analyze the strain rate fluctuations along the adhesive overlap and throughout Double Cantilever Beam (DCB) joint testing.

1.3 Research methodology

The objectives of the present work were accomplished following the next research methodology:

- Comprehensive literature investigation was conducted to elucidate the current state of the art concerning polyurethane adhesives and the influence of loading rate and temperature on adhesive properties;
- Experimental tests to characterize the adhesive properties, namely bulk tensile tests, thick adherend shear tests (TAST), double cantilever beam (DCB) tests and mixed mode fracture tests;
- Study of the effect of temperature and strain rate on the adhesive properties, subjecting the specimens to different temperatures and loading rates;
- Analysis of strain rate fluctuations using Digital Image Correlation (DIC) and comparison of true strain rate and engineering strain rate.

1.4 Thesis outline

This thesis is divided into seven distinct sections. The first chapter provides an overview of the problem addressed, as well as the objectives, background and motivation behind it. The second chapter comprehends a review of adhesive bonding, the different adhesives' classification, failure modes and joint design. As one of the purposes of this work is to study and comprehend how different loading and environmental conditions affect adhesives' properties, a brief review of the topic is also presented. Subsequently, there is an assessment of the existing approaches for failure load prediction. The third chapter consists of a description of the experimental procedure. The fourth chapter presents the experimental results along with their respective analysis. A more detailed analysis and thorough exploration of the results regarding the behaviour of Adhesive A under various temperatures and loading rates are described in Paper A. Additionally, the analysis of strain rate in different adhesives is also more extensively covered in Paper B. The fifth chapter provides a summary of the appended documents, and, the last two chapters summarize the main conclusions of the work and provide insight into suggestions for future work.

Chapter 2

State of the art

2.1 Adhesive bonding

Adhesive bonding is a highly multi-functional joining technique and can be used to bond many dissimilar materials together. A variety of joint strengths can be achieved, ranging from low-strength sealants and caulks used only to fill gaps and voids, to high-strength structural adhesives commonly used in the automotive and aerospace industries [**?**].

Kinloch [**?**] defines an adhesive as a substance that, when applied to the surfaces of materials, can join them together and resist separation. However, there are other materials that do not fit this definition yet exhibit the phenomenon of adhesion, such as paints and printing inks. This phenomenon of adhesion is defined as the molecular attraction exerted between two substances resulting from intermolecular forces established between their surfaces [**?**].

This adhesive technology has been utilized for many years, with adhesives made from a range of natural products such as bones, skins, fish, milk, and plants. Nonetheless, significant evolution only commenced a few years ago with the advent of synthetic polymers. This is attributed to the requirement for most technological applications to possess a certain set of characteristics that enable easy adhesion to varied materials and the ability to transmit considerable load [**?**].

A bonded joint is formed by connecting two surfaces of similar or different materials using non-metal fillers and adhesives. Three stages can be distinguished in the formation of an adhesive joint. Initially, the adhesive is required to be in a solid state so that it can flow easily over the surface and adequately wet the substrates to be bonded, resulting in effective adhesion. In the second stage, the adhesive must be hardened to provide good load-bearing capacity. Pressure-sensitive adhesives are exceptional in that they do not require a hardening stage as they remain permanently sticky. It is crucial to consider that the joints' performance and durability will be significantly impacted by various variables, such as joint design and environmental factors, so an understanding of these issues is required to achieve the best results with this technology [**?**, **?**].

As previously mentioned, adhesive bonding allows various types of plastics and composites to be bonded to themselves and to other materials such as metals, wood, fabric, film or paperboard. Assuming a clean substrate surface, most materials can be bonded using adhesive to a similar or

dissimilar material. For challenging materials, such as those with low surface energy such as PE, PP, or PTFE, primers or special surface preparation procedures can significantly improve bondability. Additionally, substrates may take various forms, such as blocks, films, sheets, particles, sandwich structures, or honeycomb cores. This technique presents an increasing alternative to mechanical fastening [**?**]. Adhesively bonded structures offer more uniform stress distribution across the bonded area, resulting in increased stiffness and load transmission and subsequently reducing weight and cost, in contrast to conventional joining technologies like riveting and welding, as illustrated in Figure 2.1. Though they are simple and fast, mechanical fasteners, which use bolts, screws, rivets or pins to join two or more materials together, can also introduce holes and discontinuities into the structure, which can reduce strength and stiffness, increase weight and originate stress concentrations. On the other hand, welding is a method that involves the application of heat and pressure to join two or more materials together. It is a durable technique capable of withstanding high loads and temperatures, however, it necessitates considerable expertise and equipment and has the potential to cause distortion and residual stress in the structure [**?**, **?**].

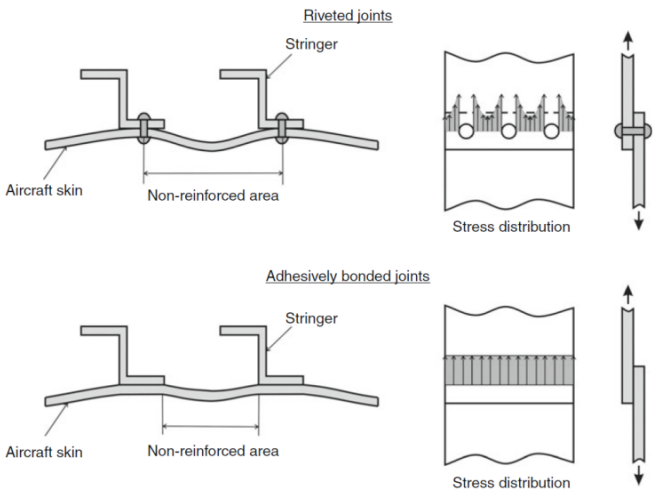


Figure 2.1: Stress distribution for different joining methods [**?**].

In addition to achieving better and uniform stress distribution along the bondline, adhesive bonding technology offers numerous advantages [**?**, **?**]:

- The adhesive joint has good damping properties due to the uniform distribution combined with the polymeric nature of the adhesive. This also provides high fatigue strength;
- Versatile joining method capable of joining dissimilar materials;
- Adhesives are capable of efficiently bonding thin plates, making them ideal for creating lightweight structures. This is a major application of structural adhesives, which do not necessitate additional components. Consequently, considerable cost savings and a reduction in labour for processing can be achieved;
- This process is easily applied with automated systems;

- Joint design becomes highly adaptable to this technology, facilitating the introduction of new concepts and materials to the industry;
- It is a durable assembly technique that creates a continuous, almost uniform seal that is visually impermeable to gases and liquids. The intimate bonding of the surfaces assists in preventing corrosion.

However, this joining method does have some drawbacks [**?**, **?**]:

- In order to increase joint strength, it is necessary to reduce peeling and cleavage stresses;
- Limited shelf lives and working lives for some adhesives;
- Adhesives, like polymers, have limited resistance to extreme environmental conditions, including temperature and humidity;
- An appropriate surface preparation is required to achieve good interfacial strength and a durable joint, such as solvent cleaning, mechanical abrasion, or chemical treatments;
- Temperature is required for some adhesives in order for them to harden, which can be an economical drawback;
- As the bonding is not immediate in most cases, tools are needed to keep the substrates in place;
- Difficult quality assurance.

2.1.1 Classification of adhesives

There are various methodologies available to categorise adhesives. They can be classified based on their chemical and physical characteristics, as well as their reaction and processing conditions. This classification aids in determining the method of application and setting of the adhesive, as well as in assembly and fixturing. In turn, this relates to the nature and purpose of the objects being bonded, which inevitably simplifies adhesive selection [**?**]. Some of the methods used to categorise an adhesive include:

- Polymer base, natural or synthetic;
- Functionality in the polymer "backbone";
- Physical forms;
- Chemical families;
- Functional type.

It is important to note that all classifications considered eventually overlap with each other [**?**, **?**].

Regarding polymer base classification, adhesives can be natural or synthetic. Natural adhesives encompass vegetable- and animal-based adhesives, consisting of organic materials such as casein, bone, and resin, as well as inorganic adhesives such as sodium silicate. They are cost-effective, simple to apply, and have a lengthy storage life. These adhesives rapidly develop tackiness but possess weak strength properties. The majority of them are soluble in water and use water as a solvent. Synthetic adhesives refer to all adhesives except natural adhesives (i.e. elastomeric, thermoplastic, thermosets, and alloys). All structural adhesives are included in this category [**?**].

In terms of functionality in the polymer "backbone", adhesives can be grouped as thermosetting, thermoplastic, elastomer or hybrid. These materials cannot be heated and melted after the initial curing process. The curing cycle of thermosetting adhesives occurs through a chemical reaction either at room temperature or at an elevated temperature, depending on the type of adhesive utilized. Two-part components have longer shelf lives and usually cure at room temperature or faster at moderately high temperatures, whereas one-part systems typically require elevated temperatures to cure and have a limited shelf life. When cured, thermosetting adhesives form densely crosslinked structures. Thermoplastics, unlike thermosetting plastics, do not cross-link during curing and are able to be melted without undergoing significant changes in their properties. The systems are one-part components and are designed to harden as soon as they cool from a molten state or when a solvent or liquid vehicle evaporates [**?**, **?**]. Elastomers are rubber-like polymers that possess flexibility and are highly deformable [**?**]. They can attain reversible elasticity through a cross-linking process, with the curing cycle differing depending on adhesive type and form. It is noteworthy that this material does not undergo complete melting [**?**]. Hybrid adhesives are a combination of thermosetting, thermoplastic or elastomer adhesives, in order to create an adhesive that incorporates the beneficial properties of each compound. Rigid resins are combined with flexible, tough elastomers or thermoplastics to provide improved peel strength and energy absorption [**?**].

The functional classification categorises adhesives as either structural or non-structural. Structural adhesives possess high strength and permanent properties, and are used to transfer loads between adherents in their respective service environments. They are generally cross-linked or thermosetting polymers, although some thermoplastic polymers are used in certain structural applications. Non-structural adhesives, such as hot-melts, pressure-sensitive adhesives, and others, do not need to withstand significant loads [**?**, **?**, **?**].

A commonly employed method for distinguishing between adhesives is through their physical composition. Various adhesive systems are offered in distinct forms, including the most frequent options such as [**?**]:

- Liquid - Easily applied by using mechanical spreaders such as rollers, spraying, or brushing;
- Paste - Paste adhesives possess high viscosities, which enable them to be applied to vertical surfaces with minimal sagging or dripping. These bodied adhesives can serve as gap fillers and sealants;

- Powder - It is generally unfeasible to utilise adhesives in solid form. These substances must be subjected to heat or dissolved in a solvent to transition to a liquid state, providing the means for them to be applied to surfaces;
- Film, tape - These adhesives provide a bond line with a consistent thickness and have the benefits of not requiring dosing and are easy to dispense;
- Among others.

Regarding chemical families, thermosets, thermoplastics and elastomers are the most relevant. One of the most crucial and commonly employed thermosets is epoxy adhesive. These structural, cross-linked, and versatile adhesives are known for their strength and brittleness, but they can be formulated to become flexible and tough without losing their tensile strength. The curing cycle for the epoxy can take place at either room or elevated temperatures. It can readily adhere to a wide range of substrates and has excellent environmental resistance. Polyimides are among the most crucial thermoplastics in use today. They exhibit excellent thermomechanical properties, can withstand high temperatures, and possess remarkable toughness. They are widely employed as structural adhesives in the aerospace and automotive industries. Polyurethanes are becoming increasingly common in the automotive industry as elastomers. The formation of a polyurethane elastomer involves three main steps. First, the polyol is reacted with the diisocyanate to form a simple chain. The second step involves chain extension, which occurs when the terminal isocyanate in the reaction product reacts with an –OH group of another polyol. The final step is the formation of an elastomer through curing (further chain extension). Polyol molecular structure can be used to create a cross-linked polymer through the use of either a hydroxyl or a diamine. The polymer's stiffness and thermal resistance depend on the size, flexibility and functionality of the polyol and the portion of the isocyanate group linking with the hydroxyl group. Cryogenic conditions can also able to be withstood [**?**, **?**].

2.1.2 Failure mode and joint design

A joint may fail due to a failure in adhesion, a failure in cohesion, or a combination of both, as illustrated in Figure 2.1. It is important to note that adhesive failure refers to the breakdown of the bond between the adhesive and the adherend at the interface between them. A cohesive failure, on the other hand, occurs when the adhesive layer remains on the adherend after the failure. The cohesive failure of the adherend occurs when the adherend fails before the adhesive. Table 2.1 outlines each failure mode and its relation to bond quality.

Table 2.1: Failure mode as an inference to bond quality. Adapted from [**?**]

Failure mode	**Inference**
Adhesive failure (interfacial)	Cohesive strength >interfacial strength
Mixed failure mode	Interfacial strength = Cohesive strength
Cohesive failure (within the material)	Interfacial strength >Cohesive strength

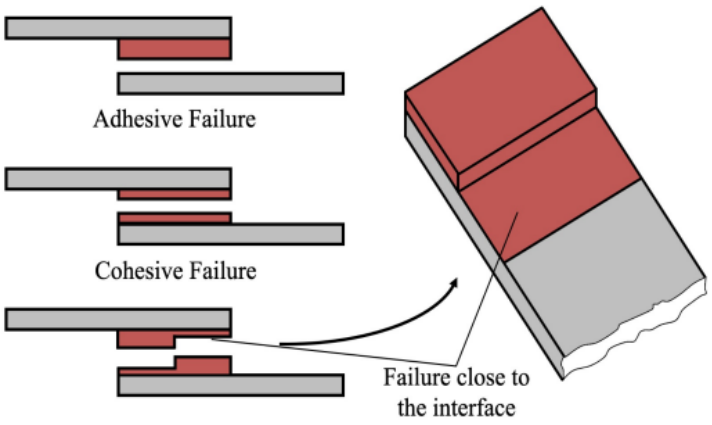


Figure 2.2: Failure modes of adhesively bonded joints.

The adhesive joint's strength, in the absence of external or environmental factors, depends on the mechanical properties of the joint's materials, the degree of interfacial contact, and the residual stresses within the joint. The design of the joint aims to achieve the highest strength possible for a specified area of bonding. When designing joints primarily for adhesive bonding, the adhesive's fundamental characteristics should dictate the appropriate joint design. Adhesive bonds act over surface areas, not single points and therefore, the joint ought to be designed with the goal of reducing stress concentration [**?**, **?**]. The designer should aim to eliminate stress concentrations which can diminish the strength and service life of the joint. Localised stresses are sometimes difficult to detect. Another cause of shrinkage in achieved cure is the release of volatiles, which may become trapped. Internal stresses decrease as adhesive thickness decreases, thus reducing the tendency to entrap volatiles. Air may become trapped at the interface if the viscosity of the adhesive is excessively high, does not flow smoothly during curing, or fails to wet the substrate.

Joints experience various forms of stress during their lifespan. Figure 2.3 illustrates the stress types that adhesive joints are exposed to. When subject to pure compression, joint failure is less likely compared to other loading conditions, although the use of compression loads is very restricted. Under shear, an even load is imposed along the bonded area, making use of all bonded areas and resulting in an economical joint that is highly resistant to failure. When forces acting perpendicular to the joint are distributed uniformly over the entire bond area, tensile stress develops. If loads are applied at an angle other than completely axial, cleavage and peel stresses may result. As adhesives generally have poor resistance to cleavage and peel, joints intended to withstand tension loads ought to have physical restraints in place to guarantee axial loading. Peel and cleavage loads exhibit comparable stress distribution, which is concentrated at one end of the joint. The adhesive's peel strength can be as little as 1% of its shear strength, but adhesives with low modulus and elasticity often exhibit greater peel strengths. This type of stress can be minimised by using a symmetrical joint, such as a double lap. When designing a joint, it is important to consider the loading mode and ensure that peel and cleavage stresses are minimised and shear stresses are maximised [**?**, **?**, **?**].

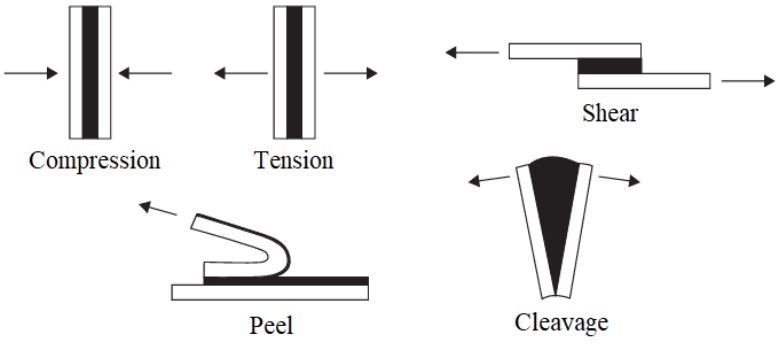


Figure 2.3: Types of adhesive loading conditions. Adapted from [**?**].

There are methods that, if employed and implemented during joint design, can enhance joint efficiency. It is important that a high percentage of the bonded area contributes to the strength of the joint. Additionally, the adhesive should be subjected to stress in the direction of its maximum strength and minimized in the direction in which it is weakest. Joints used in adhesive bonding are shown in Figure 2.4. The joint ought to support all loads on the part. In structural joints, the load in one adherend should transfer through the adhesive layer to the other joint component.

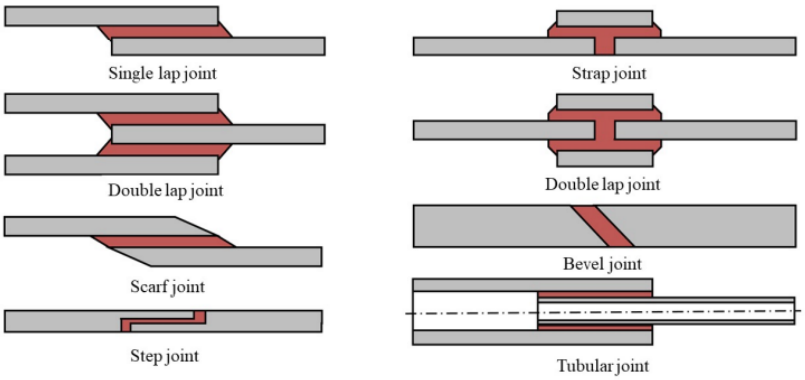


Figure 2.4: Types of joints used in adhesive bonding.

2.2 Effect of strain rate and temperature

To tackle the issues connected to the factors impacting the ultimate performance of the joint, it is imperative to examine the conduct of the material under various loading rates and environmental circumstances [**?**]. By enhancing the precision of fracture mechanism models, it becomes feasible

to anticipate the conduct of bonded structures, refine the structures' efficiency, and devise adhesives that are more robust. There has been increasing interest in comprehending the mechanical behaviour of adhesive bonds when subjected to variable loading rates and temperatures. Several studies have investigated how these variables affect the strength and fracture behaviour of different adhesive materials, such as crash-resistant epoxy and polyurethane adhesives. As there are multiple research works revealing the conspicuous rate dependency of numerous adhesives [**?**].

Recent studies have revealed new trends in strain rate and temperature effects on tensile, shear and fracture. In relation to tensile and shear properties, Borges et al. [**?**] and Jia et al. [**?**] identified a considerable strain rate dependence. Borges et al. [**?**] found that tensile and shear strength increased as the loading rate increased. However, Jia et al. [**?**] discovered that this behaviour was only consistent at room temperature. For other temperatures, the stiffness of the adhesive decreased with increasing loading rates, specifically at negative temperatures. In the study undertaken by Machado et al. [**?**], an increase in temperature led to a decrease in tensile strength, whilst an increase in strain rate resulted in an increase. Several authors investigated whether different testing methodologies could influence the results of studying fracture behaviour. Bidadi et al. [**?**] conducted a study to investigate the impact of loading rate on the mixed mode fracture behaviour of an epoxy resin material. The findings revealed that increasing the loading rate significantly reduced the fracture loads and corresponding resistance values for each mode-mixity. This was attributed to a reduction in the size of the fracture process zone at the crack tip in higher loading rates. But Borges et al. [**?**] did not verify the same in their study, the energy release rate increased as a function of the loading rate for all mode mixities in both adhesives under study.

As it is imperative to comprehend the obstacles linked with applying adhesives in the industry it is vital to assess the effectiveness of bonded connections under high load rates and impact circumstances, particularly as adhesives are polymers and thus display viscoelastic and viscoplastic traits [**?**]. Therefore, it is crucial to comprehend the variations in the mechanical properties of materials during exposure to different strain rates and temperatures since they are highly sensitive to such parameters [**?**, **?**, **?**]. However, it is objectively necessary to consider the sensitivity to strain rate in order to fully understand the changes in mechanical properties such as fracture energy. Thus, it is crucial to comprehend how strain rate may fluctuate throughout a constant speed fracture examination. It should be emphasised that loading rate and strain are separate concepts, as although they are linked, they concern different aspects of material performance. In several studies, the effect of test speed on adhesive fracture energy has been investigated. However, only a small number of studies focused on the strain rate sensitivity of fracture energy, and these were primarily limited to numerical simulations and specific conditions.

Viana et al. [**?**] studied the influence of loading rate on a crash-resistant epoxy while varying the temperature conditions. The findings indicate that under quasi-static conditions, the specimens' absorbed energy (SLJ) decreased with an increase in temperature. This decline is attributed to the adhesive's decrease in yield stress with higher temperatures. The research carried out by Jia et al. [**?**, **?**] studying ductile polyurethane adhesives showed a similar trend. In both scenarios, a correlation was observed between an increase in loading rate and a decrease in critical fracture en-

ergy. However, under quasi-static conditions, when analyzing mode I fracture, the critical energy release rate decreased with temperature. In contrast, at higher loading rates, the mode II fracture energy reduced with an increase in temperature.

Understanding the behaviour of the mechanical properties of both the adhesive and the substrate facilitates the creation of strain rate-dependent models, confirming enhanced joint designs that can withstand dynamic loads during impact [**?**, **?**]. This topic has received significant attention in this field. Nonetheless, the majority of the published research concerning the impact of strain rate on adhesive fracture toughness neglects to explain sufficiently how the authors determine the strain rate and its variance before the crack tip in a fracture test [**?**, **?**, **?**, **?**]. Some studies discuss test speed instead of the strain rate [**?**, **?**, **?**, **?**]. In certain instances, the nominal strain rate is determined by multiplying the test speed by the adhesive thickness [**?**]. However, this calculation fails to accurately reflect the actual strain rate encountered by the adhesive layer.

Using the TDCB (tapered double cantilever beam) test, Marzi et al [**?**] and Karac et al [**?**] conducted strain rate studies on a crash-optimised structural adhesive and a rubberised epoxy adhesive, respectively. Rapid mode I loading does not result in significant variations in strain rate during crack propagation, according to Marzi et al [**?**]. Based on their results, they also established a numerical correlation between crosshead velocity and average strain rate. A correlation between the strain rate at the crack tip and the test speed was established by Karac et al [**?**] in a previous study using an analytical beam with an elastic foundation. In the context of mode II tests, Marzi [**?**] investigated an epoxy-based adhesive, conducting a strain rate analysis via tapered end-notched flexure (TENF) tests. The author defined shear strain rate as the ratio of local velocity to adhesive thickness. Leffer et al. [**?**] discovered that, during an ENF test, the shear deformation rate at the crack tip varied significantly from the start of the test until failure occurred, for a constant crosshead displacement, also for an engineering epoxy adhesive. Jia et al [**?**] numerically investigated polyurethane adhesives at high strain rates, showing consistent strain rate variation according to different impact conditions. To conduct this research, the authors propose a process that relies on strain rates weighted averages to determine the adhesive's effective strain rate in the setting of numerical simulation under high strain rates. The model was calibrated and verified using experimental data acquired from tests involving DCB, ENF, and thick adherend shear tests (TAST). This study demonstrated a strong concordance between experimental results and numerical projections, thereby verifying the effectiveness of the strain rate determination method.

Using a numerical methodology, Nunes et al. [**?**] analysed the strain rate during both crack initiation and propagation in DCB and ENF test configurations of a single-component epoxy adhesive specially designed to withstand crash conditions. The researchers observed that the strain rate experienced prior to failure varied significantly along the bond line at constant testing velocities and was much lower than that observed during DCB tests. Additionally, they found that modifications in displacement velocity would have an equivalent effect on the strain rate.

Chapter 3

Experimental procedure

3.1 Materials

Three different polyurethane adhesives were used in this work, which will be referred to as Adhesive A, Adhesive B and Adhesive C. All adhesives in question are two-component structural polyurethanes specially developed for use in the automotive industry with different purposes. Table 3.1 shows the general adhesive specifications as the respective curing cycles.

Table 3.1: Adhesives specifications.

Adhesive	Type of adhesive	Adhesive thickness	Cure cycle	Post-cure cycle
Adhesive A	Polyurethane 2K	4 mm	24h @ 23 ºC	4h @ 80 ºC
Adhesive B	Polyurethane 2K	1 mm	24h @ 23 ºC	4h @ 80 ºC
Adhesive C	Polyurethane 2K	2 mm	7 days @ 23 ºC	-

The mechanical and physical properties of each adhesive are listed in Table 3.2.

Table 3.2: Adhesives mechanical and physical properties.

Property	Adhesive A	Adhesive B	Adhesive C
Aspect	Liquid	Paste	Paste
Tg [ºC]	-5	15	-45
Tensile strength [MPa]	7	15	15
Elongation at break [%]	110	25	100

The DCB specimens used were machined from DIN 40CrMnMo7 steel, which is high-strength steel, in order to avoid plastic deformation of the substrates during testing. The general properties of the substrates can be found in Table 3.3.

Table 3.3: Substrate mechanical properties.

Young's Modulus [MPa]	Poisson's ratio
210000	0.3

3.2 Manufacturing of specimens

3.2.1 Bulk test

Tensile properties were obtained by testing bulk specimens with a dogbone shape. These specimens were initially obtained through an injection mould. Some authors in the literature consider that for 2-component adhesives the injection mould enables defect-free specimens [**?**], however, the properties obtained on these tests were not as expected. The second implemented technique that promoted a better compromise of tensile properties, Young's modulus and tensile strength, using the desired thickness, consists of the manufacture of bulk material plates under pressure, as illustrated in Figure 3.1.

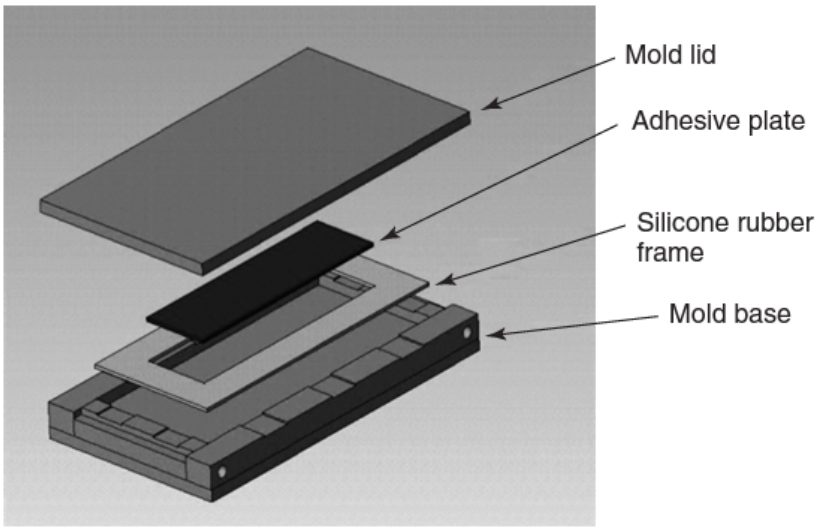


Figure 3.1: Exploded view of the mould to produce plate specimens under hydrostatic pressure [**?**].

For the manufacture of the adhesive plate, uncured material is poured into a rectangular-shaped mould and pressed between steel plates. The thickness of the plate is controlled using a silicon rubber frame contouring the material. This restrains the adhesive within the mould and provides hydrostatic pressure. To guarantee a straightforward future removal of the adhesive plate, two silicone sheets are positioned above and below the silicone frame, preventing the adhesive from adhering to the metal plates of the mould. Once the mould is closed, it is placed into a hydraulic press at 30 bar to minimize the presence of air bubbles (voids) that could originate from the mixing of this two-component polyurethane adhesive. Subsequently, after being fully cured, the adhesive plate is machined into a dogbone shape following the British standard BS 2782 [**?**] to obtain the configuration in Figure 3.2.

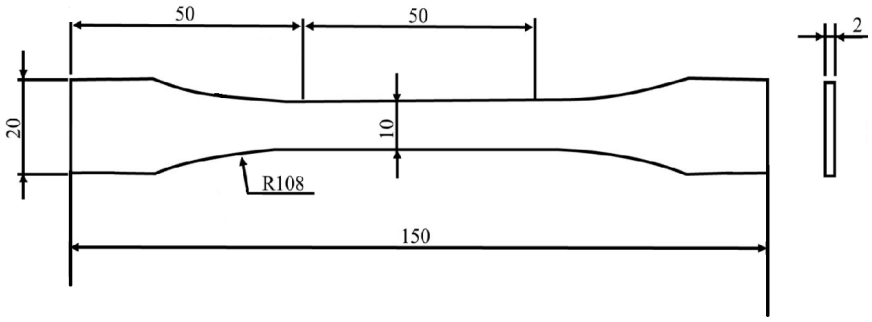


Figure 3.2: Tensile specimen geometry, dimensions in mm.

To allow the software GOM to capture and record the displacement between two different points on the specimen for specimens tested at high and low temperatures, the surface of the specimen was sprayed with a layer of white paint followed by a thin and speckled layer of black paint, as observed in Figure 3.3

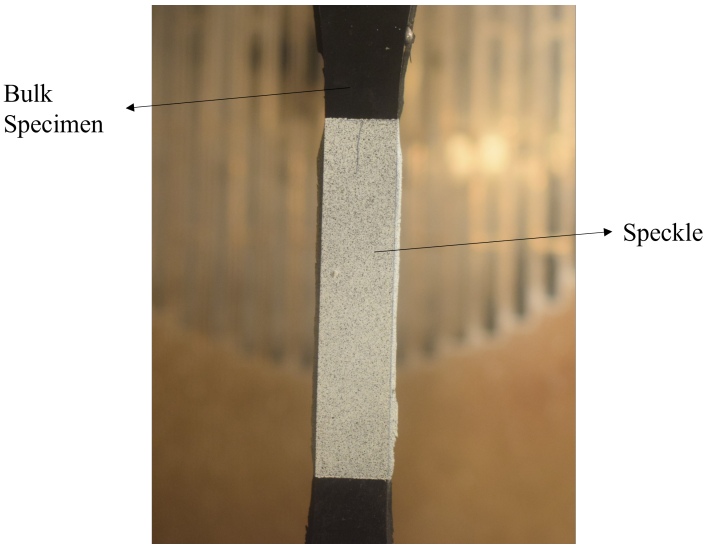


Figure 3.3: Bulk specimen with speckle for DIC analysis.

3.2.2 Thick adherend shear test

This testing method enables the assessment of the shear properties of adhesives. Each specimen is produced with an adhesive thickness of 5 mm, employing 1.5 mm shim tabs to ensure improved control of the overlap and to avoid the occurrence of tensile stresses during testing. The specimen's geometry can be found in Figure 3.4.

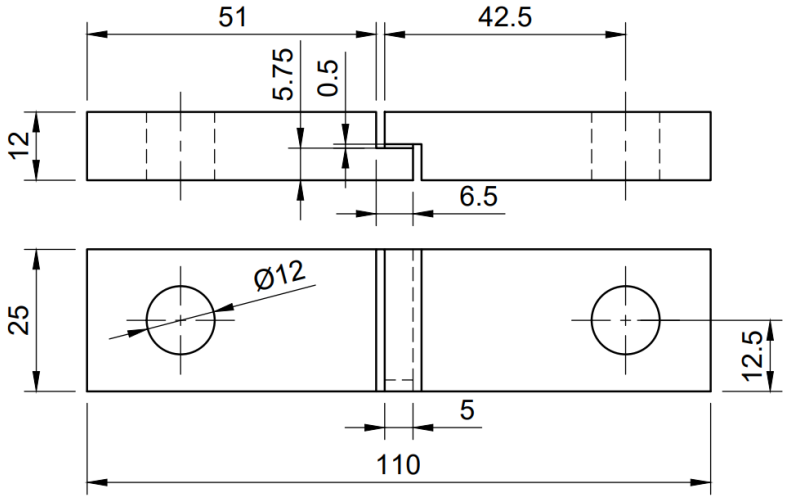


Figure 3.4: TAST specimen geometry, dimensions in mm [**?**].

Before the adhesive application, all TAST specimens underwent sandblasting to eliminate iron oxides during the sandblasting procedure, generating a surface more amenable to adhesion and preventing interfacial failure. Subsequently, the surface was cleansed with acetone to remove any surface grease [**?**, **?**, **?**]. A primer was additionally employed to enhance the adhesive bonding to the surface.

Upon placing the bottom TAST onto the mould, the adhesive is applied to its surface. Subsequently, the top TAST and the shims are positioned. Once any excess adhesive is cleaned, the mould is closed and left to cure during the respective adhesives' cure cycle time.

After the curing process is complete, the specimens must be extracted from the mould and gently cleaned on the sides to eliminate any adhesive residue. The shims need to be removed, and the side surfaces should be cleaned with acetone.

In order to measure the displacement of the specimens during the test, Digital Image Correlation (DIC) was employed. The aforementioned speckle method from the previous section was also utilized, as shown in Figure 3.5.

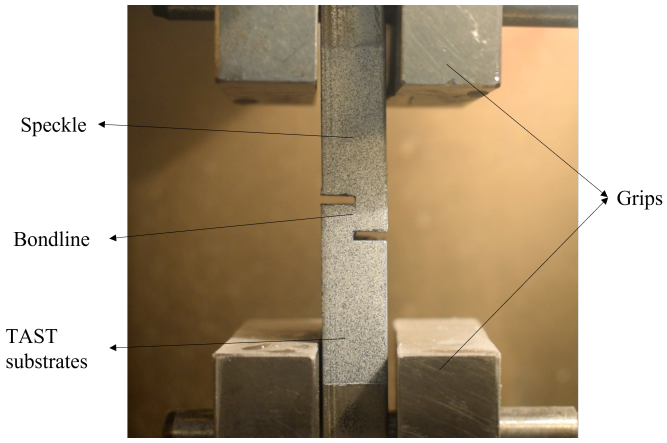


Figure 3.5: TAST specimen with speckle for DIC analysis.

3.2.3 Double cantilever beam

In order to determine the fracture energy in mode I and mixed mode, DCB specimens were manufactured. This specimen consists of the bonding of two beams with the same length and thickness, as depicted in Figure 3.6.

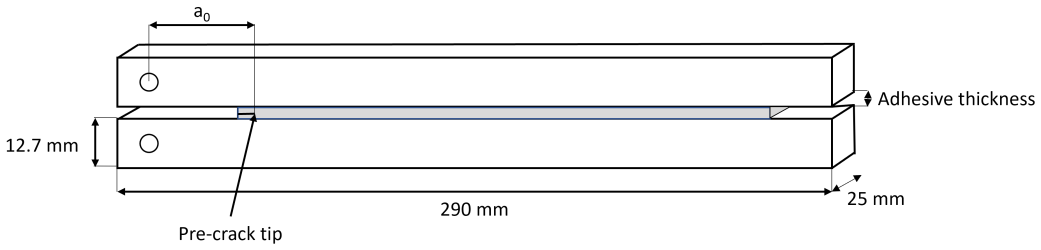


Figure 3.6: DCB specimen.

The first step of the manufacturing process also involves sandblasting and cleansing the surface with acetone for improved adhesion. After cleaning the surface, and before applying adhesive, the joints intended for the adhesive A application were primed. Regarding Adhesive C, in an initial study, it was noted that after testing, the adhesive did not exhibit promising toughness properties as expected, and the failure mode observed was not as anticipated.

Consequently, an analysis was conducted to identify the type of treatment required on the surface to achieve a better bond between the adhesive and the substrate, as well as to better characterize the properties in question. Therefore, two joints were tested for each applied treatment, as shown in Figure 3.7:

- 2 joints prepared with Primer;
- 2 joints prepared with Aktivator + Primer;

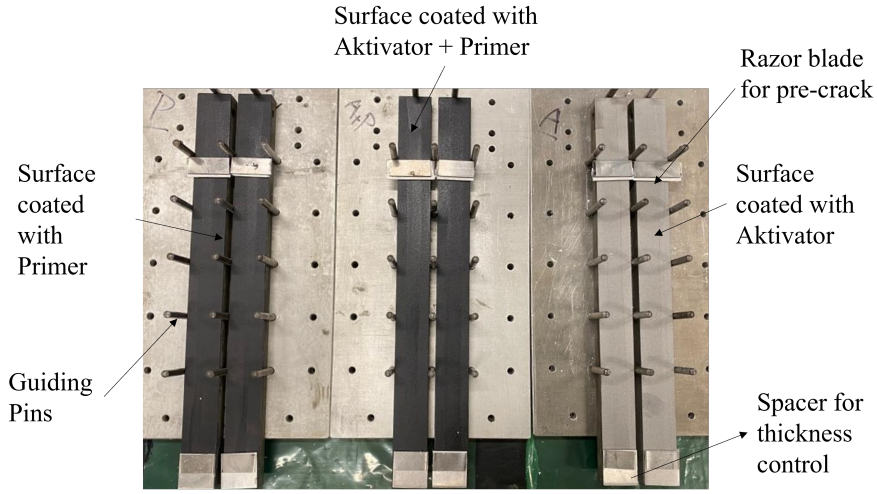


Figure 3.7: DCB specimens with respective surface treatments.

- 2 joints prepared with Aktivator.

The specimens subjected to primer treatment exhibited superior outcomes; thus, subsequent specimens were exclusively fabricated with primer application.

3.3 Testing procedure

Two separate testing machines were utilized for the various characterizing tests. For both tensile and shear predictions an INSTRON® 3367 universal testing machine, equipped with a 30 kN load cell was used. On the other hand, mode I and mixed mode fracture tests were conducted employing an INSTRON® 8801 testing equipment, featuring a 100 kN load cell. For the execution of tests at different temperatures (60 ºC and -30 ºC), two distinct thermal chambers were used. To evaluate the temperature effect on tensile and shear properties, an INSTRON® 3119-606 thermal chamber was utilized, and liquid nitrogen was employed to conduct the tests at -30 ºC. Regarding fracture tests, due to the limited space within the aforementioned thermal chamber, a custom thermal chamber was employed, specifically designed for previous tests [**?**].

3.3.1 Bulk test

All the bulk specimens were subjected to tensile loading conditions until failure. To characterize the adhesive under tensile loading, a quasi-static loading rate of 1 mm/min was employed. An extensometer was also utilized to measure the strain of the specimens, and this data was combined with the load recorded from the testing machine during testing at room temperature, 23 ºC. The mentioned setup can be found in Figure 3.9 The stress-strain curves obtained enabled the assessment of the young modulus, tensile strength, and maximum elongation of the adhesive in question.

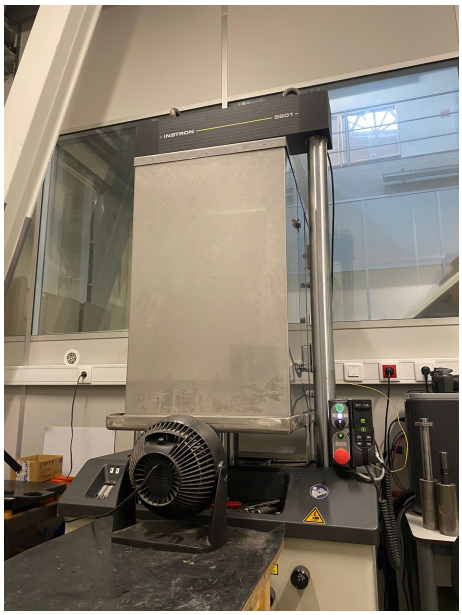


Figure 3.8: Thermal chamber for DCB and mixed mode testing.



Figure 3.9: Setup to test bulk specimens at room temperature.

For extreme temperatures, utilizing an extensometer for strain measurement proved impractical; hence, Digital Image Correlation (DIC) was employed instead. To accomplish this, a camera was deployed to capture the test, and subsequently, the frames were processed using GOM software.

3.3.2 Thick adherend shear test

TAST specimens were shear loaded to evaluate the shear characteristics of the specimen. These specimens were pin-attached to their respective grips and pulled in a way that ensured pure shear-loading effects. For all tested temperatures, the applied force was measured using the machine's load cell, and displacement was tracked using Digital Image Correlation (DIC).

3.3.3 Mode I fracture test

To determine mode I fracture energy DCB tests were performed. Both load and displacement were recorded by the machine for mode I testing, however, for strain rate analysis, DIC was also implemented to establish a correlation between the machine data and the true/engineering loading and strain rate of the specimens.

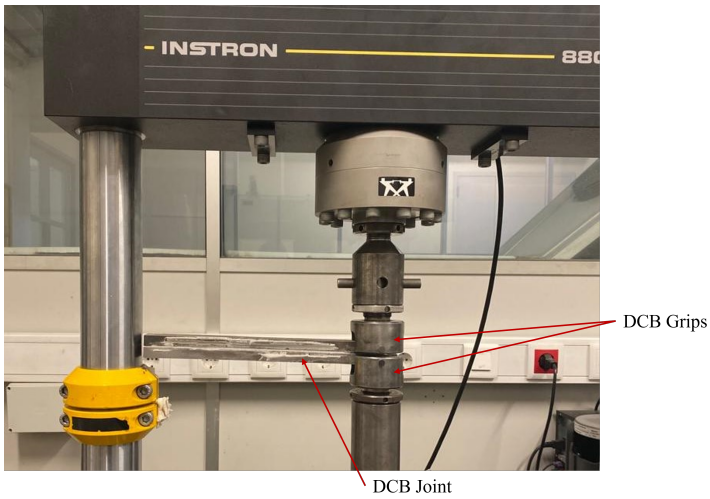


Figure 3.10: DCB setup.

3.3.4 Mixed mode fracture test

A mixed mode apparatus was used to simulate the considered mixed mode situations. This equipment, Figure 3.11, has previously passed multiple validating standard fracture tests [**?**], indicating that the weight of the equipment does not affect the expected fracture energy [**?**].

This device allows a wide range of phase angles between 0º and 90º. Figure 3.12 illustrates how to alter the geometrical configurations by varying the distances denoted as s1, s2, s3, and s4.

As the apparatus beam lengths are modified, the balance of forces is necessarily altered. As a result, separate forces are applied to the top (F1) and lower (F2) adherends. During the test, LVDTs were employed to track the displacement of each substrate.

$$F_1 = F\frac{s_1}{s_3} \qquad F_2 = F\frac{s_1 s_4}{s_3(s_3+s_4)} \tag{3.1}$$

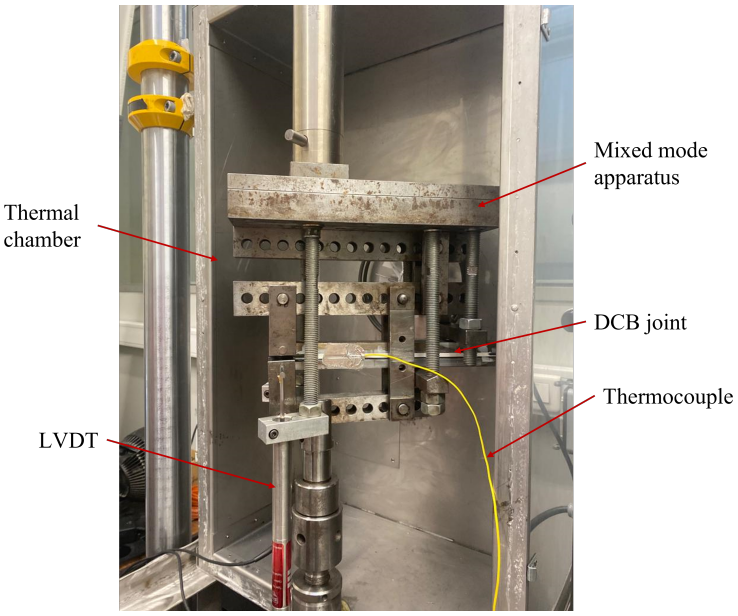


Figure 3.11: Apparatus used for mixed mode testing.

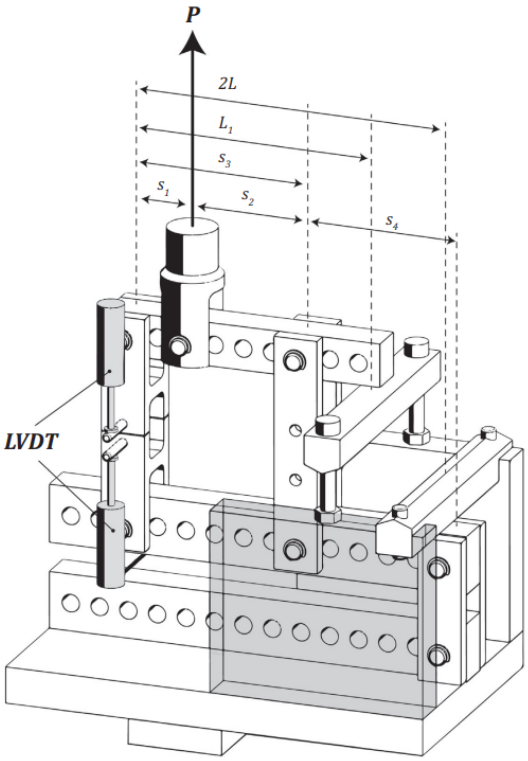


Figure 3.12: Schematic representation of the apparatus used for mixed mode testing [**?**].

The measurements obtained from the two LVDTs are denoted as δ_1 for the upper adherend and δ_2 for the lower adherend. As a result, the displacement specific to each mode can be expressed

as follows:

$$\delta_I = \delta_1 - \delta_2 \qquad \delta_{II} = \frac{1}{2}(\delta_1 - \delta_2) \tag{3.2}$$

As a result, the load delivered by the machine combines modes I and II. The terms PI and PII are defined by

$$P_1 = \frac{F_1 - F_2}{2} \qquad P_2 = F_1 + F_2 \tag{3.3}$$

The theoretical mode ratio ϕ is determined by

$$\Phi_{apparatus} = arctan\left(\frac{\sqrt{(3)}\left(\frac{F_1}{F_2}+1\right)}{2\left(\frac{F_1}{F_2}-1\right)}\right) \tag{3.4}$$

The fracture energy values for a mixed mode test are obtained by considering the mixed mode loading as the combination of a mode I loading DCB, opening mode) and a mode II loading (ENF, sliding mode), as depicted in Figure 3.13.

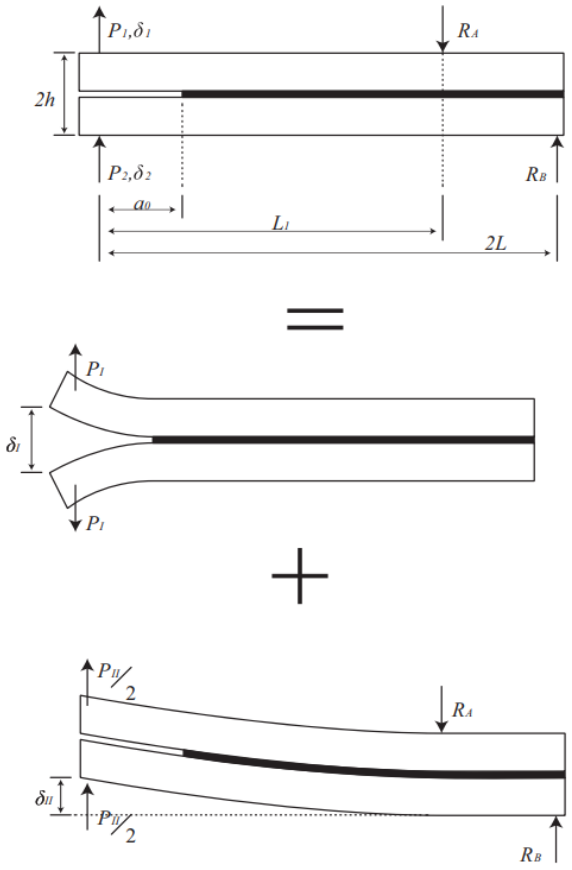


Figure 3.13: Mixed mode loading conditions [**?**].

At alternative test temperatures, a thermocouple was employed to monitor the temperature of the adhesive layer throughout the experiment, as shown in figure 3.11.

Table 3.4 summarizes the fracture test conditions considered in this study.

Table 3.4: Summary of test conditions, Fracture test.

	Temperature		
	Low temperature -30 ºC	**Room temperature 23 ºC**	**High temperature 60 ºC**
Quasi-static	Adhesive A (Mode I + Mixed mode 45º)	Adhesive A (Mode I + Mixed mode 45º/60º)	Adhesive A (Mode I + Mixed mode 45º)
0.2 mm/min		Adhesive C (Mode I + Mixed mode 45º)	Adhesive C (Mode I + Mixed mode 45º)
Intermediate Speed	Adhesive A (Mode I + Mixed mode 45º)	Adhesive A (Mode I + Mixed mode 45º)	Adhesive A (Mode I + Mixed mode 45º)
200 mm/min	Adhesive C (Mode I)	Adhesive C (Mode I + Mixed mode 45º)	
High Speed	Adhesive A (Mode I + Mixed mode 45º)	Adhesive A (Mode I + Mixed mode 45º)	Adhesive A (Mode I + Mixed mode 45º)
6000 mm/min		Adhesive C (Mode I + Mixed mode 45º)	

3.4 Data reduction approach

Data reduction approaches such as the Compliance Calibration Method and Corrected Beam Theory rely on the monitoring of the crack length during propagation, which is not simple and viable for mixed-mode testing [**?**]. Given the potential for significant errors in calculating fracture energies, the CBBM has been demonstrated to be a much more suitable option. Ahead of the crack tip, an FPZ is developed due to the nucleation of multiple micro-cracks through the adhesive thickness and classification, as shown in Figure 3.14. This FPZ makes it difficult to identify the precise location of the crack tip. When the material in question exhibits high ductility, the material will present an extensive FPZ ahead of the crack tip, which will influence the measured toughness, as a considerable amount of energy is dissipated within it [**?**, **?**]. These classical methods are not developed to consider this phenomenon, yet, CBBM takes into account the features previously mentioned.

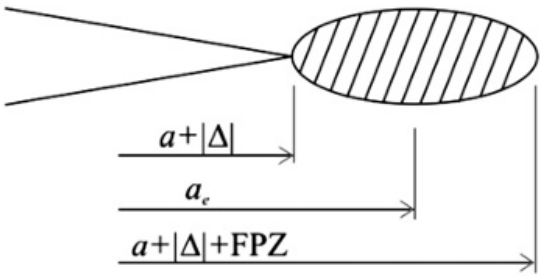


Figure 3.14: Schematic representation of FPZ and equivalent crack length concepts [**?**]

CBBM is a data reduction approach based on linear elastic fracture mechanics which does not require a crack length measurement during the test because the equivalent crack length used is estimated based only on the specimen compliance.[**?**]

The equation presented below can provide the strain energy of the specimen [**?**]:

$$U = 2\left[\int_0^a \frac{M_f^2}{2E_x I}dx + \int_0^a \int_{-h/2}^{h/2} \frac{\Gamma^2}{2G_{13}} Bdzdx\right] \tag{3.5}$$

where M_f corresponds to the substrate bending moment and I to the second moment of area for each independent substrate. The parameter τ is equal to

$$\tau = \frac{3V}{2Bh}\left(1 - \frac{z^2}{c^2}\right) \tag{3.6}$$

where V is the transverse load in each adherend for $0 \leq x \leq a$, z is the distance in the normal axis and c half of the thickness of each DCB substrate. The displacement δ can be determined using Castigliano's method, which involves applying beam theory and taking a partial derivative of the

strain energy with respect to the load P

$$\delta = \frac{\partial U}{\partial P} = \frac{8Pa^3}{E_x Bh^3} + \frac{12Pa}{5BhG_{13}} \tag{3.7}$$

Given this approach, it is possible to define the compliance of the specimen among the $P-\delta$ curve obtainable by the testing machine's acquisition data system, where $C = \delta P$. However, the classical beam theory is limited in its ability to account for all phenomena that occur during a crack opening event, such as stress concentration in the crack tip during the initial part of the pure mode I test [**?**]. Such events may have an impact on the $P-\delta$ curve, which is not accounted for by the methodology. In order to include these effects, a new parameter is introduced called the corrected flexural modulus (E_f), which replaces the value of E_1. Therefore, the altered flexural modulus of the specimen can be expressed as follows:

$$E_f = \left(C_0 - \frac{12(a_0 + \|\Delta|)}{5BhG_{13}}\right)^{-1} \frac{8(a_0 + |\Delta|)^3}{Bh^3} \tag{3.8}$$

Where C_0 represents the initial compliance and a_0 is the initial crack length. Δ is a correction factor accounting for the root rotation of the crack length size (a_0). To estimate the crack length,

$$a_{eq} = \frac{A}{6\alpha} - 2\frac{\beta}{A} \tag{3.9}$$

where the α and β coefficients can be written as

$$\alpha = \frac{8}{Bh^3 E_f} \beta = \frac{12}{5BhG_{13}} \tag{3.10}$$

and A given as

$$A = \left(\left(1 - 108\gamma + 12\sqrt{\frac{3}{a}(4\beta^3 + 27\gamma^2\alpha)}\right)\alpha^2\right)^{1/3} \tag{3.11}$$

where the last parameter γ corresponds to the negative value of the compliance.

$$\gamma = -C \tag{3.12}$$

According to the CBBM criterion, the fracture energy comes from

$$G_{I_c} = \frac{6P^2}{B^2 h}\left(\frac{2a_e^2}{h^2 E_f} + \frac{1}{5G_{13}}\right) \tag{3.13}$$

For mixed-mode situations fracture energy is partitioned into distinct mode I and mode II components, permitting the individual application of CBBM to each mode.

$$C_I = \frac{8a^3}{EBh^3} + \frac{12a}{5BhG} \tag{3.14}$$

$$C_{II} = \frac{3a^3 + 2LL_1^2}{2EBh^3} + \frac{6LL_1}{5BhG(2L - L_1)} \tag{3.15}$$

where E and G correspond, respectively, to Young's and shear moduli of the adhesive, B is the joints' width, a is the crack length and h is the specimen's thickness. L and L_1 are defined in Figure 3.12. For mode I part, the formula of the equivalent crack length is presented by [**?**]:

$$a_{eq_I} = \frac{A}{6\alpha} - \frac{2\beta}{A} \tag{3.16}$$

knowing that,

$$A = \left(\alpha^2 - 108\alpha^2 C_I + 12\alpha^2 \sqrt{\frac{3}{\alpha}(4\beta + 27C_I\alpha)} \right)^{1/3} \tag{3.17}$$

$$\alpha = \frac{8}{Bh^3 E_f} \qquad \beta = \frac{12}{5BhG} \tag{3.18}$$

The following equation represents the formula for the mode II part [**?**]:

$$a_{eq_{II}} = \left[\frac{2}{3} \left(\left(C_{II} - \frac{6LL_1}{5BhG(2L - L_1)} \right) Bh^3 E - \frac{2}{3} LL_1^2 \right) \right]^{1/3} \tag{3.19}$$

The fracture toughness values for each mode can be determined using the following equations, which take into account the relationships between different modes of fracture [**?**].

$$G_I = \frac{9P_I^2}{B^2 h} \left(\frac{a_{eq_I}^2}{h^2 E_{fI}} + \frac{1}{5G} \right) \tag{3.20}$$

and for mode II

$$G_{II} = \frac{9P_{II}^2 a_{eq_{II}}^2}{16B^2 E_{fII} h^3} \tag{3.21}$$

In this experiment, DIC was used to study the variation of strain rate as a function of crack size. To ensure proper alignment between the test specimen and the camera, a laser beam technique was used to maintain perpendicularity between the DCB and the camera. Figure 3.15 displays the concluding setup, which involved a 3D printed part that placed the laser perpendicular to the specimen.

The digital camera captured the specimen displacement during the test. The images were then extracted and post-processed. The use of DIC enabled the measurement of specimen displacement near the interface, along the adhesive layer and the calculation of true and engineering strain rates for various points on the joint and during the test period. Displacement data was acquired by analysing the recorded images with GOM Correlate software. Two reference points were selected, one on each substrate, to measure displacement during testing. Initially, the quality of the speckle was verified to ensure that these points could be traced in every test frame. Subsequently, the displacement between the reference points was tracked by the software over time.

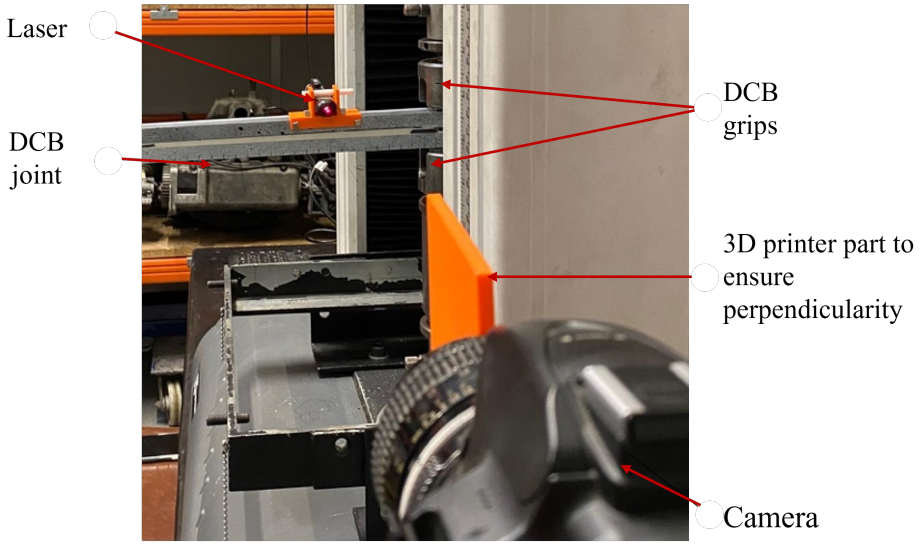


Figure 3.15: Laser beam method for guaranteeing perpendicularity between the DCB joint and the camera.

Once the values for the displacement have been extracted, it is possible to calculate the values for the strain rate. The definition of engineering strain rate for a material that experiences dynamic loading is typically expressed through the following equation:

$$\dot{\varepsilon}_{Engineering} = \frac{d\varepsilon}{dt} = \frac{d}{dt}\left(\frac{L(t) - L_0}{dt}\right) = \frac{v(t)}{L_0} \tag{3.22}$$

where time *(t)* is measured in seconds in this study, *L0* is the initial adhesive thickness, *L(t)* is the adhesive thickness at time *t*, and *v(t)* is the velocity. Thus, the strain rate is determined as the velocity at which paired points on the two sides of the adhesive layer move away from each other, divided by the initial adhesive thickness. However, it is important to consider that this velocity depends on both time and distance from the loading point. This equation is applied in DCB tests to assess the adhesive layer's strain rate in mode I. Nonetheless, the equation provides an engineering strain rate, whereas numerical simulations employ the true strain rate. The actual strain rate may significantly deviate from its engineering value, especially with more pliable adhesives and thicker bond lines as in the present study. The true strain rate considers the actual change in deformation occurring within the adhesive layer during its deformation. The true strain was calculated using the following expression:

$$\dot{\varepsilon}_{True} = \frac{ln\left(\frac{L(t)}{L(t-1)}\right)}{dt} \tag{3.23}$$

where *L(t)* represents the thickness value at time *t*, *(t-1)* is the adhesive thickness of the increment prior to *t*, and *dt* corresponds to the time interval between both increments.

Chapter 4

Results and discussions

As a consequence of this study, two articles were authored, both of which are appended herewith. While an in-depth analysis of the findings is expounded in these two papers, a concise overview of the results is also provided in this section. Any subsequent mention with the nomenclature QS, ISR and HSR will be relative to the quasi-static condition (0.2 mm/min), intermediate strain rate (200 mm/min) and high strain rate (6000 mm/min), respectively. For simplicity, low temperature (-30 ºC), room temperature (23ºC) and high temperature (60 ºC) will be referred to as LT, RT and HT, respectively.

4.1 Strength tests

Figure 4.1 illustrates a comparison of the stress-strain curves of all adhesives tested under QS conditions at room temperature.

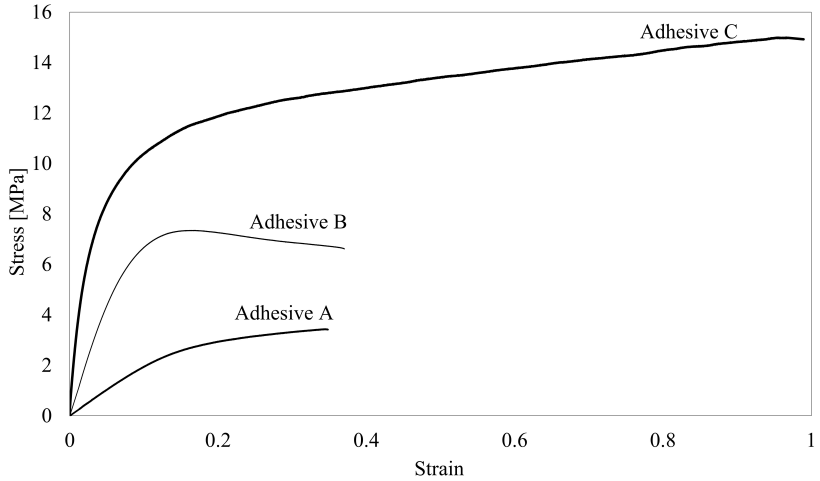


Figure 4.1: Tensile strength results for all adhesives under 1 mm/min at 23 ºC.

Of the three adhesives, it is evident that adhesive C exhibits superior tensile strength, rigidity, and maximum strain at failure, at room temperature, making it the most ductile of the three. Adhesive B follows closely behind, with adhesive A showing the least favourable properties among the three.

The impact of temperature on adhesive joints is a significant area of research, as service temperatures are frequently encountered in practice. Below or above standard room conditions, the service temperature is a crucial factor in determining adhesive performance. This relationship is due to the glass transition phenomenon which significantly affects adhesive properties with temperature. When the temperature exceeds the adhesive's T_g, it experiences more elongation but experiences lower strength and stiffness.

Notably, the results presented in 4.2 and 4.3 provide significant information regarding the adhesive's reaction to changing temperatures, making it a useful resource for engineering and material design applications. Moreover, comprehending the interdependence between rigidity and ductility at different temperatures can guide the selection and optimisation of adhesives tailored to specific operating environments, ultimately improving the reliability and performance of adhesive-bonded systems. In Figures 4.2 and 4.3, the impact of temperature on the properties of adhesive C is evidently exhibited. Both tensile and shear properties are presented with meticulous attention to detail, demonstrating distinctive behaviour across a range of temperature conditions.

It is worth noting that at -30ºC, the adhesive displays greater stiffness and strength, indicating its suitability for low-temperature environments. This behaviour is accompanied by a level of ductility, owed to the adhesive's T_g being -45ºC, enabling flexibility to be retained even at sub-zero temperatures.

At temperatures above 23 ºC, a reduction in strength and an increase in maximum strain are noticeable, especially for tensile properties. The deterioration of properties resulting from exposure to varying temperatures under quasi-static conditions has also been researched by multiple authors, that found similar trends. Na et al [**?**] tested adhesive joints of varying composition at different temperatures and found that the joint's strength diminishes with elevated temperature. Deb et al. [**?**] investigated the impact of various extension rates and temperatures by employing double lap joints bonded with a rubber-toughened adhesive based on an epoxy resin. Their findings suggested that the adhesive strength decreases as the temperature rises, due to its softening effect. However, below room temperature, the joint strength increased.

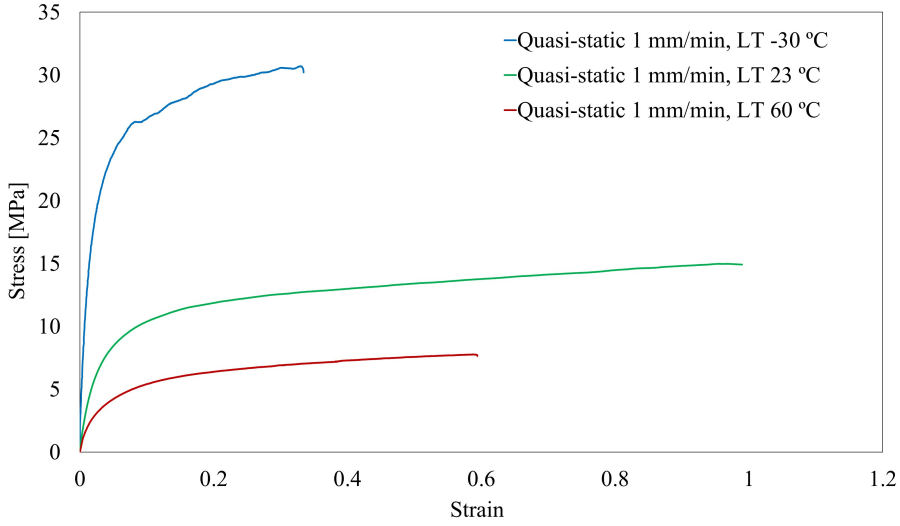


Figure 4.2: Bulk test results for adhesive C under quasi-static loading rate.

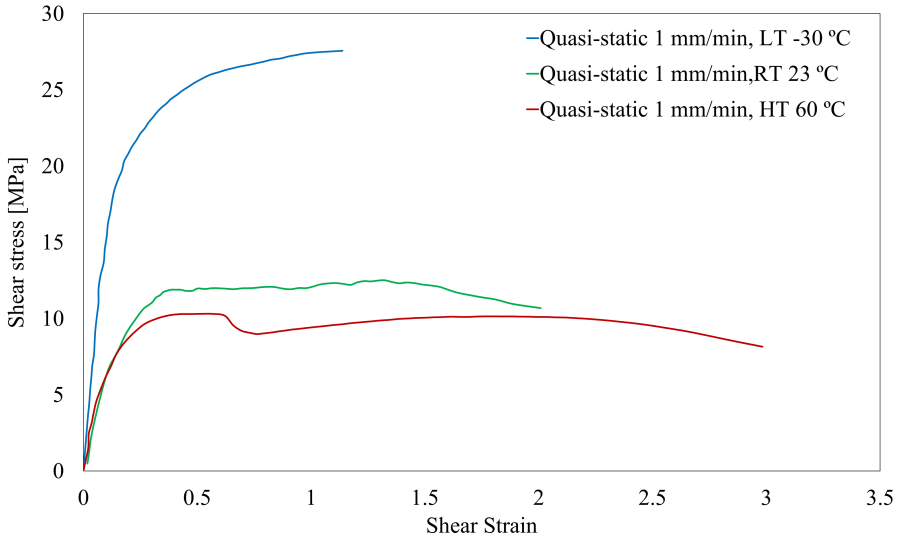


Figure 4.3: TAST results for adhesive C under quasi-static loading rate.

Taking both bulk and TAST results into consideration, it is evident that strength tests demonstrate a significant influence of temperature on the adhesive's tensile behaviour. However, for pure shear solicitation (TAST), the adhesive's behaviour appears almost independent of temperature. Tensile strength markedly decreased with increased temperature, while shear strength remained almost constant. Regarding strain at failure, the parameter decreased with temperature during the tensile test, while it increased for the shear solicitation test. This increase may have been caused by a slight rotation of the substrates, leading to a small error in the maximum strain. However, similar trends have already been reported by other authors. Lopes et al. discovered that temperature has an important impact on adhesive properties under tensile/mode I loading, whereas, under

pure shear/mode II loading, the adhesive is almost insensitive to temperature variations. Thus, the value of properties would stay consistent, or may even rise [**?**].

4.2 Fracture energy: Effect of loading rate and temperature

4.2.1 Adhesive A

In the context of fracture toughness, it is vital to acknowledge that its value fundamentally relies on the stress and displacement encountered by the specimen prior to failure. Hence, a thorough analysis requires investigating both these factors to comprehend completely the correlation between temperature and loading rate's impact on fracture energy.

For adhesive A, all fracture samples resulted in cohesive failure within the adhesive (see Figure 4.4). The surfaces of the fractures at room temperature and high temperature displayed crack origination at the pre-crack tip which then bends towards one of the interfaces and spreads in close proximity to the interface, invariably within the adhesive layer. For LT, the adhesive exhibits minimal ductility, which inhibits the crack from propagating to one side of the DCB joint. Therefore, the crack propagates in a linear manner at the mid-thickness of the adhesive layer, rather than at one of the interfaces.

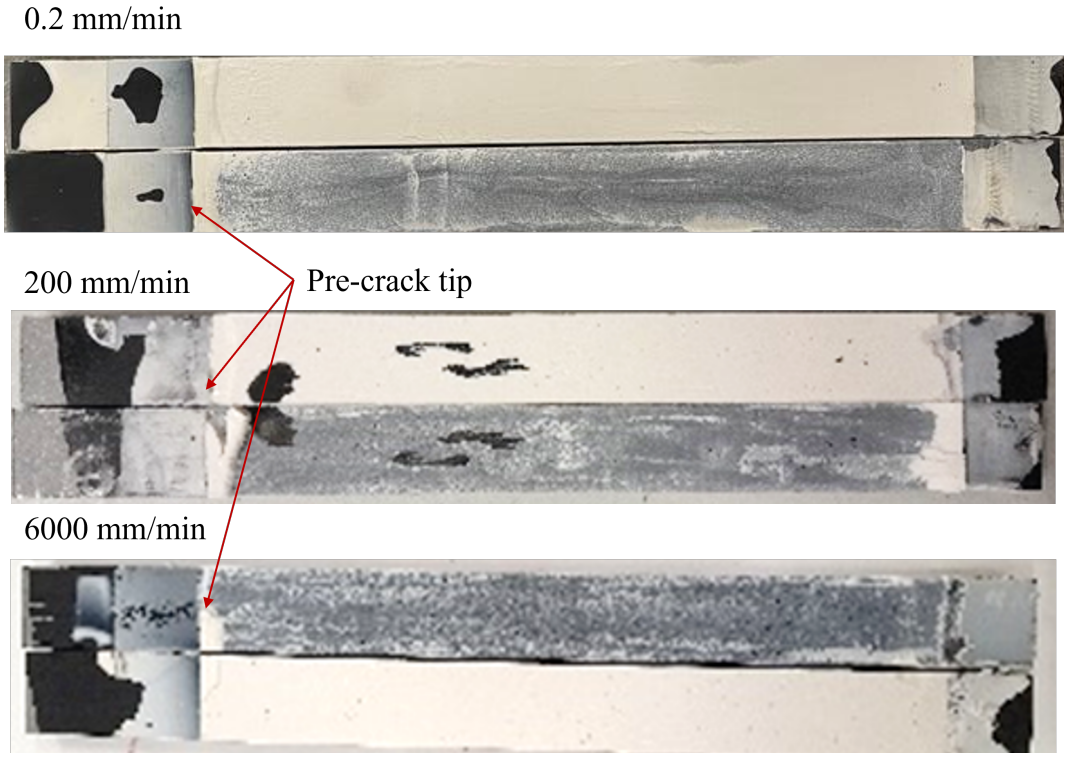


Figure 4.4: Fracture surface of adhesive A after testing at 23 ℃ for different loading rates under pure mode I.

The findings demonstrate that an increased loading rate has a significant impact on joint fracture toughness. This highlights the importance of considering loading rates when evaluating the fracture properties of materials or structures, as they can have a significant impact on overall structural integrity and performance. Understanding these effects is essential in creating and preserving sturdy and dependable components, especially in situations where rapid or dynamic loading conditions are prevalent [**?**]. At loading rates lower than 200 mm/min, the fracture energy values displayed similarity due to the material's ability to dissipate energy through plastic deformation and microcrack propagation in both fracture modes. Nevertheless, with increasing loading rates, the material exhibited a stiffer response, allowing for less energy dissipation and leading to a more brittle behaviour. Consequently, there was a marked disparity between mode I and mode II fractures, wherein G_{II} decreased more rapidly, rendering it extremely sensitive to increased strain rates at lower temperatures.

When considering the mechanical properties, it is important to note that there are numerous factors that can affect them. Two key parameters to consider include the testing temperature and the T_g of the adhesive. The testing temperature is crucial in evaluating a material's performance, as it can significantly affect its stiffness, strength, and ductility. Understanding how a material's T_g corresponds to testing conditions is essential as it directly impacts the adhesive's structural integrity. In the field of material characterization, it is imperative to consider these factors to assess a material's behaviour under different modes of loading thoroughly. While analysing Figure 4.5, which shows the effect of strain rate on fracture energy in pure mode I for 23 and 60 ºC, it is clear that the sensitivity to strain rate is practically similar at both temperatures (in pure mode I).

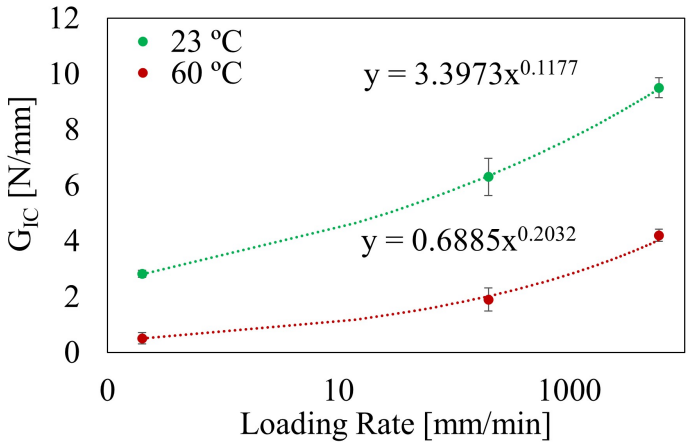


Figure 4.5: Effects of loading rate on the fracture energy mode I - adhesive A

In the examination of Figure 4.6 results, an abrupt decrease in the crucial fracture energy was noticed at temperatures beneath the glass transition temperature T_g for both mode I and mode II constituents of mixed mode fracture energy. Additionally, an inconsistency between G_I and G_{II} was observed at loading rates over 200 mm/min at low temperatures (LT).

On the other hand, the fracture energy of adhesive A increased when exposed to temperatures

above its glass transition point (23°C and 60°C) while the loading rates were increased. In most cases, this trend remained consistent except for the transition from a loading rate of 200 mm/min to 6000 mm/min at room temperature while in the mode II aspect of mixed mode. As previously noted, mode I and mode II exhibited different behaviours under high strain rates. Throughout the experiment, it was maintained precise control over the rate of displacement, and the apparatus was configured with a 45-degree phase angle for mixed mode testing prior to commencement. However, as the strain rate increased, a noticeable discrepancy between the values for mode I and mode II emerged, as mentioned previously. It would be expected that the strain rate would be the same for both modes, but mode I is clearly growing at a faster rate, leading to the suggestion that the mode mixity is changing to pure mode I fracture behaviour. With these aspects in mind, a comparative analysis of fracture energies was carried out, focusing on strain rate and each fracture mode. Based on the fracture energies, it is evident that lower temperatures exhibit reduced sensitivity to strain rate. This phenomenon can be attributed to an increased sensitivity to strain rate resulting from temperatures exceeding the T_g, with different responses for mode I and mode II fractures.

It should be noted that the tests carried out controlled the displacement rate and not the strain rate. Despite the fact that the loading rate was set to a constant value for each specimen tested, the strain rate exhibits different behaviour for mode I and mode II due to the different sensitivities associated with each mode, explaining why there is an increasing discrepancy between these two modes. Further experiments and numerical analysis should be carried out to understand how this phenomenon affects each mode.

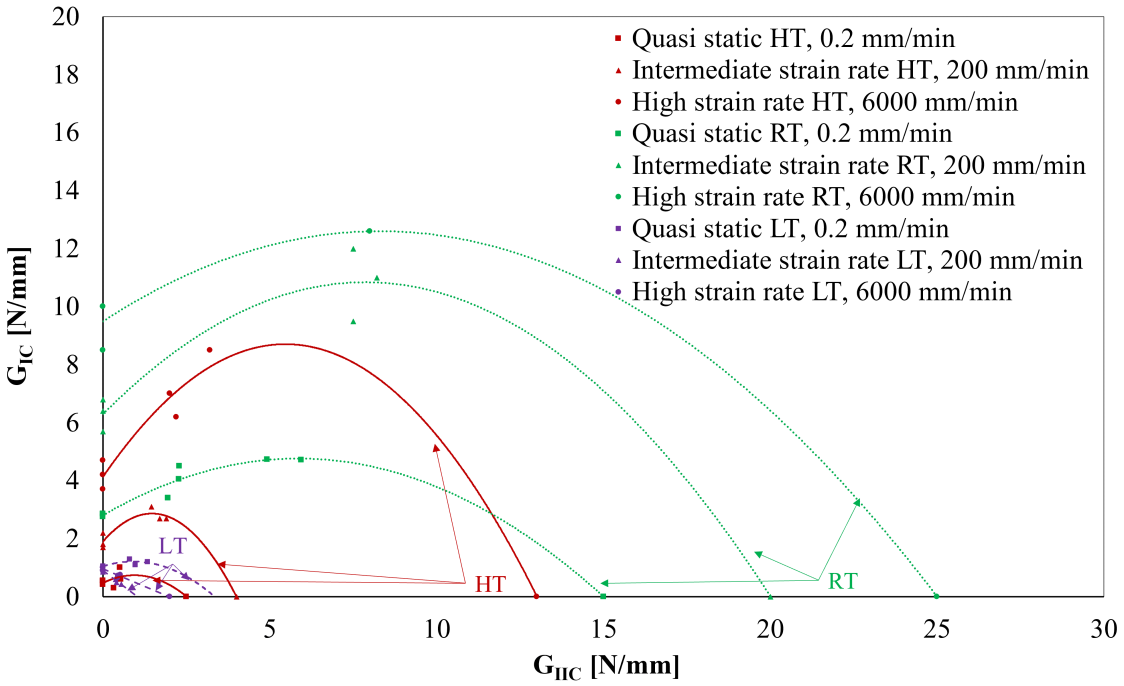


Figure 4.6: Fracture envelope of adhesive A.

At a temperature of 60°C, the fracture energy parameters show comparable behaviour for strain rates below 200 mm/min. However, at higher strain rates, G_{II} demonstrates a tenfold increase in value from its original state under quasi-static conditions, whereas G_I increases by a factor of 12.

This occurrence can be attributed to the heightened mobility of polymer chains within the PU adhesive at elevated temperatures. This improved mobility permits superior energy dissipation and deformation before fracture, resulting in increased values of both G_I and G_{II}. However, this impact is particularly noticeable for G_I, which is related to crack opening and the separation of bonded surfaces during mode I loading. This necessitates a greater displacement of the adhesive perpendicular to the crack plane. In contrast, G_{II} concerns crack sliding and shear deformation of the adhesive, necessitating less extensive deformation within the crack plane. Therefore, the rise in energy dissipation and high-temperature deformation has a more substantial impact on G_I than G_{II}.

Based on these findings, it is evident that, for this adhesive, G_I displays marginally greater sensitivity to strain rate at elevated temperatures when compared to mode II. This point was also reported for an epoxy adhesive by Lopes et al. [**?**]. When comparing the results obtained at 23°C and 60°C, it becomes clear that room temperature (23°C) is more vulnerable to strain rate impacts than the higher temperature of 60°C. Therefore, based on the presented results, the optimal adhesive performance was achieved at higher loading rates (6000 mm/min) and room temperature (23 ºC), with a G_I of approximately 13 N/mm and G_{II} of around 7 N/mm.

Although closer results to mode II were not accomplished, the quadratic polynomial approximation used to construct a fracture envelope from these results enables an extrapolation to be formulated for mode II.

For more comprehensive details, reference should be made to the attached paper A, which discusses how temperature and loading rate influence the fracture energy of adhesive A under mixed mode conditions.

4.2.2 Adhesive B

Based on the fracture test results of this adhesive under various loading rates, it is evident that the fracture energy rises with the loading rate in pure mode I and mixed mode. Sekiguchi et al. [**?**] similarly noted a positive correlation between mode I fracture energy and loading rate for a rubbery polyurethane adhesive. In addition, Figure 4.7 indicates that G_{IC} increases nearly linearly on a logarithmic scale. In terms of mixed mode loading (see Figure 4.8), G_{II} demonstrates linearity with an increasing loading rate at 23 ºC. However, this is not the case for the G_I component of the mixed mode, which is shown to be more sensitive to variation in loading rate at higher test speeds under 23 ºC compared to mode II.

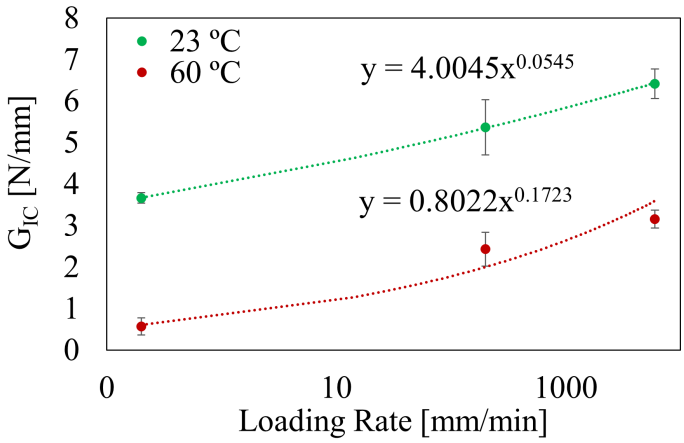


Figure 4.7: Effects of loading rate on the fracture energy mode I - adhesive B.

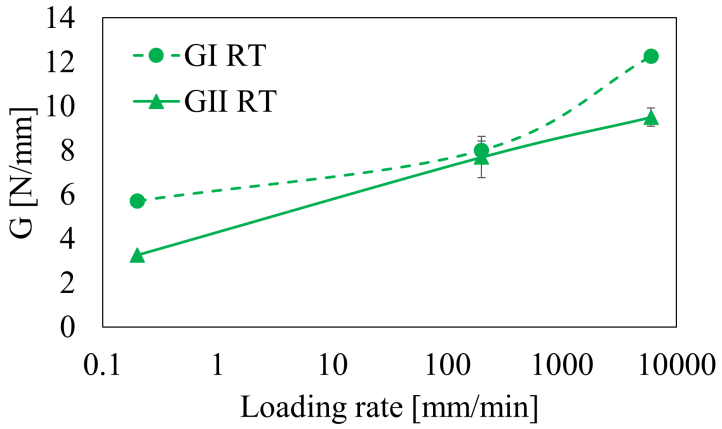


Figure 4.8: Fracture energy as a function of loading rate for adhesive B, mixed mode.

For adhesive B, all fracture specimens demonstrated cohesive failure within the adhesive. Moreover, with the increase in loading rate, the specimens displayed a smoother fracture surface, as shown in Figure 4.9.

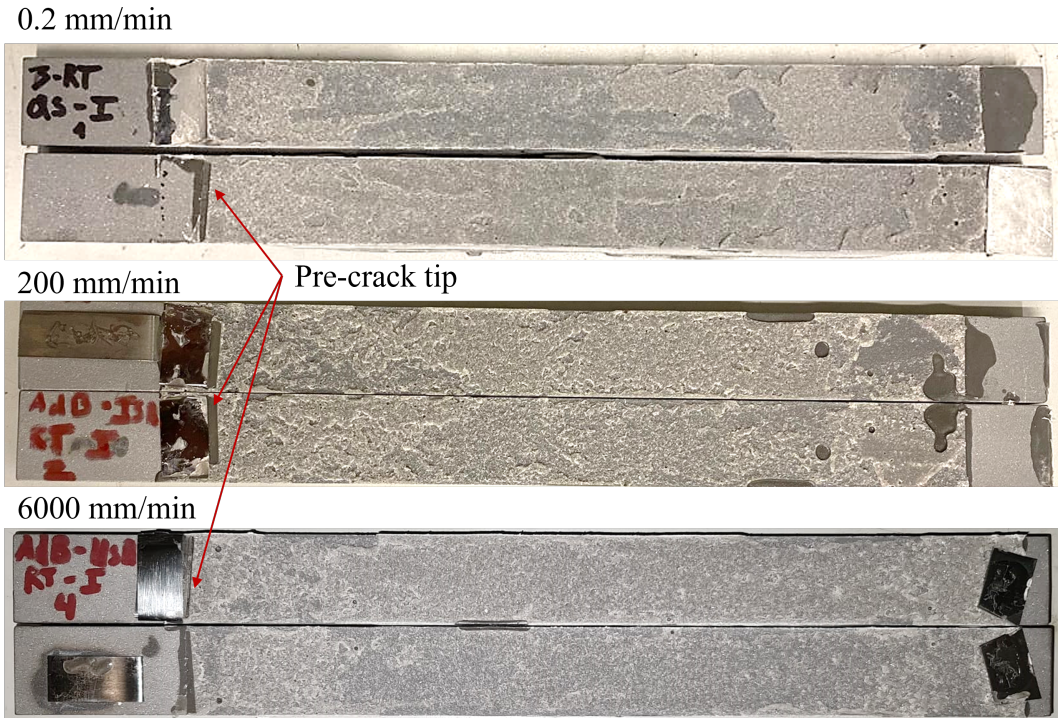


Figure 4.9: Fracture surface of adhesive B after testing at 23 ºC for different loading rates under pure mode I.

The impact of temperature on the fracture behaviour of the adhesive was evaluated through DCB tests. All tested conditions were performed above the adhesive's T_g. According to the results shown in Figure 4.7, pure mode I exhibited an 84% reduction in G_{IC} (quasi-static condition) with temperature increasing, from 3.66 N/mm to 0.57 N/mm, and a reduction of approximately 50% at higher loading rates. These findings confirm that fracture toughness degradation occurred at high testing temperatures under pure mode I conditions. Banea et al. [**?**] also reported a decrease in mode I fracture energy with temperature, which was more pronounced when the temperature was close to the T_g of the adhesive.

Regardless of the testing temperature, it is evident that the adhesive exhibits a consistent pattern in mode I fracture energy with increasing loading rates. Specifically, there is an almost linear growth of the G_{IC} with loading rate in logarithmic scale. It is evident that the sensitivity to strain rate at both temperatures is almost identical, as the lines are almost parallel (with similar slopes).

The fracture envelope determined is presented in Figure 4.10. The fracture envelopes for each adhesive exhibit uniform shapes, indicating a rise in the energy release rate as the loading rate increases. Although a closer approach to mode II could not be obtained, the application of a quadratic polynomial approximation to generate a fracture envelope from these data enables the development of an extrapolation for mode II.

Based on the findings, the adhesive exhibited superior performance at elevated loading rates (6000 mm/min) and room temperature, with a G_I of about 12.3 N/mm and G_{II} of roughly 9.5

N/mm.

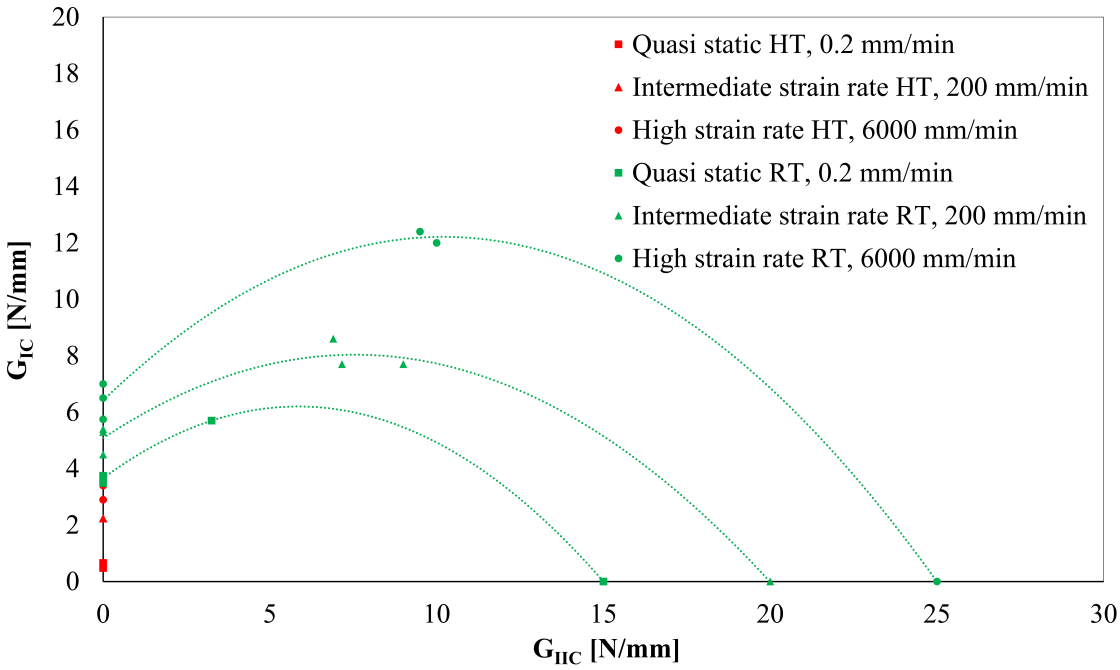


Figure 4.10: Fracture envelope of adhesive B.

4.2.3 Adhesive C

After considering the fracture envelope depicted in Figure 4.11 and analyzing Figure 4.12, it can be confirmed that the fracture energies of adhesives B and C exhibited comparable behaviours at 23 °C as the loading rates increased up to 200 mm/min. At intermediate speed, during the transition from 200 mm/min to 6000 mm/min at room temperature, the fracture energy of the mode II part of the mixed mode did not increase as rapidly as mode I. In fact, between intermediate and high test speeds at room temperature, G_I increased by approximately 89.19%, whereas G_{II} increased by 15.75%. Once again, mode I and mode II part of the mixed mode display distinct behaviours at high strain rates, as noted in the results of adhesives A and B. As the loading rate increases, a clear discrepancy between the G_I and G_{II} values arises, as previously mentioned. It would be expected that both modes have the same strain rate. However, it appears that mode I is growing at a faster rate. This suggests, once again, that the mode mixity is changing to pure mode I fracture behaviour, despite verifying the 45º phase angle before testing. According to these findings, it is evident that mode I is more responsive to strain rates than mode II for a given temperature.

In spite of the fact that a closer approximation to mode II could not be reached, creating a fracture envelope using a quadratic polynomial approximation allows for the formulation of an extrapolation towards mode II.

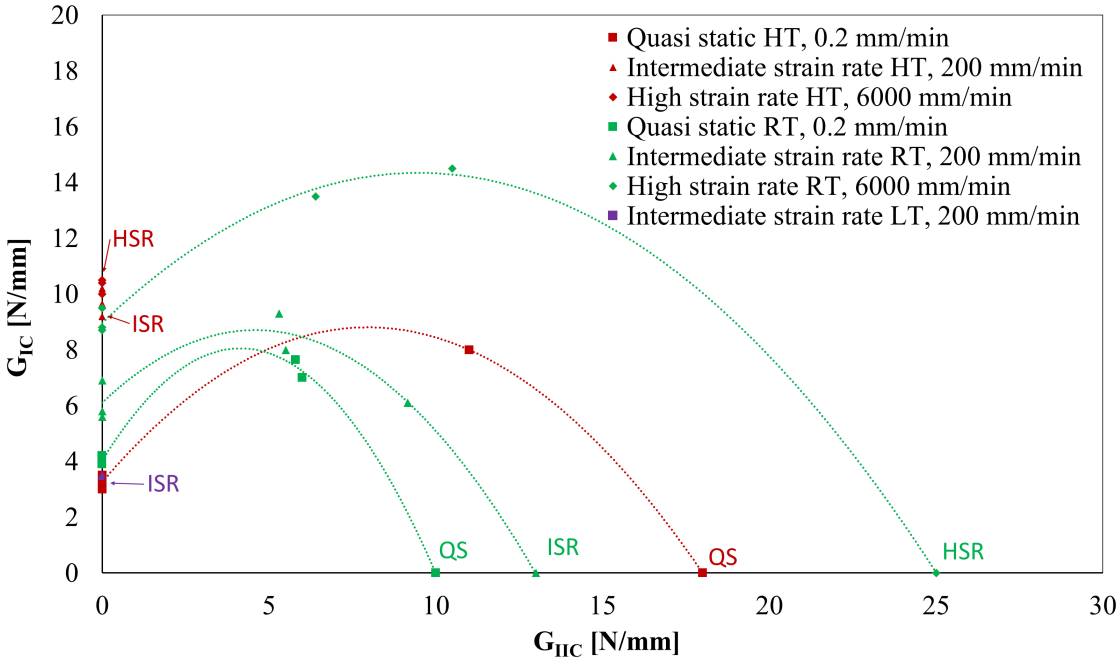


Figure 4.11: Fracture envelope of adhesive C.

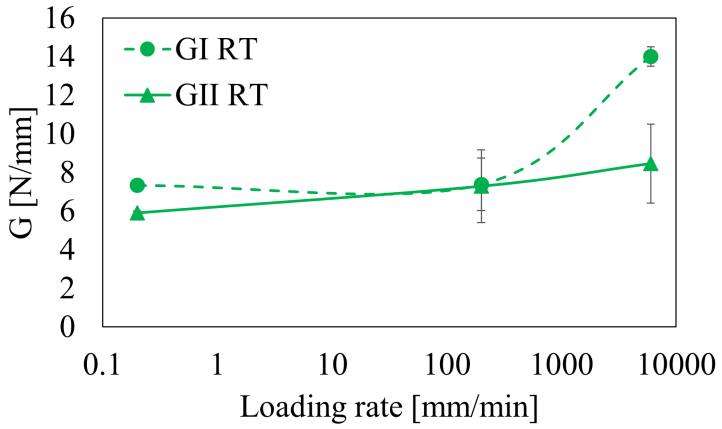


Figure 4.12: Fracture energy as a function of loading rate for adhesive C, mixed mode.

For adhesive C, all fracture specimens exhibited cohesive failure within the adhesive. Additionally, with an increase in loading rate, the specimens displayed a fracture surface that had a more uniform distribution of adhesive between the two substrates, as exhibited in Figure 4.13.

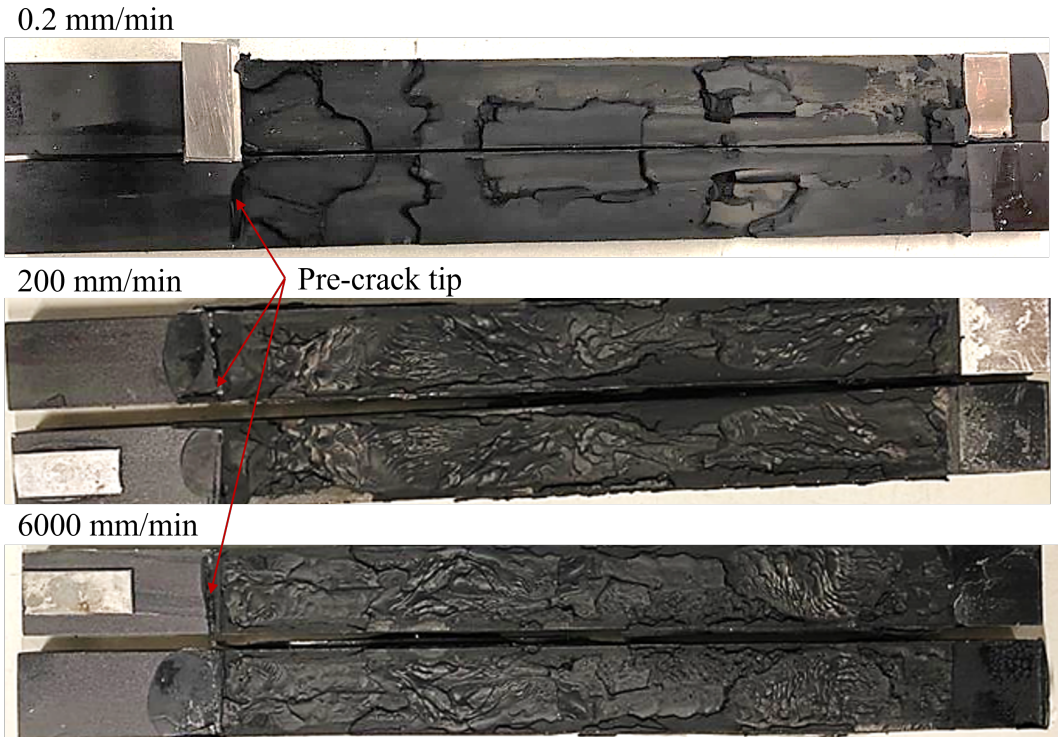


Figure 4.13: Fracture surface of adhesive C after testing at 23 ºC for different loading rates under pure mode I.

In pure mode I (see Figure 4.14), for loading rates between 200 and 6000 mm/min, G_{IC} increases more significantly at 23 ºC, and at 60 ºC a plateau seems to form, where the adhesive becomes less sensitive to loading rates. As a result, there is ongoing development of strain rate insensitivity at elevated temperatures.

Considering that both 23°C and 60°C cover a significant range of the adhesive's T_g, it appears that adhesive C is relatively unaffected by temperature under quasi-static conditions in pure mode I, as shown in Figure 4.14. However, in the case of ISR and HSR, elevating the temperature actually enhances the G_{IC}, resulting in this adhesive being more appropriate for high-temperature applications when loaded in pure mode I, in contrast to adhesives A and B.

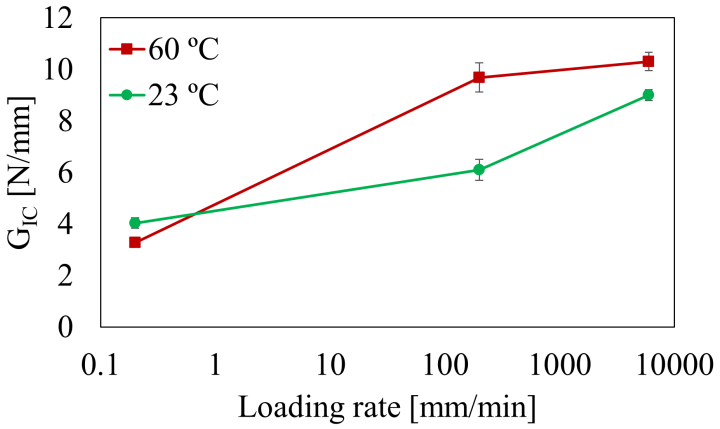


Figure 4.14: Effects of loading rate on the fracture energy in mode I - adhesive C

However, upon analysing the fracture energy outcomes for a loading rate of 0.2 mm/min in mixed mode (refer to Figure 4.15), G_I exhibited less sensitivity to temperature than mode II. In Figure 4.11, it can be observed that at 0.2 mm/min and higher temperatures, the curve shifted significantly to the right and displayed increased mode II values. Yet, it should be noted that further experimentation is needed to support this observation since only one result for mixed mode is available at this quasi-static, high-temperature condition. Additional results could alter the curve behaviour.

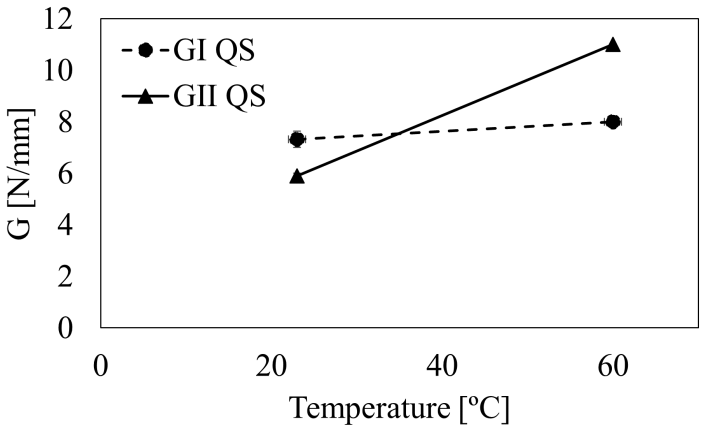


Figure 4.15: Fracture energy as a function of temperature for adhesive C, mixed mode.

Based on the findings, the adhesive's performance was optimal when subjected to elevated loading rates of 6000 mm/min at room temperature, resulting in a G_I of about 14 N/mm and a G_{II} of approximately 8.45 N/mm. However, based on the results of the mode I fracture test and the observed increase in fracture energy under mixed mode with rising temperature, it is highly probable that adhesive C will yield superior outcomes under greater strain rates at 60 ºC.

A comparison of the fracture energy in pure mode I between all adhesives for all tested loading rates is established in Figure 4.16. The results show that adhesive B has a linear increase in fracture energy with increasing loading rate, at both room and high temperatures, on a logarithmic scale. Conversely, adhesives A and B experience degradation in fracture energy with temperature increase whereas adhesive C displays an increase in resistance to crack propagation. This could be elucidated by the proportion of polyol and isocyanate segments in the composition of each adhesive. If additional segments of every group are connected together, more urethane groups will be formed. This, in turn, increases cross-linking density, resulting in greater resistance to temperature [**?**].

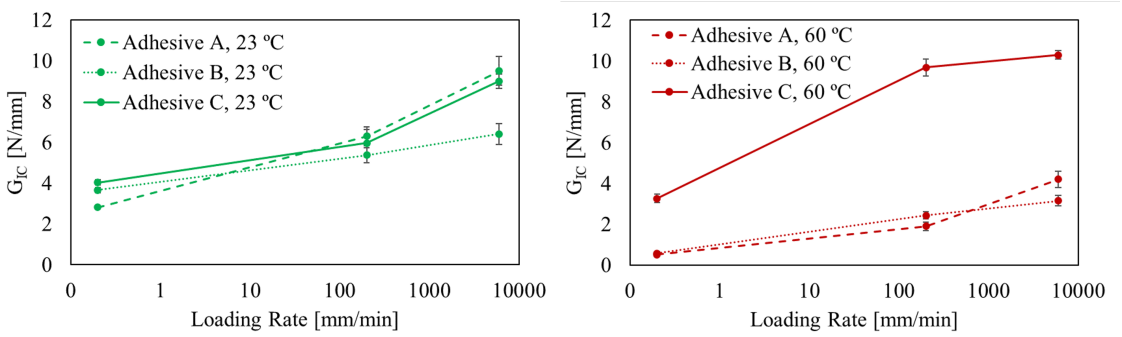


Figure 4.16: Fracture energy as a function of loading rate in mode I, comparison between adhesives A, B and C.

4.3 Strain rate study in DCB joints

Studying the variation of strain rate during material testing is essential to understand the behaviour of adhesives under diverse conditions, including a wide range of strain rates and temperatures. These data are fundamental parameters for ensuring structural safety, as adhesives must have the capability to withstand different loading conditions, exhibit deformation while maintaining structural integrity, and effectively transmit loads without compromising the joint's integrity. The influence of strain rate on material behaviour is of paramount significance, as it may vary across small or large scales, impacting the determination of critical fracture energy values.

The conditions tested in the mode I fracture test are outlined in Table 4.1.

The figures that follow present the objective data from the strain rate analysis conducted for all tested conditions. The graphs depict the evolution of strain and strain rate over time at different points of overlap, providing insight into the varying parameters of the bond line. During each test, the crack size was determined for both adhesives using the CBBM data reduction method. An additional analysis of the crack tip position was conducted using DIC to attain a more precise location.

Table 4.1: Strain rate analysis, testing conditions.

Testing Conditions		**Room Temperature, 23 ºC**		**Low Temperature, -30 ºC**
Adhesive	**Thickness**	0.2 mm/min	200 mm/min	200 mm/min
Adhesive A	4 mm	X	X	X
	0.5 mm		X	
Adhesive C	2 mm	X	X	X

As the distance between the substrates increases, there is a corresponding increase in strain at each point of overlap. Experimental results for adhesives A and C, subjected to quasi-static testing at ambient conditions of 23°C, are illustrated in Figure 4.17 and Figure 4.18. It is evident that adhesive A displays strain and strain rate measurements that are approximately half those observed for adhesive C.

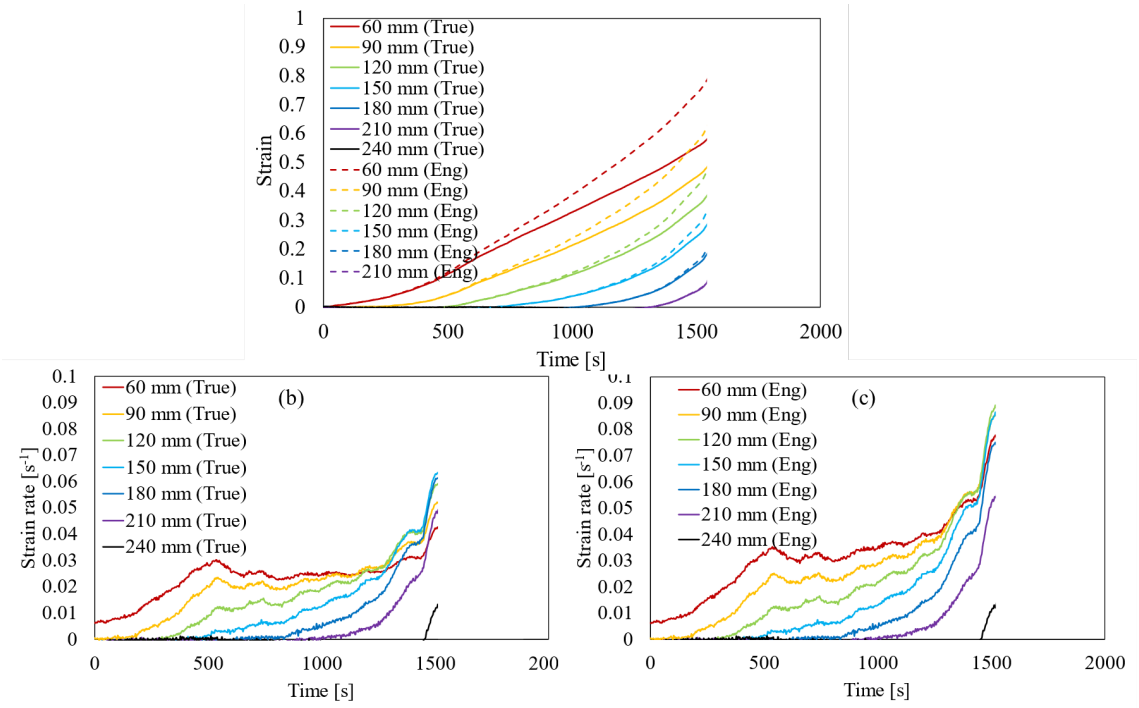


Figure 4.17: True and engineering strains and strain rates over time for various points across the overlap (adhesive A under quasi-static conditions at 23 °C): (a) strain values as a function of time (b) true strain rate as a function of time (c) engineering strain rate as a function of time.

Considering the data presented in Figures 4.19 and 4.20, it is clear that the strain rate at the crack tip will exhibit a wider range of variation as the test speed increases.

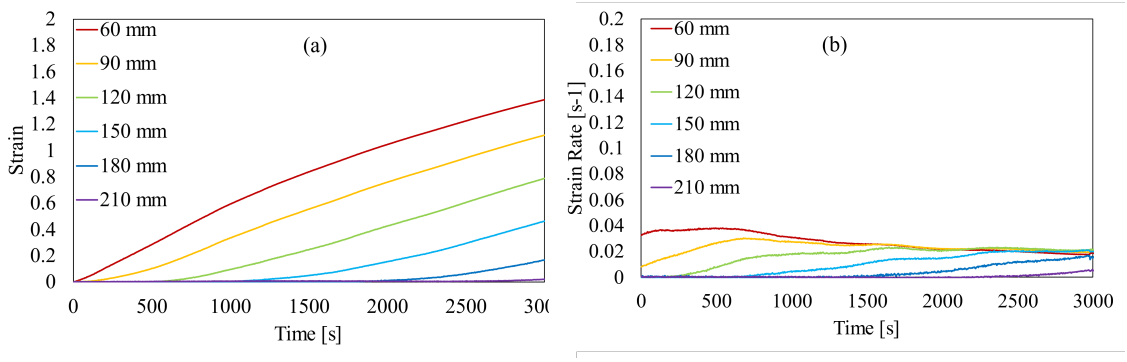


Figure 4.18: True strains and strain rates over time for various points across the overlap (adhesive C under quasi-static conditions at 23 °C): (a) strain values as a function of time (b) true strain rate as a function of time.

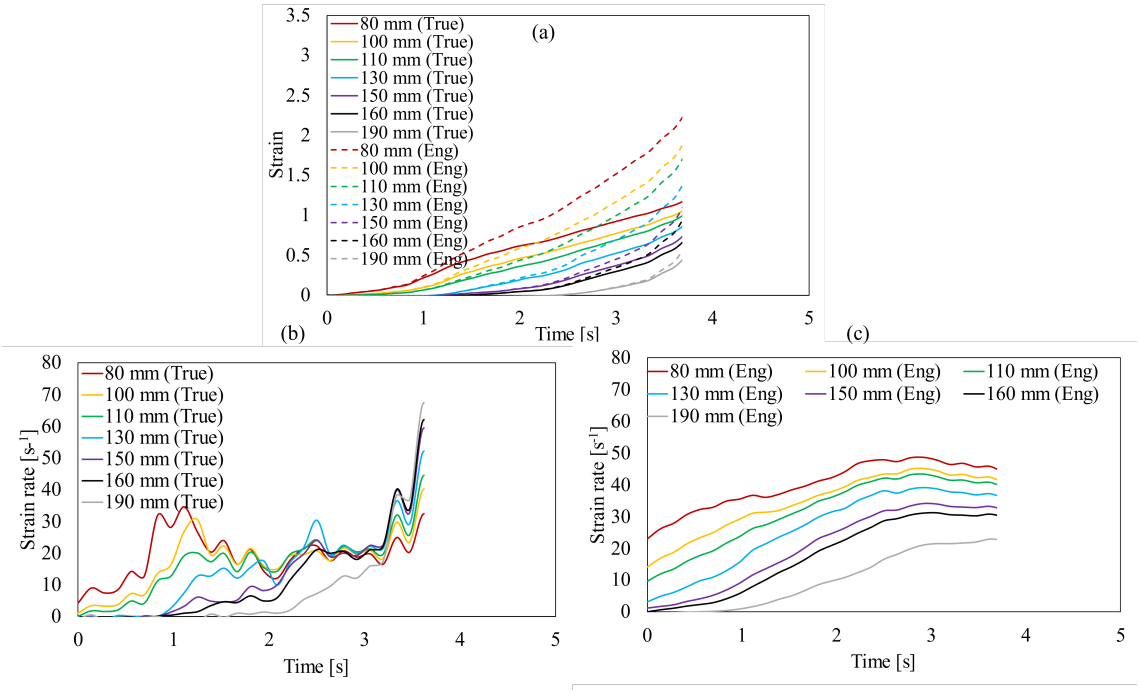


Figure 4.19: True and engineering strains and strain rates over time for various points across the overlap (adhesive A under 200 mm/min loading rate at 23°C): (a) strain values as a function of time (b) true strain rate as a function of time (c) engineering strain rate as a function of time.

At lower temperatures, the strain values causing failure decrease due to the brittle nature of the adhesive material. This brittleness causes cracks to propagate quickly, which results in a significant decrease in the duration of the testing process. When an adhesive is exposed to these conditions, particularly low temperatures and increased strain rates, energy accumulates in a limited region near the crack tip as the adhesive material has limited deformability. This stored energy is subsequently released when it reaches a critical threshold, causing an abrupt and rapid expansion of the crack, which initiates the energy release process [**?**].

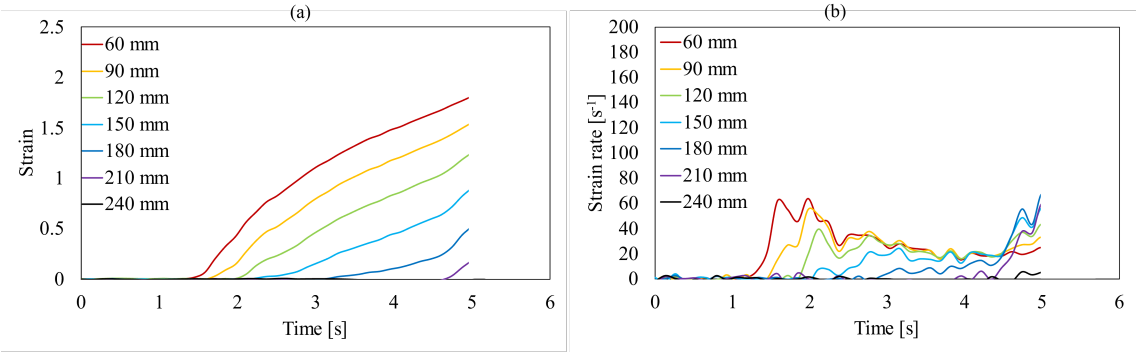


Figure 4.20: True strains and strain rates over time for various points across the overlap (adhesive C under 200 mm/min at 23 °C): (a) strain values as a function of time (b) true strain rate as a function of time.

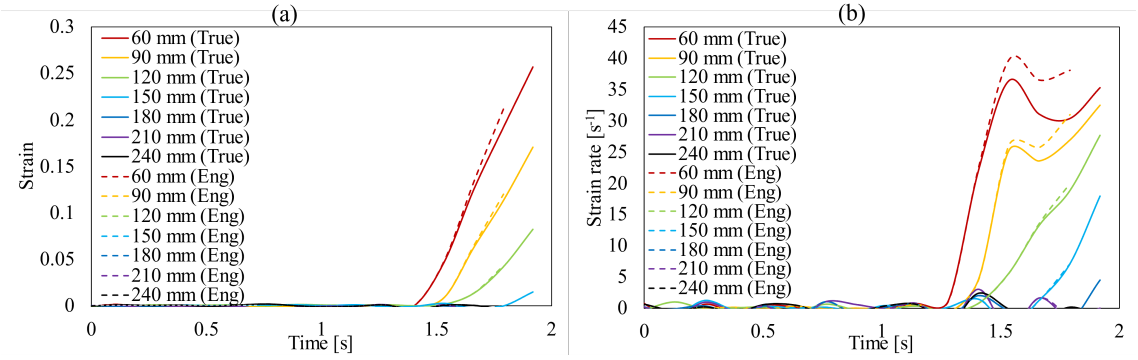


Figure 4.21: True strains and strain rates over time for various points across the overlap (adhesive A under 200 mm/min at -30 °C): (a) strain values as a function of time (b) true and engineering strain rate as a function of time.

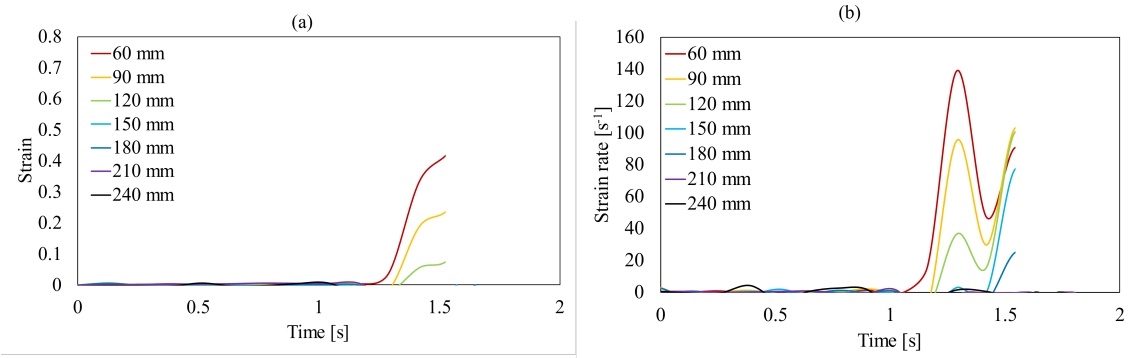


Figure 4.22: True strains and strain rates over time for various points across the overlap (adhesive C under 200 mm/min at -30 °C): (a) strain values as a function of time (b) true strain rate as a function of time.

Brittle polymers display distinct behaviour in comparison to ductile adhesives, which are characterised by more mobile polymer chains. This leads to dissimilar strain rate-dependent responses in such circumstances. Consequently, as temperature decreases, susceptibility to strain rate diminishes. At low temperatures, the joint failed abruptly. A stable crack propagation along the entire bondline was not observable.

When establishing a comparison of both the true and engineering elongation rates for all the conditions tested for adhesive A, it clearly shows significant differences, particularly where the material was more flexible. A prominent instance is the comparison between the curves for specimens tested at 200 mm/min at room and low temperatures. In low temperatures, adhesive A demonstrates less variation in both engineering and true strain rate values, compared to the values obtained from tests performed at room temperature. Furthermore, there is a greater discrepancy in values observed when comparing tests conducted at higher loading rates and quasi-static condition but at the same test temperature.

4.3.1 Effect of adhesive thickness on strain rate and fracture energy

Different studies have shown that plastic deformation occurs throughout the depth of the adhesive and that the energy dissipation is directly proportional to the thickness of the adhesive layer [**?**]. Therefore, a research study was conducted to investigate the effect of adhesive thickness on the range of strain rates of adhesive A. In this study, two DCB joints with different thicknesses (4 mm and 0.5 mm) were subjected to a loading rate of 200 mm/min and tested at a temperature of 23 ºC.

Figure 4.23 shows the variation of fracture energy with thickness for adhesive A. The results illustrate an increase in fracture energy of approximately 31.25% with increasing thickness. It has been observed that when the adhesive is capable of plastic deformation, a plastic zone forms before the crack tip, resulting in a damaged zone [**?**]. It has been demonstrated by Kinloch and Shaw [**?**] that the adhesive fracture toughness is linked to the dimensions of the plastic zone, and the constraining influences from the dual adherents regulate the plastic zone dimensions. Therefore, this study explains the rise in adhesive fracture toughness due to the adhesive having the ability to create bigger plastic zones before fracture occurs, as the adhesive layer becomes thicker. As a result, plasticity extends throughout the entire adhesive thickness.

In Figure 4.24 it is apparent that during the initial stage of the test, both the specimen with 4 mm adhesive thickness and the specimen with 0.5 mm have consistent and similar crack propagation rates. However, towards the end of the test just before complete failure, there is a sudden and significant increase in crack size for the specimen with a thicker bondline. The cause of this may be attributed to the sudden reduction in load and the coalescence of the crack.

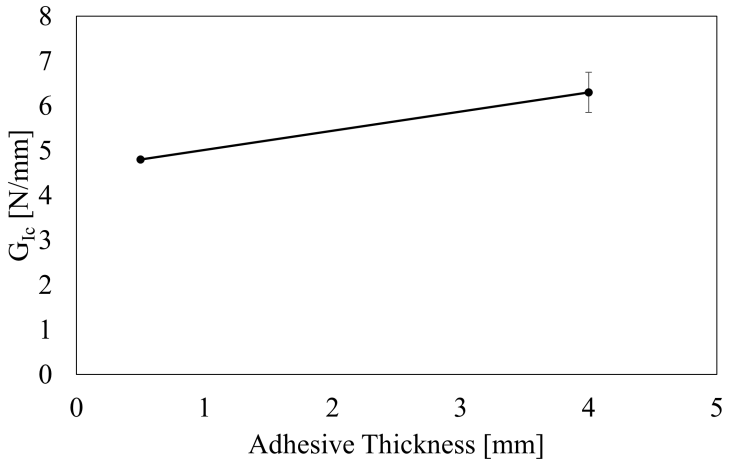


Figure 4.23: Fracture energy as a function of thickness of adhesive A.

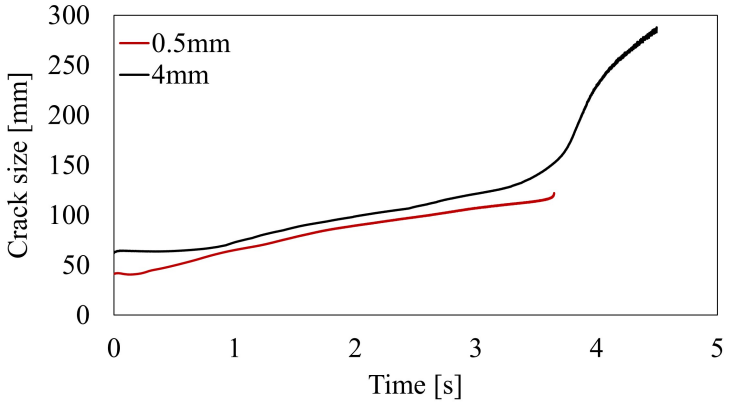


Figure 4.24: Crack size as a function of time of adhesive A, different thicknesses.

The decrease in thickness by a factor of 8 resulted in a rise in strain rate for the equivalent test speed, albeit not to the same degree as demonstrated in Figure 4.25. The strain rate values for the broader bondline range between 10 to 30 s^{-1}, whereas for the 0.5 mm adhesive layer, they range between 40 and 120 s^{-1}. When designing a joint, it is essential to consider the thickness of the adhesive layer as the range of strain rate variation increases with a thinner layer. Despite this, it is worth noting that thin joints have a significant strain rate variation at the crack tip, particularly when exposed to higher loading rates.

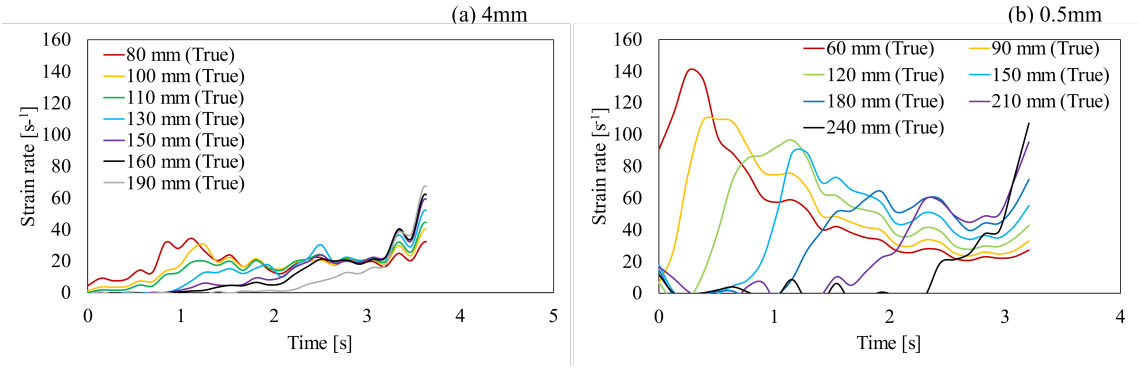


Figure 4.25: Investigation into the influence of thickness on the strain rate of adhesive A under testing Conditions of 200 mm/min at a temperature of 23 ℃: (a) Utilizing an adhesive thickness of 4 mm, (b) employing an adhesive thickness of 0.5 mm."

For more comprehensive details, reference should be made to the attached paper B.

Chapter 5

Summary of the appended documents

5.1 Paper A

From High Strain Rates to Elevated Temperatures: Investigating Mixed-Mode Fracture Behaviour in a Polyurethane Adhesive

---

This article primarily focuses on the study of how certain factors, such as loading rate and temperature, influence the final performance of the adhesive. To understand the impact of these parameters on the fracture energy of the polyurethane adhesive studied, mixed-mode bending tests were performed. The specimens were subjected to different loading rates (0.2 mm/min, 200 mm/min, and 6000 mm/min). The test temperatures ranged from -30 to 60 °C. The data reduction approach implemented in this study was a compliance-based beam method. By analysing and studying the variations in the adhesives' properties under different conditions, a deeper understanding of the effect of temperature and strain rate was developed.

5.2 Paper B

Exploring strain rate variation in the adhesive layer during constant speed mode I fracture tests: loading speed and test temperature effects

---

This paper aims to comprehend the strain rate sensitivity of the fracture energy, as opposed to the loading rate sensitivity of two different polyurethane adhesives subjected to mode I loading conditions. The study experimentally examines strain rate variations under constant loading rates and investigates how test speed affects the strain rate in mode I fracture tests. The impact of testing temperature on the strain rate is also explored by performing tests at -30 ºC and 23 ºC. Digital image correlation (DIC) and tracking methods are employed to improve the understanding of strain rate characteristics in these tests. To analyse the effect of loading rate on strain rate, the tests were conducted at different speeds as well. The influence of adhesive thickness on the strain rate has been also explored. It was experimentally found that the strain rate at the crack tip will vary even at a constant loading rate. The variation in strain rate is mainly evident in tests performed at higher loading rates, where the strain rate range increased. The tests performed at low temperatures revealed less variation of strain rate (adhesive A varied between 14-26 s^{-1} and adhesive C kept an approximate value of 21 s^{-1}) than the ones tested under the same loading rate condition at 23 ºC (adhesive A varied between 11-30 s^{-1} and adhesive C kept an approximate value of 20-55 s^{-1}. For the same adhesive, thicker bondlines are less likely to cause a substantial error in fracture energy results than thinner bondlines.

Chapter 6

Conclusion

The investigation into how loading rate and temperature impact the mode I and mixed mode fracture behaviour of three polyurethane adhesives has offered valuable insight into the mechanical characteristics and response of adhesives in various loading conditions and service temperatures. It has aided in deepening the comprehension of how the strain rate fluctuates along the overlap during the fracture test, across various testing scenarios and thicknesses. The investigation examined three loading rates (0.2 mm/min, 200 mm/min and 6000 mm/min) and three separate temperatures (-30 ºC, 23 ºC, 60 ºC) under mixed mode loading conditions. Also, the study evaluated the true and engineering strain rates for mode I for two polyurethane adhesives (adhesives A and C) under two loading rates (0.2 mm/min and 200 mm/min) at two temperatures (-30°C and 23°C).

Based on the research conducted and the obtained results, several key conclusions can be drawn. With regard to the effect of temperature and loading rate on adhesives' properties:

- For Mode I and Mixed Mode, the critical strain energy release rate is considerably impacted by the operating temperature. Additionally, the loading rate is a significant determinant of this parameter, with its effect varying depending on the temperature at which the sample is exposed;

- Furthermore, it was found that the maximum load the specimen can bear increases with the rising loading rate, but this effect is mainly seen at temperatures above T_g.

- As far as mode I is concerned, adhesive A behaves more stiff and brittle at low temperatures compared to the results of the sample tested at 23ºC. However, adhesive C maintains its rigidity and somewhat of its pliability since the temperature at which it was tested, -30ºC, still exceeds the adhesive's T_g, unlike adhesive A. At temperatures exceeding T_g, adhesives A and B experienced a decline in fracture energy, yet exhibited comparable behaviour in response to an increase in G_{IC} regardless of the test temperature. Conversely, the fracture energy of adhesive C rose with elevated testing temperatures. When designing joints that will operate in extreme temperatures, it is important to select an adhesive that is appropriate

for the application. Therefore, the use of polyurethanes with high ratios of polyol and isocyanate should be considered for extreme temperatures, as they offer superior temperature resistance.

- Both strain rate and temperature exert comparable influences on the mixed mode, encompassing mode I and mode II. However, it appears that mode I is more sensitive to these effects overall.

- In summary, all three adhesives displayed their maximum mixed mode performance under comparable conditions, featured by high loading rates (6000 mm/min) and normal room temperature. Under these conditions, adhesive A exhibited its peak performance with a G_I of around 13 N/mm and a G_{II} of approximately 7 N/mm. Adhesive B had its best performance, yielding a G_I of roughly 12.3 N/mm and a G_{II} of about 9.5 N/mm. Similarly, Adhesive C excelled, achieving a G_I of roughly 14 N/mm and a G_{II} of approximately 8.45 N/mm. Nevertheless, adhesive C excelled over the other options in relation to fracture energy, with a higher G_I and a similar G_{II} value, rendering it the preferable selection in the specified conditions.

With regards to the analysis of strain rate, it can be concluded that:

- Adhesive A exhibits more sensitivity to load rate and temperature fluctuations compared to adhesive C. Furthermore, adhesive A demonstrated a larger fracture process zone than adhesive C, indicating that a greater fracture process zone is more susceptible to strain rate.

- Even when a constant loading rate is maintained during testing, there are variations in strain rate, indicating that it is not consistent throughout the test process. Also, adjusting the speed of the test between two tests does not yield a variation in the strain rate values of the same magnitude. These points highlight the need to maintain consistent strain rate control during testing.

- The strain rate variation under a given condition increases with the loading rate, indicating its significance, particularly at high test speeds. However, the strain rate remains largely stable at low temperatures. Therefore, when designing adhesive joints for a specific feature, considering the impact of these factors is crucial. For instance, the fracture energy relies on load and displacement and, hence, on strain. Therefore, it is crucial to consider these phenomena when designing adhesive joints that are effective. As most applications, particularly within the automotive industry, encounter high loading rates, there is a significant variation in strain rates, making it challenging to forecast the mandatory energy for an existing crack to disseminate.

- In situations where the adhesive becomes more flexible, the true and engineering strain rates will differ more. The best agreement between both strain rates was observed at low temperatures.

- The decrease in thickness did not demonstrate the anticipated correlation in strain rate measurements. The strain rate values have increased for thinner bond lines. However, the size of the fracture process zone has reduced, thereby leading to a decrease in the fracture energy of the adhesive.

Chapter 7

Future work

Given that car crashes involve impact speeds higher than those tested in this study, it would be worthwhile to analyse the behaviour of the tested adhesives at increased test speeds and evaluate the impact of temperature.

Additionally, characterizing the behaviour of adhesive C under varying loading rates at temperatures below its T_g would help elucidate its performance in a more brittle state.

Furthermore, investigating the impact of quasi-static rates at -30 ºC on strain rate for both adhesives could yield valuable information, for a better comparison of the fracture energy as a function of strain rates for different temperatures.

In order to evaluate the behaviour of these adhesives numerically, it could be worthwhile to develop a numerical model suitable for these adhesives, after which it could be possible to compare the numerical and experimental results for the way strain rate varies along the overlap.

References

[1] Adams R. D. Da Silva, L. F. Joint strength predictions for adhesive joints to be used over a wide temperature range. *International Journal of Adhesion Adhesives*, pages 362–379, 2007.

[2] Marques E. A. S. da Silva L. F. Machado, J. J. M. Adhesives and adhesive joints under impact loadings: An overview. *The Journal of Adhesion*, pages 421–452, 2018.

[3] Costa M. Banea M. D. Da Silva L. F. M. Viana, G. M. S. O. A review on the temperature and moisture degradation of adhesive joints. *Journal of Materials: Design and Applications*, pages 488–501, 2017.

[4] Öchsner A. Adams R. D. Da Silva, L. F. *Handbook of Adhesion Technology*. Springer Science Business Media, 2011.

[5] da Silva L. F. Carbas R. Campilho R. D. Banea, M. D. Effect of material on the mechanical behaviour of adhesive joints for the automotive industry. *Journal of adhesion science and Technology*, pages 663–676, 2017.

[6] Borges C. S. Marques E. A. Carbas R. J. Akhavan-Safar A. Antunes D. P. Lopes A. M. da Silva L. F. Nunes, P. D. Numerical assessment of strain rate in an adhesive layer throughout double cantilever beam and end notch flexure tests. *Journal of Process Mechanical Engineering*, pages 415–425, 2020.

[7] M. J. Troughton. *Handbook of plastics joining: a practical guide*. William Andrew, 2008.

[8] A. J. Kinloch. *Adhesion and adhesives: science and technology*. Springer Science Business Media, 1987.

[9] E. M. Petrie. *Handbook of Adhesives and Sealants*. McGraw-Hill, 2007.

[10] Akhavan-Safar A. Carbas R. J. C. Marques E. A. S.-Goyal R. da Silva L. F. M. Antelo, J. Replacing welding with adhesive bonding: an industrial case study. *International Journal of Adhesion and Adhesives*, 13, 2022.

[11] Mittal K. L. Pizzi, A. *Handbook of Adhesive Technology (Second Edition)*. CRC Press, 2017.

[12] Landrock A. H. Ebnesajjad, S. *Adhesives Technology Handbook*. William Andrew Publishing, 2014.

[13] I. R. Clemitson. *Polyurethane casting primer*. CRC Press, 2011.

[14] J. Shields. *Adhesives Handbook*. Elsevier, 2013.

[15] C. A. Harper. *Handbook of Plastics, Elastomers, and Composites*. McGraw-Hill Education, 2002.

[16] Shimamoto K. Akiyama H. Sato C. Houjou, K. Effect of test temperature on the shear and fatigue strengths of epoxy adhesive joints. *The Journal of Adhesion*, page 2599–2617, 2022.

[17] Alfano G. Škec, L. Experimental and numerical study of rate-dependent mode-i failure of a structural adhesive. *The Journal of Adhesion*, page 1323–1355, 2023.

[18] Nunes P. D. P. Akhavan A. Marques E. A. S. Carbas R. J. C. Alfonso L. Silva L. F. M. Borges, C. S. P. Influence of mode mixity and loading rate on the fracture behaviour of crash-resistant adhesives. *Theoretical and Applied Fracture Mechanics*, 2020.

[19] Hui D. Yuan G. Lair J. Lau K. T. Xu F. Jia, Z. Mechanical properties of an epoxy-based adhesive under high strain rate loadings at low temperature environment. *Composites PartB*, pages 132–137, 2016.

[20] Hayashi A. Nunes P. D. P. Marques E. A. S. Carbas R. J. C. Sato C. Da Silva L. F. M. Machado, J. J. M. Strain rate dependence of a crash resistant adhesive as a function of temperature for the automotive industry. *Journal of Materials: Design and Applications*, pages 2189–2203, 2019.

[21] Googarchin H. S. Akhavan-Safar A. da Silva L. F. M. Bidadi, J. Loading rate effects on mixed-mode i/ii fracture envelope of epoxy resins with nonlinearbehavior. *Theoretical and Applied Fracture Mechanics*, 2023.

[22] Marques E. A. S. Carbas R. J. C. Akhavan-Safar A. Da Silva L. F. M. Nunes, P. D. P. Dcb tests at constant strain rate using crash-resistant epoxy adhesives: A numerical and experimental approach. *Journal of Automobile Engineering*, pages 3234–3242, 201.

[23] S. Hartshorn. 1986.

[24] W. C. Wake. Theories of adhesion and uses of adhesives: a review. *Polymer*, 1978.

[25] Machado J. Carbas R. Costa M. Da Silva L. F. M.-Vaz M. Banea M. D. Viana, G. Strain rate dependence of adhesive joints for the automotive industry at low and high temperatures. *Journal of Adhesion Science and Technology*, pages 2162–2179, 2018.

[26] Yuan G. Hui D. Feng X. Zou Y. Jia, Z. Effect of high loading rate and low temperature on mode i fracture toughness. *Theoretical and Applied Fracture Mechanics*, pages 79–92, 2019.

[27] Yuan G. Hui D. Feng X. Zou Y. Jia, Z. Effect of high strain rate and low temperature on mode ii fracture toughness. *International Journal of Adhesion and Adhesives*, pages 105–112, 2018.

[28] Marques E. A. S. da Silva L. F. Machado, J. J. M. Adhesives and adhesive joints under impact loadings: An overview. *The Journal of Adhesion*, 2018.

[29] Hayashi A. Sato C. Sekiguchi, Y. Analytical determination of adhesive layer deformation for adhesively bonded double cantilever beam test considering elastic–plastic deformation. *The Journal of Adhesion*, 2020.

[30] Ting R. Y. Moulton R. J. Riew C. K. Siebert A. R. Bascom, W. D. The fracture of an epoxy polymer containing elastomeric modifiers. *Journal of Materials Science*, 1981.

[31] Rushford J. L. Rose W. S. Hunston D. L. Riew C. K. Bitner, J. L. Viscoelastic fracture of structural adhesives. *The Journal of Adhesion*, 2006.

[32] Bullman G. W. Hunston, D. L. Viscoelastic fracture behaviour for different rubber-modified epoxy adhesive formulations. *Int J Adhes Adhes*, 1985.

[33] Grapotte D. Cayssials F. Lataillade, J. L. The impact resistance of ctbn- modified epoxy adhesive joints. *Journal de Physique IV Colloque*, 1994.

[34] Anders Biel. Constitutive behaviour and fracture toughness of an adhesive layer, 2005.

[35] Kapania R. K. Johnson E. R. Dillard D. A. Jacob G. C. Starbuck J. M. Makhecha, D. P. Rate-dependent cohesive zone modeling of unstable crack growth in an epoxy adhesive. *Mechanics of Advanced Materials and Structures*, 2009.

[36] He J. Hunston D. Hoffman D. Raghavan, D. Strain rate dependence of fracture in a rubber-toughened epoxy system. *The Journal of Adhesion*, 2010.

[37] Hesebeck O. Brede M. Kleiner F. Marzi, S. A rate-dependent cohesive zone model for adhesively bonded joints loaded in mode i. *Journal of Adhesion Science and Technology*, 2009.

[38] Blackman B. R. K. Cooper V. Kinloch A. J. Sanchez S. R. Teo W. S. Ivankovic A. Karac, A. Modelling the fracture behaviour of adhesively-bonded joints as a function of test rate. *Engineering Fracture Mechanics*, 2011.

[39] S. Marzi. Measuring the critical energy release rate in mode ii of tough, structural adhesive joints using the tapered end-notched flexure (tenf) test. *The European Physical Journal Special Topics*, 2012.

[40] Alfredsson K. S. Stigh U. Leffler, K. Shear behaviour of adhesive layers. *International Journal of Solids and Structures*, 2007.

[41] Yuan G. Feng X. Zou Y. Jia, Z. Numerical study on the mechanical behavior of a polyurethane adhesive under high strain rate. *Composites Part B: Engineering*, 2019.

[42] Dillard D. A. Blackman B. Adams R. D. Da Silva, L. F. *Testing Adhesive Joints: Best Practices*. John Wiley Sons, 2012.

[43] Bs 2782-0:2011 methods of testing plastics. introduction. Standard, 2011.

[44] Adhesives — determination of shear behaviour of structural adhesives — part 2: Tensile test method using thick adherends. Standard, 2019.

[45] Bu H. Ma W. Zhang P. Zhan X. Wang, F. Influence of the different surface treatments on fracture property of cfrp adhesive joint. *Journal of Adhesion Science and Technology*, pages 961–975, 2022.

[46] Sekiguchi Y. Shimamoto K. Akiyama H. Sato C. Houjou, K. Energy release rate and crack propagation rate behaviour of moisture-deteriorated epoxy adhesives through the double cantilever beam method. *The Journal of Adhesion*, pages 1016–1030, 2023.

[47] Xian G. Wang, W. Effects of steel surface treatment with silanized carbon nanotubes on the bonding properties between steel and epoxy adhesive. *The Journal of Adhesion*, pages 297–319, 2023.

[48] Diogo Rafael Coelho Oliveira de Andrade Santos. Characterization of the fatigue threshold of structural adhesives for automotive applications. Technical report, Faculdade de Engenharia da Universidade do Porto, 2022.

[49] Filipe José Palhares Chaves. Fracture mechanics applied to the design of adhesively bonded joints. Technical report, Faculdade de Engenharia da Universidade do Porto, 2013.

[50] Carbas R. Marques E. Viana G. Da Silva L. F. M. Costa, M. An apparatus for mixed mode fracture characterization of adhesive joints. *Theoretical and Applied Fracture Mechanics*, pages 94–102, 2017.

[51] Campilho R. D. S. G. Gonçalves J. P. M. De Moura, M. F. S. F. Crack equivalent concept applied to the fracture characterization of bonded joints under pure mode i loading. *Composites Science and Technology*, page 2224–2230, 2008.

[52] L. F. M. Da Silva. *Modeling of Adhesively Bonded Joints*. Springer Berlin, 2008.

[53] Mu W. Qin G. Tan W. Pu L. Na, J. Effect of temperature on the mechanical properties of adhesively bonded basalt frp-aluminum alloy joints in the automotive industry. *International Journal of Adhesion and Adhesives*, pages 138–148, 2018.

[54] Malvade I. Biswas P. Schroeder J. Deb, A. An experimental and analytical study of the mechanical behaviour of adhesively bonded joints for variable extension rates and temperatures. *International Journal of Adhesion and Adhesives*, pages 1–15, 2008.

[55] Akhavan-Safar A. Carbas R. J. C. Marque E. A. S. Goyal R. Jennings J. da Silva L. F. M. de Castro Lopes, F. V. B. The role of loading mode on the property degradation of adhesives at high temperatures. *Fatigue Fracture of Engineering Materials Structures*, pages 1848–1863, 2023.

[56] Xu F. Li Z. Zhang C. Feng, W. Mode fracture toughness of adhesively bonded composite joints under high loading rate conditions. *The Journal of Adhesion*, 2023.

[57] YAMAGATA Y. SATO C. SEKIGUCHI, Y. Mode i fracture energy of adhesive joints bonded with adhesiveswith different characteristics under quasi-static and impact loading. *Journal of The Adhesion Society of Japan*, 53(10):330–337, 2017.

[58] da Silva L. F. Campilho R. D. S. G. Banea, M. D. Temperature dependence of the fracture toughness of adhesively bonded joints. *Journal of Adhesion Science and Technology*, 24(11-12):2011–2026, 2010.

[59] Webster D. C. Chattopadhyay, D. K. Thermal stability and flame retardancy of polyurethanes. *Progress in Polymer Science*, 34(10):1068–1133, 2009.

[60] Akhavan-Safar A. Carbas R. J. Marques E. A. Wenig S. da Silva L. F. Perez, M. Loading rate and temperature interaction effects on the mode i fracture response of a ductile polyurethane adhesive used in the automotive industry. *Materials*, 2022.

[61] da Silva L. F. M. Campilho R. D. Banea, M. D. The effect of adhesive thickness on the mechanical behavior of a structural polyurethane adhesive. *The Journal of Adhesion*, pages 331–346, 2015.

[62] Fernlund G. Spelt J. K. Papini, M. The effect of geometry on the fracture of adhesive joints. *International Journal of Adhesion and Adhesives*, pages 5–13, 1994.

[63] Shaw S. J. Kin Loch, A. J. The fracture resistance of a toughened epoxy adhesive. *The Journal of Adhesion*, pages 59–77, 1981.

Appendix A

Paper A

polymers

MDPI

Article

From high strain rates to elevated temperatures: Investigating mixed mode fracture behaviour in a polyurethane adhesive

Maria Ribas [1], Alireza Akhavan-Safar [2,*], Nicolas Pigray [1], Ricardo J.C. Carbas [2,*], Eduardo A.S. Marques [1], Catarina S.P. Borges [1], Sabine Wenig [3] and Lucas F.M. da Silva [1]

[1] Faculdade de Engenharia, Universidade do Porto, Rua Dr. Roberto Frias, 4200-465, Porto, Portugal.
[2] Institute of Science and Innovation in Mechanical and Industrial Engineering (INEGI), Rua Dr. Roberto Frias, 4200-465 Porto, Portugal.
[3] Sika Automotive AG, Kreuzlingerstrasse 35, 8590 Romanshorn, Switzerland.
* Correspondence: Alireza Akhavan-Safar (Email: aAkhavan-Safar@inegi.up.pt), Ricardo J.C. Carbas (Email: RCarbas@fe.up.pt).

Abstract: The investigation of the behaviour of adhesive joints under high strain rates is an active area of research, primarily due to the widespread use of adhesives in various industries, including automotive manufacturing. Understanding how adhesives perform when subjected to high strain rates is crucial for designing vehicle structures. Additionally, it is particularly important to comprehend the behaviour of adhesive joints when exposed to elevated temperatures. Therefore, this study aims to analyse the impact of strain rate and temperature on the mixed mode fracture characteristics of a polyurethane adhesive. To achieve this, mixed mode bending tests were conducted on test specimens. These specimens were subjected to three different strain rates (0.2 mm/min, 200 mm/min, and 6000 mm/min) and tested at temperatures ranging from -30 °C to 60 °C. The crack size was measured using a compliance-based method during the tests. For temperatures above T_g, the maximum load supported by the specimen increases with an increasing loading rate. G_I increased by a factor of 35 for intermediate strain rate and 38 for high strain rate from low temperature (-30 °C) to room temperature (23 °C). G_{II} also increased for the same conditions by a factor of 25 and 95 times, respectively.

Keywords: Polyurethane adhesive; fracture energy; temperature; loading rate; mixed mode

Citation: Ribas, M.; Akhavan-Safar, A.; Pigray, N.; Carbas, R.J.C.; Marques, E.A.S.; Borges, C.S.P.; Wenig, S.; da Silva, L.F.M. **From high strain rates to elevated temperatures: Investigating mixed mode fracture behaviour in a polyurethane adhesive.** *Polymers* **2023**, *volume number*, x. https://doi.org/10.3390/xxxxx

Academic Editor(s):

Received: date
Revised: date
Accepted: date
Published: date



Copyright: © 2023 by the authors. Submitted for possible open access publication under the terms and conditions of the Creative Commons Attribution (CC BY) license (https://creativecommons.org/licenses/by/4.0/).

1. Introduction

Over the course of recent years, adhesive bonding has been undergoing continuous evolution and increasingly entering the industry more and more. In contrast to bonding methods such as riveting, which result in stress concentration zones adjacent to the holes, and, welding, which complicates the joining process of dissimilar materials, adhesives enable a more advantageous and uniform distribution of the stress and production of lighter structures. Adhesives have gained widespread utilization across various industrial sectors, primarily due to their numerous advantages. In the automotive industry, specifically, polyurethanes have emerged as a favoured adhesive family. This preference is attributed to the exceptional properties and high bonding strength exhibited by polyurethane adhesives. They are commonly used to bond diverse materials for structural applications that are frequently exposed to conditions favourable to material degradation and bond deterioration, such as humidity, vibrations, and temperature fluctuations, among others. These conditions may deteriorate the joint strength as shown in some researches [1].

Fracture energy is a key property of adhesives, particularly when it comes to joint design that follows the damage tolerance philosophy. Damage tolerance refers to the ability of a joint or structure to withstand and tolerate the presence of flaws or damage

without experiencing catastrophic failure. In this context, fracture energy plays a critical role. It represents the energy required to propagate a crack through an adhesive joint, and it is a measure of the adhesive's resistance to crack growth.

When designing joints based on the damage tolerance philosophy, it is essential to select adhesives with high fracture energy. Adhesives with a higher fracture energy can absorb more energy before crack propagation occurs, thereby providing greater resistance to failure. By incorporating adhesives with high fracture energy into joint designs, engineers can enhance the overall durability and reliability of structures, as these adhesives are better able to withstand the presence of cracks or flaws and prevent them from propagating further. The fracture of a component may occur under different loading conditions such as shear, tensile, and even mixed mode loading, which is the most realistic scenario since the components are constantly under numerous stresses. Consequently, the fracture toughness of the polyurethane adhesive will be influenced by its surroundings, including the strain rate and temperature it experiences. This shows the importance of improving the design and manufacture of bonded structures, so it is possible to enhance their longevity and safety.

To address the challenges related to the conditions that affect the final performance of the joint, it becomes necessary to investigate how the material itself behaves under different loading rates and environmental conditions [2]. By improving the accuracy of fracture mechanism models, it is possible to predict the behaviour of bonded structures, optimize the performance of the structures, and develop more durable adhesives.

In recent years, there has been a growing interest in understanding the mechanical behaviour of adhesive joints under different loading rates and temperatures. Several studies have explored the impact of these variables on the strength and fracture behaviour of various adhesive materials, including crash-resistant epoxy and polyurethane adhesives. Since there are a numerous study that found many adhesives to be noticeably rate dependent [3].

However, despite the number of recent studies, new trends have been set regarding strain rate and temperature effect on tensile, shear, and fracture properties. Concerning tensile/shear properties, Borges et al. [4], Jia et al. [5] and Machado et al. [6] revealed an incredibly dependent strain rate effect. Borges et al. [4] concluded that both tensile and shear strength increased with increasing loading rate, although, Jia et al. [5] found a similar type of behaviour at room temperature, the same was not so linear for other temperatures, where the stiffness of the adhesive even decreased while increasing loading rates at negative temperatures. In the study conducted by Machado et al. [6], for all displacement rates, the increase in temperature led to a decrease in tensile strength and the increase in strain rate led to an increase in tensile strength. Some authors verified if there could be any methodology that could influence the results of the tests in the study of fracture behaviour. Nunes et al. [7] studied a special test procedure where DCB tests were performed with the crack tip at a constant strain rate throughout the test, and it was revealed to be more consistent than tests performed at constant test speed, this is supported by the fact that the standard deviation of the test results decreased.

The strain rates experienced in an adhesive layer during testing using two commonly employed fracture toughness specimen configurations, DCB and ENF, were investigated by the same author. The primary goal was to comprehend the influence of adhesive properties on the progression of strain rate. The results demonstrated substantial variability in the strain rate along the bond line during DCB tests conducted at a consistent cross-head displacement rate. Specifically, the strain rate exhibited a threefold increase at the commencement of the test in comparison to its value at the end [8]. Regarding fracture behaviour, despite the few numbers of studies conducted, it remains an extensive unexplored field due to its conflicting results. Viana et al. [9] explored the strain rate dependence of a crash-resistant epoxy under low and high-temperature conditions and found out that the energy absorbed by the specimens (SLJ) under quasi-static conditions showed a decreasing trend with temperature due to the decrease of adhesive yield stress with temperature. Something similar was found by Jia et al. [10] [11], where in both cases, the critical fracture

energy in question decreased with increasing loading rate, however, in mode I, the critical energy release rate decreased with the temperature drop for the quasi-static condition while G_{IIc} decreased with increasing temperature for higher strain rates. This aspect, however, was not investigated in the study conducted by Borges et al. [12]. The aim of this study was to create a finite element model (cohesive zone model also reviewed by Tserpesa et al. [13] that accurately represents the mechanical behaviour of adhesives under mode I fracture conditions, while also taking into account the dependence of properties on strain rate. With increasing strain rates, the two adhesives studied showed an increase in ultimate stress and critical energy release rate.

Bidadi et al. [14] intended to carry out a study of the effects of loading rate more in-depth, verifying its influence in mixed mode fracture behaviour in an epoxy resin material. According to the results, fracture loads and corresponding fracture resistance values for each mode-mixity were decreased significantly by increasing the loading rate. This was reasoned by the fact that there was a reduction in the crack tip fracture process zone size in higher loading rates. But Borges et al. [4] did not verified that, in both adhesives under study, the energy release rate, for all mode mixities, increased as a function of the loading rate.

Perez et al. [15] aimed to fill the research gap on the strain rate and temperature effects of polyurethane adhesives, with results showing that increasing the loading rate significantly increased the maximum strength of DCB specimens, with the greatest sensitivity observed at room temperature.

Although there have been numerous studies investigating the effects of temperature and strain rate on adhesive behavior, the majority of these studies have focused on epoxy adhesives rather than polyurethanes. As a result, there is a noticeable research gap when it comes to understanding the behavior of polyurethane adhesives under varying temperature and strain rate conditions. Specifically, there is a lack of research on how strain rate and temperature interact with each other in mixed mode conditions for polyurethane adhesives. Mixed mode fracture, which involves a combination of different loading modes, has received less attention from researchers when considering various strain rates. This limited focus on mixed mode fracture and strain rate variations in polyurethane adhesives means that there is still much to learn about their behavior and response under different loading conditions. Taking this into account, the main aim of this work is to fulfil this research gap and understand the fracture behaviour of this polyurethane adhesive under different loading rates and temperatures. To do that, mixed mode testing was performed for three different test speeds (quasi-static 0.2 mm/min, intermediate strain rate 200 mm/min, and high strain rate 6000 mm/min) and three different temperatures (Low temperature -30 ^{o}C, room temperature with approximately 23 ^{o}C and high-temperature 60 ^{o}C).

2. Experimental details

In this work, fracture envelopes of a polyurethane adhesive were determined at three different loading rates each at three different temperatures. Any subsequent mention with the nomenclature QS, ISR and HSR, will be relative to the quasi-static condition (0.2 mm/min), intermediate strain rate (200 mm/min), and high strain rate (6000 mm/min), respectively. A loading angle (mode mixity) of 45^{o} was implemented on a mixed mode apparatus. However, at quasi static mixed mode condition for room temperature, a mode mixity of 60^{o} was also adopted, for a more precise estimation of G_{IIc} for quasi-static loading condition. The experimental details are explained in the following sections.

2.1. Materials

DCB specimens were manufactured using high strength steel (PM300) substrates. Throughout the course of this study, a ductile polyurethane-based adhesive with mechanical properties modified for industrial applications was used. The glass transition temperature, T_g, of the adhesive is -5 ^{o}C.

Detailed information regarding both the physical and mechanical properties of the adhesive is presented in Table 1.

Table 1. Physical and mechanical properties of the polyurethane adhesive at room temperature [15].

Property	Polyol	Isocyanate	Mixed
Specific gravity at 25ºC (g/cm^3)	1.57	1.22	-
Viscosity at 25ºC ($mPa.s$)	7000	20	1100
T_g (^oC)		-5	
Maximum tensile strength (MPa)		3.4 ± 0.09	
Maximum tensile strain (%)		33.4 ± 1.34	
Young's Modulus (MPa)		20.3 ± 1.23	

2.2. Specimens' geometry and manufacturing procedure

Figure 1. illustrates the specimen geometry and respective adhesive thickness (4mm).

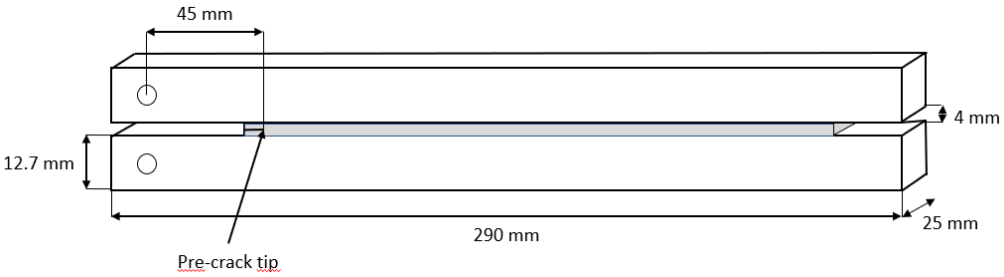


Figure 1. DCB specimen geometry

The first step of the manufacturing procedure was to sandblast the substrate surfaces. This surface treatment intends to enhance the adhesion of the adhesive to the surface, by removing the iron oxides during the sandblasting process, creating a more adhesion friendly surface and preventing the occurrence of interfacial failure [16] [17] [18].

The surface was then cleaned with acetone to remove any grease that might be on the surface. A primer (Primer-206, Sika) was then applied to improve the adhesion of the adhesive to the surface.

A typical mould for producing DCBs (Figure 2) typically comprises of top and bottom plates with holes for the guide pins that hold the DCBs in place while the adhesive is being applied. Though, to ensure that enough of the poured adhesive is retained within the joint during the curing cycle, the usual mould had to be modified by adding 3D printed pieces due to the very low viscosity of the adhesive used in this study and the very thick bond line that was required. In order to guarantee a constant pre-crack size, a razor blade was used. This was positioned so that the initial crack had a length equivalent to 45 mm, as shown in Figure 1. This sheet was also sandwiched by two steel spacers in order to make a 4 mm thickness to position the crack in the middle of the adhesive layer. Besides this spacer responsible for positioning the razor blade, a 4 mm spacer was also inserted after the adhesive layer for a better bond line thickness control.

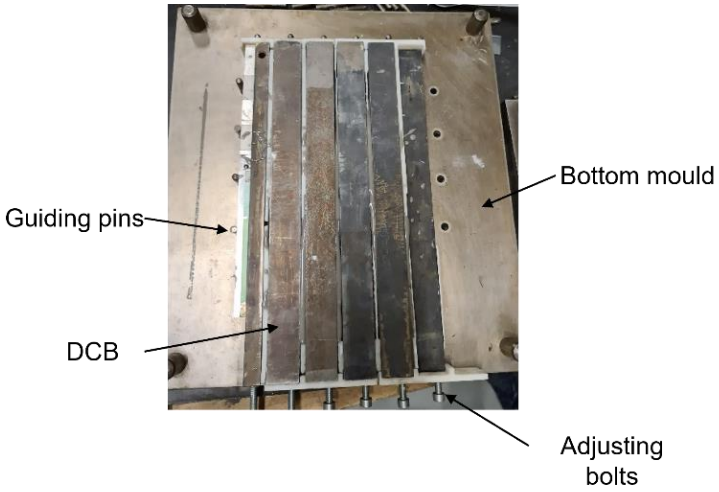


Figure 2. DCB specimens' setup, only missing the top plate.

After manufacturing, the curing process of the adhesive commences with an initial stage of 24h at room temperature. Subsequently, a post-curing process ensues, involving an additional 4h stage duration at 80 °C.

2.3. Test methods

To perform mixed-mode fracture tests, several loading rates were taken into consideration. For each loading rate, the joints were tested at various temperatures, including low temperature, room temperature, and high temperature, always under mixed-mode settings. Table 2 summarizes the test conditions considered in this study.

Table 2. Summary of test conditions.

		Temperature		
		Low Temperature -30 °C	Room Temperature 23 °C	High Temperature 60 °C
Loading Rate	Quasi-static 0.2 mm/min	Mixed mode test (45°)	Mixed mode test **(45°/60°)**	Mixed mode test (45 °)
	Intermediate Speed 200 mm/min	Mixed mode test (45 °)	Mixed mode test (45°)	Mixed mode test (45 °)
	High Speed 6000 mm/min	Mixed mode test (45 °)	Mixed mode test (45°)	Mixed mode test (45 °)

All the tests were performed using an Instron 8801 servo-hydraulic testing machines equipped with a load cell rated to ±100kN. A special, in-house-built thermal chamber was used to conduct experiments at various temperatures. To simulate the considered mixed-mode conditions, a mixed-mode apparatus was utilized. This equipment has previously undergone several validating standard fracture tests, confirming that the weight of the apparatus does not significantly affect the expected fracture energy [19]. To ensure the substrate alignment during the curing cycle, a special mould was employed during the manufacturing process. Metal spacers were also calibrated to allow a better control of the bond line thickness of the adhesive, which had 4 mm.

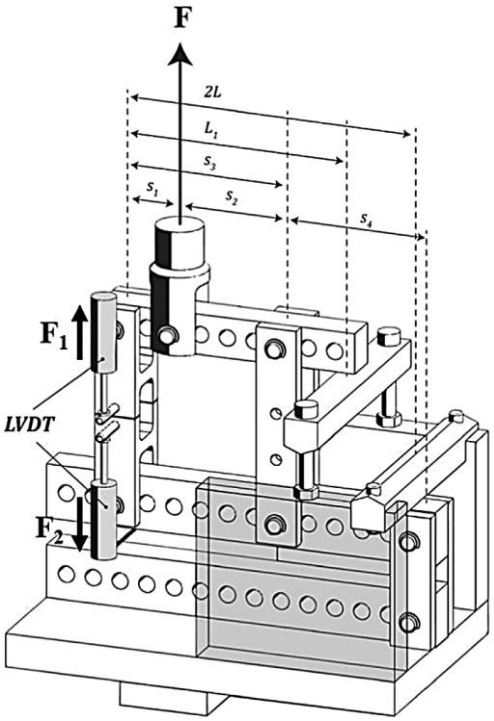


Figure 3. Schematic representation of the apparatus used for mixed mode testing [19].

Different mode mixities may be achieved for mixed-mode settings by adjusting the beam lengths (s_1 to s_4) in the mixed-mode apparatus. The forces exerted on the specimen's top (F1) and bottom (F2) arms will alter as the beam length changes.

$$F_1 = F \times \frac{s_1}{s_1} \quad (1)$$

$$F_2 = F \times \frac{s_1 s_4}{s_3 \times (s_3 + s_4)} \quad (2)$$

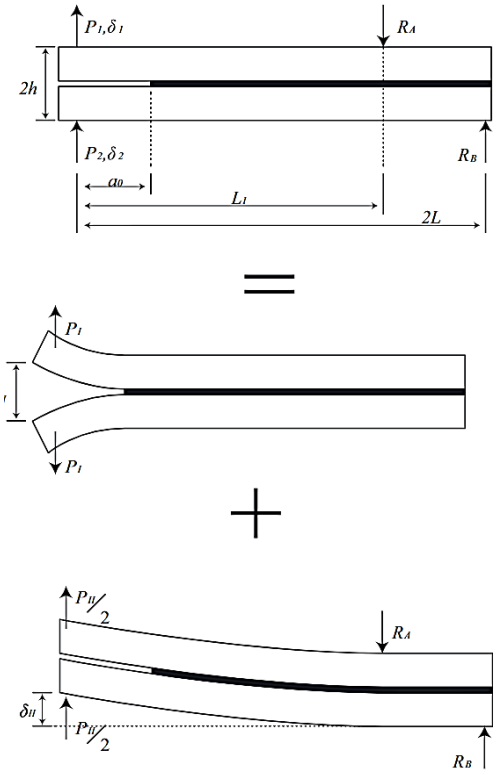


Figure 4. Mixed mode loading conditions [19].

As a result, mode I and mode II are combined in the load delivered by the machine. P_I and P_{II}, are established by

$$P_I = \frac{F_1 - F_2}{2} \tag{3}$$

$$P_{II} = F_1 + F_2 \tag{4}$$

And the mode ratio (φ) is determined as below:

$$\varphi_{apparatus} = \tan^{-1}\left\{\frac{\sqrt{3}\times\left(\frac{F_1}{F_2}+1\right)}{2\times\left(\frac{F_1}{F_2}-1\right)}\right\} \tag{5}$$

3. Data Reduction Approach

Accurate crack length measurement during fracture testing is challenging since the equipment design may limit visual monitoring and introduce additional measuring errors that may not be taken into account. During crack propagation, particularly in the case of the tested flexible polyurethane, a fracture process zone (FPZ) forms around the crack tip. This region experiences damage, leading to energy loss. When evaluating the length of the crack, it is important to consider the impacts of this FPZ and the energy dissipation caused by the damage. While using CBBM, a data reduction method based on linear elastic fracture mechanics, it is not necessary to monitor the crack length during testing, because an equivalent crack length is used, instead of the real crack length. Compliance based beam method, as the name says, is based only on the specimen compliance (C) from which the equivalent crack length can be estimated.

The fracture energy is divided into pure mode I and mode II components for mixed mode, allowing a separate application of CBBM for each mode [20].

$$C_I = \frac{8a^3}{EBh^3} + \frac{12a}{5BhG} \tag{6}$$

$$C_{II} = \frac{3a^3 + 2LL_1^2}{2EBh^3} + \frac{6LL_1}{5BhG(2L - L_1)} \tag{7}$$

where E and G are the Young's and shear moduli of the adhesive, respectively, and a is the crack length, B is the width of the joint, and h is the thickness of the specimen. L and $L1$ are defined in Figure 3. CBBM also considers the FPZ in the equivalent crack length (a_{eq}), that is possible to determine through specimen's compliance. For mode I, the formula is represented by Costa et al. [19]

$$a_{eqI} = \frac{A}{6\alpha} - \frac{2\beta}{A} \tag{8}$$

knowing that A is calculated as below:

$$A = \left(\alpha^2 + 108\alpha^2 C_I + 12\alpha^2\sqrt{\frac{3(4\beta + 27C_I\alpha)}{\alpha}}\right)^{\frac{1}{3}}, \alpha = \frac{8}{Bh^3E_f}, \beta = \frac{12}{5BhG} \tag{9}$$

For mode II, the formula is represented by the following equation [19]

$$a_{eqII} = \left[\frac{2}{3}BEh^3\left(C_{II} - \frac{6LL_1}{5BhG(2L - L_1)}\right) - \frac{2}{3}LL_1\right]^{1/3} \tag{10}$$

The fracture toughness values for each mode are then given by the following equations, considered the mode mixity relations [19].

$$G_I = \frac{9P_I^2}{B^2h}\left(\frac{a_{eqI}^2}{h^2E_{fI}} + \frac{1}{5G}\right) \tag{11}$$

$$G_{II} = \frac{9P_{II}^2 a_{eqII}^2}{16B^2E_{fII}h^3} \tag{12}$$

4. Results and Discussion

In the following discussion, all graphs and results presented are relative to tests conducted at different temperatures and loading rates, however all have the same mode mixity set to 45º.

4.1. Joint strength as a function of temperature and loading rate

In Figure 5, the behaviour of the load displacement curve when the adhesive is subjected to different temperatures, while maintaining the loading rate at 0.2 mm/min is represented.

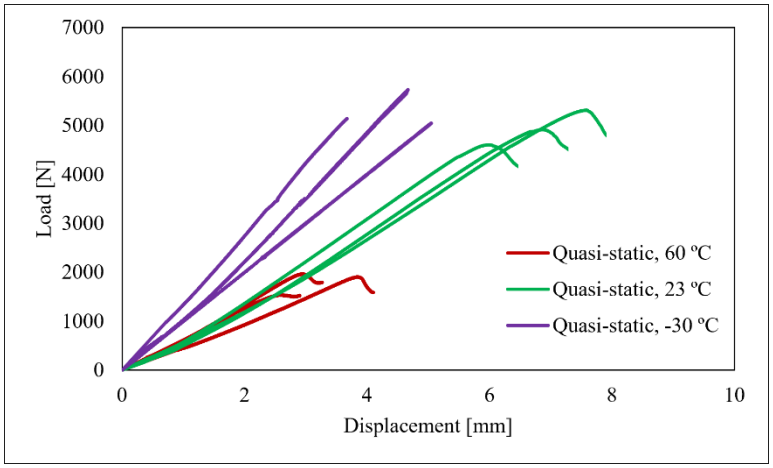


Figure 5. Load-displacement of the machine for test submitted to quasi-static condition, for a mixed mode apparatus set up at 45º.

For the temperature of -30 ºC, the adhesive shows a stiffer behaviour as indicated by the slope of the curve. This indicates that at lower temperatures, the adhesive is less flexible. This may happen as the molecular mobility decreases while transitioning from a rubbery state to a glassy state, which leads to a more compact polymer chain and subsequently a steeper slope, but still, it may maintain a high load-bearing capacity as the room temperature results, due to a window that may exist, where the adhesive does not undergo marked degradation of properties.

For temperatures above the T_g, 23 ºC and 60 ºC, both curves show similar slope, which in turn implies similar stiffness. Though, at 23 ºC, the curve has double the displacement compared to the curve at 60 ºC. This implies that the adhesive exhibits higher deformability or elongation capability at room temperature compared to higher temperatures.

Jingxin Na et. al [21] also found that the polyurethane adhesive in the study in question, maintained ductility and increased resistance at low temperatures, which led to a higher joint strength, this was due to the fact that the adhesive had a relatively low T_g. In the same study, it was found that the properties decreased with increasing temperature, such as the deformation to failure. The same was observed in Figure 5, where at 60 ºC there was a reduction of approximately 50% of deformation at failure. The greater the range between T_g. and service temperature, the greater the reduction in joint strength and properties.

D. Santos et. al [22] also also discovered significant variations in the adhesive properties depending on the test temperatures. A substantial difference was also observed between temperatures of 23 ºC and 60 ºC. Despite the adhesives exhibiting similar stiffness, the elongation of the adhesive at room temperature (23 ºC) was approximately twice as high as the results obtained at 60 ºC. This finding inherently indicates a considerable degradation of fracture properties when subjected to elevated temperatures.

Figure 6 shows the maximum load for different loading rates and temperatures. There is a clear change of the adhesive response according with the temperature and loading rate applied. By increasing the test speed from a quasi-static condition to a high strain rate, the adhesive itself was able to withstand more load for temperatures above its T_g. This may be due to the fact that when the adhesive is at temperatures below its glass transition point, the adhesive becomes more brittle, with a more solid and rigid state. At this temperature, the adhesive is more likely to crack when submitted to stress/strain, once it has less ability to dissipate energy through deformation. It is in this condition the adhesive is more sensitive to any types of defects/voids introduced during the manufacturing process.

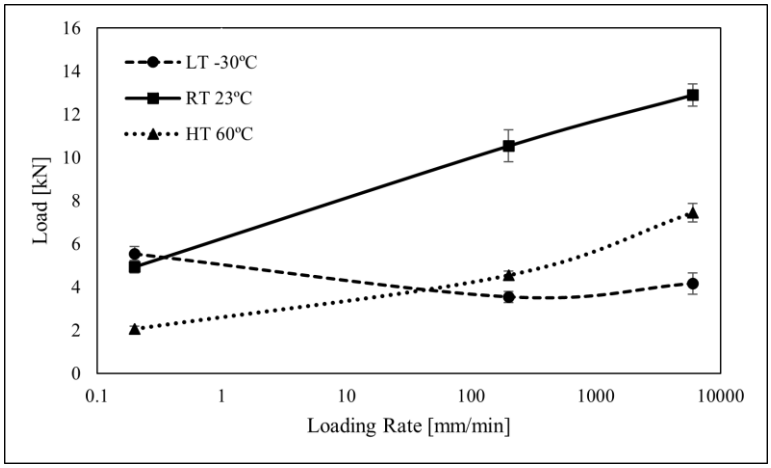


Figure 6. Maximum Load of the machine as function of Loading Rate and Temperature, for a mixed mode apparatus set up at 45º.

However, in addition to the decrease in load-bearing capacity noticeable at temperatures below T_g, which suggests that the polyurethane adhesive is negatively affected by higher strain rates at this temperature, there is also a stabilisation of the maximum load after a loading rate of 200 mm/min. It may point to a modification in the way the polyurethane adhesive deforms or a range of strain rates where its mechanical properties are less sensitive. For the adhesive under investigation, it was observed that increasing the temperature from room temperature to high temperatures did not have a substantial effect on the rate of increase in maximum load concerning strain rate. This observation is supported by the similarity in the positive slope of the curves for both room temperature and high temperature conditions as shown in Figure 5.

4.2. Effects of strain rate on mixed mode fracture energy

It should be borne in mind that fracture energy is essentially a function of the stress and displacement that the specimen has endured until failure. As a result, both factors need to be examined to fully understand how temperature and loading rate interact to affect fracture energy. The results show that a high loading rate has a significant impact on the fracture toughness of joints [23].

When analysing these results, an abrupt decrease of critical fracture energy was detected for temperature below the T_g for both mode I and mode II components of mixed mode fracture energy. It was also possible to observe a disparity between G_I and G_{II} for loading rate values higher than 200 mm/min at LT.

When the loading rate is lower than 200 mm/min, the fracture energy values are similar since the material can dissipate its energy through plastic deformation and microcrack growth in both fracture modes. However, with an increasing loading rate, the material starts to behave more rigidly and will have less time to dissipate energy, thus leading to a more brittle response. This results in a notable difference between mode I and mode II fracture since G_{II} will decrease faster, thus being more sensitive to higher strain rates at low temperatures.

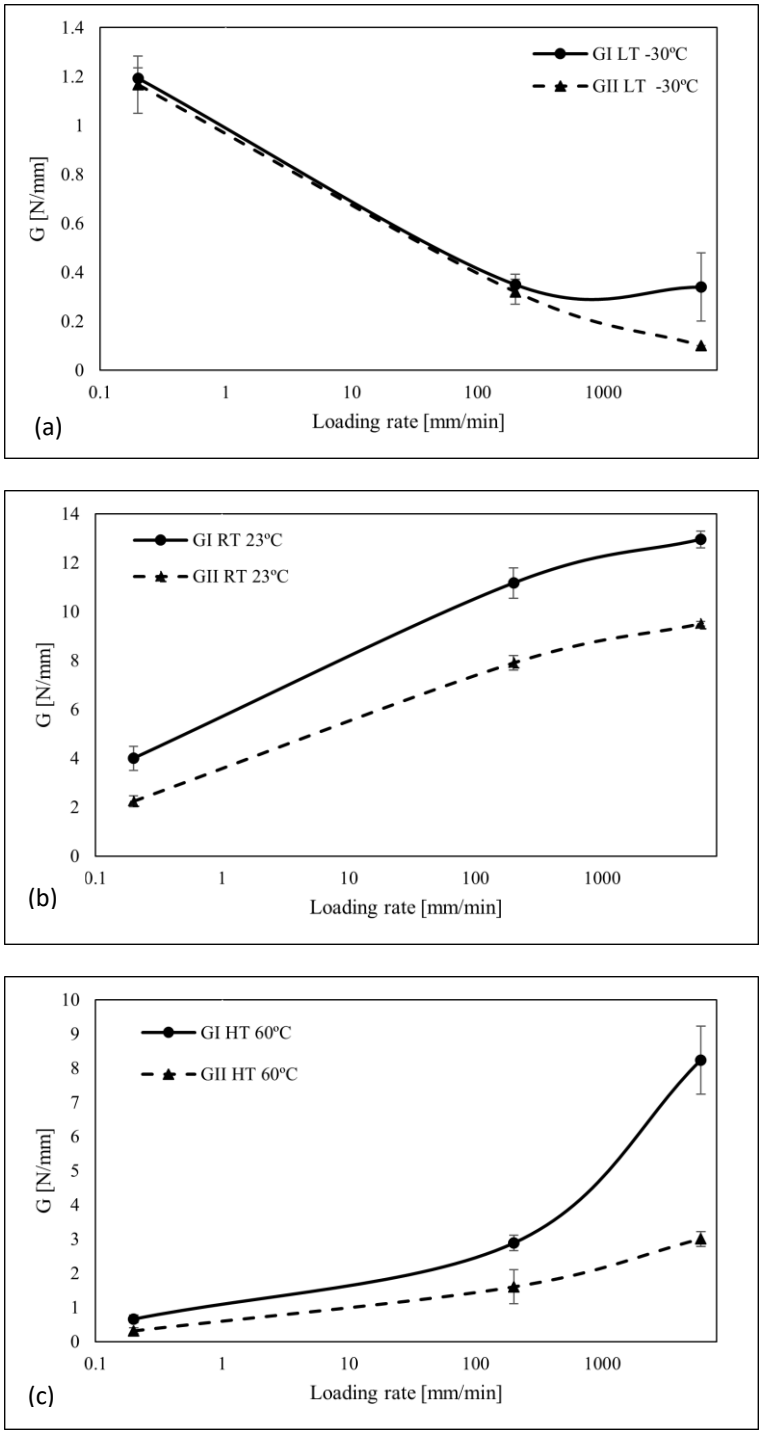


Figure 7. Critical fracture energy as function of loading rate for different temperatures: (a)Low temperature -30 ºC (b) Room Temperature 23 ºC (c) High Temperature 60 ºC, for a mixed mode apparatus set up at 45º.

On the other hand, when tested above its glass transition temperature (23 ºC and 60 ºC), both fracture energies of the adhesive increased with loading rate, except for the transition from 200 mm/min to 6000 mm/min for room temperature on mode II part of mixed mode. Once again, mode I and mode II reveal two different behaviours for high strain rates. During the test the displacement rate is controlled and the 45º phase angle used on mixed mode equipment is set on the apparatus before testing. However, as the strain rate increases, there is a clear discrepancy between the G_I and G_{II} values, as previously mentioned. It would be expected that the strain rate would be the same for both modes, but mode I is clearly growing at a faster rate, leading to the suggestion that the mode mixity is changing to pure mode I fracture behaviour. Bearing these aspects in mind, a

comparative analysis of fracture energies was conducted, with focus on the loading rate and each fracture mode. Based on Figure 8, it is evident that lower temperatures exhibit reduced sensitivity to strain rate. This phenomenon can be attributed to heightened sensitivity to strain rate resulting from temperatures surpassing the T_g, wherein the responses for mode I and mode II fractures differ.

It should be noted that in the tests conducted the displacement rate was controlled and not the strain rate. Displacement rate refers to the rate at which a material or specimen is displaced or deformed during a mechanical test, while strain rate refers to the rate at which strain develops in a material or specimen during deformation. Despite the fact that the loading rate was set to a constant value for each specimen tested, the strain rate will exhibit distinct behaviors for mode I and mode II due to disparate sensitivities associated with each mode. Further experiments and numerical analysis should be carried out to have a better understanding of this phenomenon.

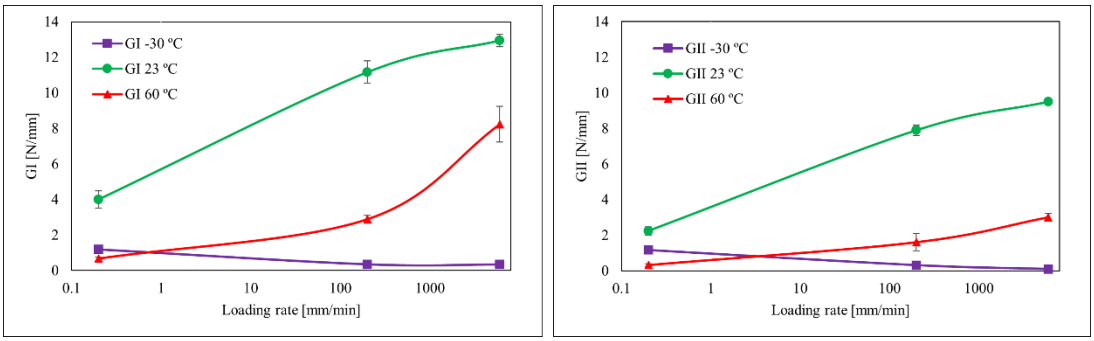


Figure 8. The effect of temperature on the fracture energy as function of loading rate for different temperatures.

For the temperature of 60 °C, the fracture energy parameters show relatively similar behaviour for strain rates lower than 200 mm/min, however, for higher strain rates, G_{II} increases about 10 times from the initial value in the quasi-static condition, while G_I increases by a factor of 12.

This may happen because, at high temperatures, the polymer chains in the PU adhesive become more "mobile", allowing a greater dissipation of energy and deformation before fracture and may increase G_I and G_{II}, but the increase is greater for G_I because this mode is associated with the crack opening and the separation of the bonded surfaces in mode I loading involves a more extensive displacement of the adhesive in the plane perpendicular to the crack. Whereas, G_{II} is associated with crack sliding and shear deformation of the adhesive which involves a less extensive deformation in the plane of the crack, therefore, the increase in energy dissipation and high-temperature deformation has a greater effect on G_I than G_{II}.

With these results in mind, it can be seen that G_I is slightly more sensitive to strain rate at high temperature than mode II.

When comparing results at 23 °C and 60 °C, in general, it can be observed that room temperature (23 °C) is more sensitive to strain rate effects compared to a temperature of 60 °C. This finding is consistent with the results presented by Jun Zhang et. al [24], which investigated the behavior of silane-modified polyurethane sealant. The study demonstrated that the material exhibited temperature dependence at a constant strain rate and rate dependence at room temperature. However, at high temperatures, the results showed lower sensitivity.

4.3. Temperature effect

Under quasi-static conditions, there was an increase of 3.4 factor in fracture energy mode I from the temperature below T_g to the temperature of the room, and this discrepancy was enhanced with increasing loading rate. However, the same was not found for

the other temperatures. In all those experiments, the critical fracture energy, for both modes, decreased when the temperature was above the room temperature, as can be verified on Figure 9.

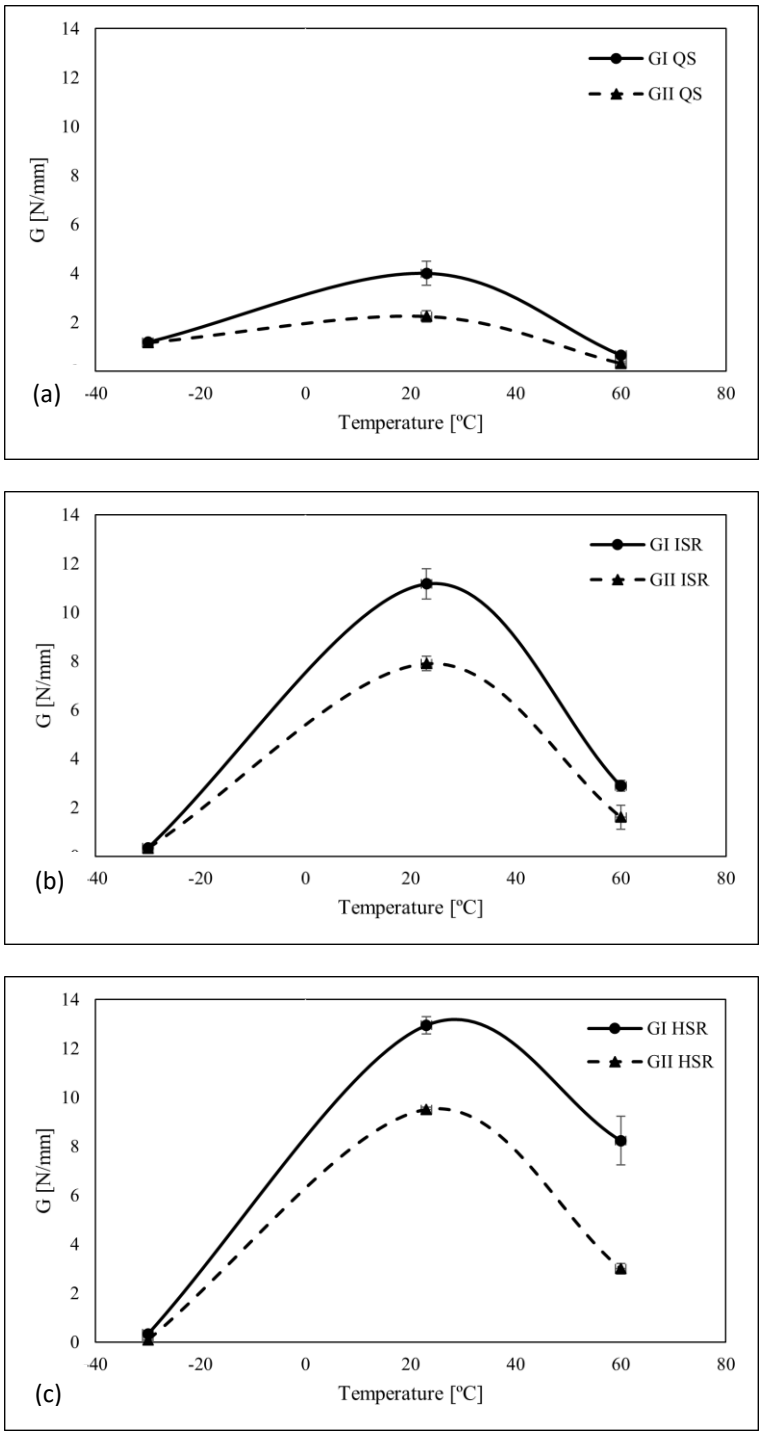


Figure 9. Critical fracture energy as function of temperature for different loading rates, for a mixed mode apparatus set up at 45º.

When an adhesive is exposed to a higher temperature than its T_g, it undergoes a reversible glass transition, in which the adhesive becomes softer and more viscoelastic. Yet, like in this case, when the adhesive is subjected to a very high temperature when compared with the glass transition temperature, thermal degradation may occur, which can lead to a permanent loss of its mechanical and adhesion properties [25].

According to the results presented, between -30 ºC and 23 ºC, there was an increase in G_I by a factor of 35 for intermediate strain rate and an increase by a factor of 38 for high

strain rate. Regarding G_{II}, fracture energy increased by a factor of 25 for intermediate strain rate and by a factor of 95, for high.

This clearly raises some questions about the sensitivity of G_I and G_{II} to strain rate and temperature. In the transition from ambient to lower temperatures it is evident that mode I exhibit a significantly greater degree of sensitivity. Within the temperature range of 23 to 60 °C, under conditions of quasi-static loading and intermediate strain rates, mode I continues to show greater sensitivity. However, at high strain rates the sensitivity of both modes appears to be comparable.

Comparing the ratio of G_I/G_{II} for intermediate (0.45) and high strain rate (2.74) at high temperature, it is clear that there is a large gap between these two values, which once again indicates the increasing discrepancy between G_I and G_{II} as the strain rate increases.

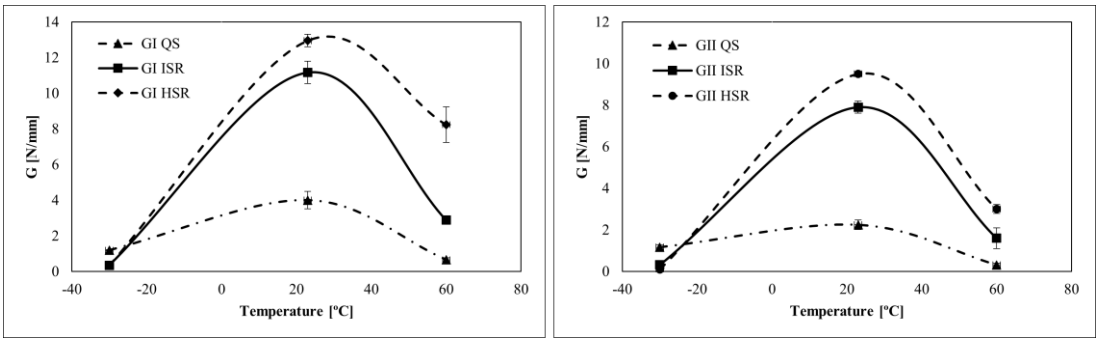


Figure 10. Fracture energy modes as function of temperature.

The best adhesive's performance was obtained for higher loading rates at room temperature and the adhesive itself showed a higher sensitivity to temperature than loading rate. The specimen subjected to high strain rate at low temperature showed the worst performance.

Lopes et al. [26] while studying the temperature effect on an epoxy adhesive subjected to different mode mixities, also concluded that the temperature sensitivity was more noticeable in tensile loading conditions when compared to shear mode and, that the tensile fracture energy dropped with increasing temperature. Santos et al. [22] also found that an increase in temperature, from 23 °C to 60 °C led to a decrease in strength and ductility for the adhesive in the study, which translated into a huge decrease in fracture toughness in mode I.

4.4. Fracture Envelope

The overall conclusion from published papers is that as the strain rate increases, structural adhesives' fracture energy generally tends to decrease [10] [11]. When exposed to impact stresses, an adhesive's basic mechanical properties, such as tensile strength, may improve, but the adhesive becomes somewhat more brittle.

Considering the experimental results, in fact, the increase of loading rate, for the same temperature, leads to a reduction of the adhesives' fracture energy for temperatures below its T_g. Yet, the same is not true for tests performed at temperatures above the glass transition temperature, namely, for room temperature and 60 °C. As previously mentioned, this may be due to the inherent viscoelastic behaviour of polymeric structures that comprise the adhesive, however, this is also what makes the adhesive and its mechanical behaviour so sensitive to loading rates.

Temperature fluctuations produce noticeable changes in the adhesive's characteristics, which in turn provide noticeably altered adhesive joint behaviour. This impact of temperature on the strength of adhesive joints has been the subject of numerous investigations and these studies state that testing at temperatures below room temperature leads to a decrease in joint toughness, while testing at higher temperatures leads to a decrease in joint strength.

Having in mind the results, there is no question that the tests performed at room temperature have the highest values of energy release rate. In other words, it can be observed that for the specimen tested at high temperatures it doesn't have as much fracture toughness when submitted to certain load rates. This is probably since the temperature of 60 ºC is too high having in mind the T_g of -5 ºC for this adhesive, therefore, the temperature in question will end up degrading the adhesive properties.

Regarding the low energy release rate values for the specimen tested at -30 ºC, this may be a result of the phenomenon related to thermally induced physical changes that at temperatures below the T_g point, the adhesive becomes more brittle.

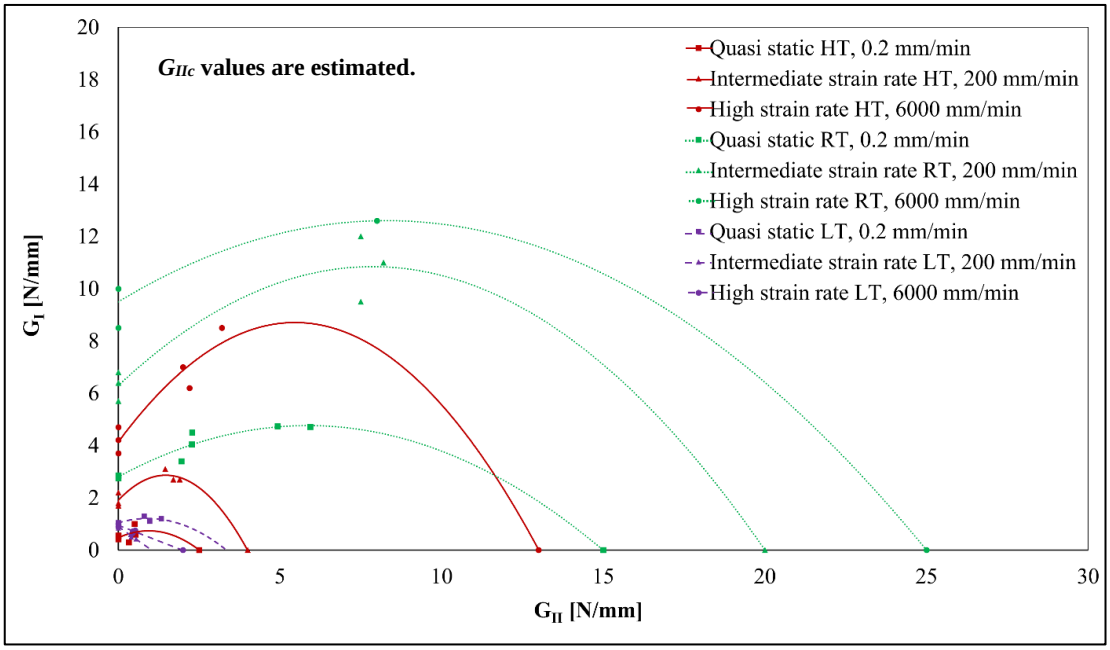


Figure 11. Fracture envelopes.

Thus, in a more general view, both temperature and strain rate influence the rate of energy release and, in a way, both variables can work in symbiosis to alter the values in different ways, allowing a greater number of applications when combined.

Figure 11 shows the fracture envelope for this adhesive. As can be seen in the figure, all the G_{IIc} values have been estimated, because if a test were performed closer to pure Mode II, with a mode mixity higher than 45º, there would be a risk of plastic deformation of the substrate before crack propagation in the adhesive layer, especially under higher strain rate conditions at high and room temperature. The results of the quasi-static test at 23 ºC, performed at a mixed mode angle of 60 ºC, were also taken into account to obtain the best possible approximation of the fracture envelope.

5. Conclusions

The study of the effects of strain rate and temperature on the mixed mode fracture behaviour of the polyurethane adhesive has provided valuable insights into the mechanical properties and behaviour of adhesives under different loading conditions and service temperature.

Thereby, the critical fracture energy for both mode I and mode II parts of mixed-mode of this polyurethane adhesive were analysed under three different loading rates (0.2 mm/min, 200 mm/min and 6000 mm/min) and three temperatures (-30ºC, 23ºC and 60ºC).

From the research carried out and the results obtained, the main conclusions drawn from this are the following:

- The critical strain energy release rate is greatly sensitive to the service temperature. The loading rate also greatly influences this parameter depending on the temperature to which the specimen is subjected.

- The maximum load supported by the specimen increases with increasing loading rate for temperatures above Tg.
- Under quasi-static conditions, the fracture energy increased around 3.4 times from below Tg to room temperature, and this disparity was exacerbated by an increase in loading rate.
- It was found that the influence of temperature is relatively more important for intermediate and high strain rate, since on the results at these two strain rates, GI increased by a factor of 35 for intermediate strain rate and 38 for high strain rate from low temperature (-30oC) to room temperature (23oC). GII also increased for the same conditions by a factor of 25 and 95 times, respectively.
- Both strain rate and temperature exert a comparable influence on both mode I and mode II of mixed mode, albeit mode I appears to exhibit, an overall, greater sensitivity to these effects.
- According to the results presented, the best adhesive's performance was obtained for higher loading rates at room temperature with a GI of approximately 13 N/mm and GII around 7 N/mm.

Acknowledgments: The second author acknowledge the individual grant No. 2020.04017.CEECIND, funded by national funds through the Portuguese Foundation for Science and Technology (FCT).

Author Contributions: Maria Ribas: Data curation, Formal analysis, Investigation, Visualization; Alireza Akhavan-Safar: Conceptualization, Supervision, Review and editing; Nicolas Pigray, Investigation, Formal analysis; Ricardo J.C. Carbas, Methodology, Supervision; Eduardo A.S. Marques, Methodology, Supervision; Catarina S.P. Borges, Investigation, Methodology; Sabine Wenig: Conceptualization, Review and editing; Lucas F.M. da Silva: Conceptualization, Review and editing, Project administration.

Institutional Review Board Statement: Not applicable.

Informed Consent Statement: Not applicable.

Data Availability Statement: Not applicable.

Conflicts of Interest: The authors declare no conflict of interest.

References

1. Tan, W., Na, J. X., & Zhou, Z. F. (2023). Effect of temperature and humidity on the creep and aging behavior of adhesive joints under static loads. The Journal of Adhesion, 99(4), 672-690.
2. Houjou, K., Shimamoto, K., Akiyama, H., & Sato, C. (2022). Effect of test temperature on the shear and fatigue strengths of epoxy adhesive joints. The Journal of Adhesion, 98(16), 2599-2617.
3. Škec, L., & Alfano, G. (2023). Experimental and numerical study of rate-dependent mode-I failure of a structural adhesive. The Journal of Adhesion, 99(8), 1323-1355.
4. Borges, C. S. P., Nunes, P. D. P., Akhavan, A., Marques, E. A. S., Carbas, R. J. C., Alfonso, L., & Silva, L. F. M. (2020). Influence of mode mixity and loading rate on the fracture behaviour of crash resistant adhesives. Theoretical and Applied Fracture Mechanics, 107, 102508.
5. Jia, Z., Hui, D., Yuan, G., Lair, J., Lau, K. T., & Xu, F. (2016). Mechanical properties of an epoxy-based adhesive under high strain rate loadings at low temperature environment. Composites Part B: Engineering, 105, 132-137.
6. Machado, J. J. M., Hayashi, A., Nunes, P. D. P., Marques, E. A. S., Carbas, R. J. C., Sato, C., & Da Silva, L. F. M. (2019). Strain rate dependence of a crash resistant adhesive as a function of temperature for the automotive industry. Proceedings of the Institution of Mechanical Engineers, Part L: Journal of Materials: Design and Applications, 233(11), 2189-2203.
7. Nunes, P. D. P., Marques, E. A. S., Carbas, R. J. C., Akhavan-Safar, A., & Da Silva, L. F. M. (2021). DCB tests at constant strain rate using crash-resistant epoxy adhesives: A numerical and experimental approach. Proceedings of the Institution of Mechanical Engineers, Part D: Journal of Automobile Engineering, 235(13), 3234-3242.
8. Nunes, P. D., Borges, C. S., Marques, E. A., Carbas, R. J., Akhavan-Safar, A., Antunes, D. P., ... & da Silva, L. F. (2020). Numerical assessment of strain rate in an adhesive layer throughout double cantilever beam and end notch flexure tests. Proceedings of the Institution of Mechanical Engineers, Part E: Journal of Process Mechanical Engineering, 234(5), 415-425.
9. Viana, G., Machado, J., Carbas, R., Costa, M., Da Silva, L. F. M., Vaz, M., & Banea, M. D. (2018). Strain rate dependence of adhesive joints for the automotive industry at low and high temperatures. Journal of adhesion science and Technology, 32(19), 2162-2179.
10. Jia, Z., Yuan, G., Hui, D., Feng, X., & Zou, Y. (2018). Effect of high strain rate and low temperature on mode II fracture toughness of ductile adhesive. International Journal of Adhesion and Adhesives, 86, 105-112.

11. Jia, Z., Yuan, G., Hui, D., Feng, X., & Zou, Y. (2019). Effect of high loading rate and low temperature on mode I fracture toughness of ductile polyurethane adhesive. Journal of Adhesion Science and Technology, 33(1), 79-92.
12. Borges, C. S. P., Nunes, P. D. P., Akhavan-Safar, A., Marques, E. A. S., Carbas, R. J. C., Alfonso, L., & Silva, L. F. M. (2020). A strain rate dependent cohesive zone element for mode I modeling of the fracture behavior of adhesives. Proceedings of the Institution of Mechanical Engineers, Part L: Journal of Materials: Design and Applications, 234(4), 610-621.
13. Tserpes, K., Barroso-Caro, A., Carraro, P. A., Beber, V. C., Floros, I., Gamon, W., ... & Rajčić, V. (2022). A review on failure theories and simulation models for adhesive joints. The Journal of Adhesion, 98(12), 1855-1915.
14. Bidadi, J., Googarchin, H. S., Akhavan-Safar, A., & da Silva, L. F. M. (2023). Loading rate effects on mixed-mode I/II fracture envelope of epoxy resins with nonlinear behavior. Theoretical and Applied Fracture Mechanics, 125, 103858.
15. Perez, M., Akhavan-Safar, A., Carbas, R. J., Marques, E. A., Wenig, S., & da Silva, L. F. (2022). Loading rate and temperature interaction effects on the mode I fracture response of a ductile polyurethane adhesive used in the automotive industry. Materials, 15(24), 8948.
16. Wang, F., Bu, H., Ma, W., Zhang, P., & Zhan, X. (2023). Influence of the different surface treatments on fracture property of CFRP adhesive joint. Journal of Adhesion Science and Technology, 37(6), 961-975.
17. Houjou, K., Sekiguchi, Y., Shimamoto, K., Akiyama, H., & Sato, C. (2023). Energy release rate and crack propagation rate behaviour of moisture-deteriorated epoxy adhesives through the double cantilever beam method. The Journal of Adhesion, 99(6), 1016-1030.
18. Wang, W., & Xian, G. (2023). Effects of steel surface treatment with silanized carbon nanotubes on the bonding properties between steel and epoxy adhesive. The Journal of Adhesion, 99(2), 297-319.
19. Costa, M., Carbas, R., Marques, E., Viana, G., & Da Silva, L. F. M. (2017). An apparatus for mixed-mode fracture characterization of adhesive joints. Theoretical and Applied Fracture Mechanics, 91, 94-102.
20. De Moura, M. F. S. F., Campilho, R. D. S. G., & Gonçalves, J. P. M. (2008). Crack equivalent concept applied to the fracture characterization of bonded joints under pure mode I loading. Composites science and technology, 68(10-11), 2224-2230.
21. Na, J., Liu, Y., Wang, Y., Pan, L., & Yan, Y. (2016). Effect of temperature on the joints strength of an automotive polyurethane adhesive. The Journal of Adhesion, 92(1), 52-64.
22. Santos, D., Akhavan-Safar, A., Carbas, R. J. C., Marques, E. A. S., Wenig, S., & da Silva, L. F. M. (2023). Load-control vs. displacement-control strategy in fatigue threshold analysis of adhesives: Effects of temperature. Engineering Fracture Mechanics, 284, 109255.
23. Feng, W., Xu, F., Li, Z., & Zhang, C. (2023). Mode I fracture toughness of adhesively bonded composite joints under high loading rate conditions. The Journal of Adhesion, 99(5), 893-909.
24. Zhang, J., Shen, H. Z., Li, H. Y., & Gu, L. F. (2021). Effects of temperature, strain rate, and cyclic loading on mechanical behavior of silane-modified polyurethane sealant. Journal of Applied Polymer Science, 138(15), 50195.
25. Viana, G. M. S. O., Costa, M., Banea, M. D., & Da Silva, L. F. M. (2017). A review on the temperature and moisture degradation of adhesive joints. Proceedings of the Institution of Mechanical Engineers, Part L: Journal of Materials: Design and Applications, 231(5), 488-501.
26. de Castro Lopes, F. V. B., Akhavan-Safar, A., Carbas, R. J. C., Marque, E. A. S., Goyal, R., Jennings, J., & da Silva, L. F. M. (2023). The role of loading mode on the property degradation of adhesives at high temperatures. Fatigue & Fracture of Engineering Materials & Structures, 46(5), 1848-1863.

Appendix B

Paper B

Exploring strain rate variation in the adhesive layer during constant speed mode I fracture tests: loading speed and test temperature effects

M Ribas[1], A Akhavan-Safar[2], P Adam-Cottard[1], RJC Carbas[2], EAS Marques[2], S Wenig[3], LFM da Silva[1]

[1]Faculdade de Engenharia, Universidade do Porto, Rua Dr. Roberto Frias, 4200-465, Porto, Portugal.
[2]Institute of Science and Innovation in Mechanical and Industrial Engineering (INEGI), Rua Dr. Roberto Frias, 4200-465 Porto, Portugal.
[3]Sika Automotive AG, Kreuzlingerstrasse 35, 8590 Romanshorn, Switzerland.

Abstract

The existing literature primarily explores fracture energy concerning test rate. However, for numerical simulations and bonded joint design, understanding the fracture energy strain rate sensitivity is key, not test speed. Even at a constant speed in fracture tests, adhesive strain rate varies during crack propagation, complicating strain rate sensitivity analysis. The current study aims to comprehend the strain rate sensitivity of the fracture energy, as opposed to the loading rate sensitivity of two different polyurethane adhesives subjected to mode I loading conditions. The study experimentally examines strain rate variations under constant loading rates and investigates how test speed affects the strain rate in mode I fracture tests. The impact of testing temperature on the strain rate is also explored by performing tests at -30 ºC and 23 ºC. Digital image correlation (DIC) and tracking methods are employed to improve the understanding of strain rate characteristics in these tests. To analyse the effect of loading rate on strain rate, the tests were conducted at different speeds as well. The influence of adhesive thickness on the strain rate was also explored. It was experimentally found that the strain rate at the crack tip varies even at a constant loading rate. The variation in strain rate is mainly evident in tests performed at higher loading rates, where the strain rate range increases. The tests performed at low

temperature revealed less variation of strain rate than the ones tested under the same loading rate condition at 23 ºC. For the same adhesive, thicker bondlines are less likely to cause a substantial error in fracture energy results than thinner bondlines.

Keywords: Polyurethane adhesives, loading mode, strain rate, fracture energy, temperature, DCB.

1. Introduction

As the modern automotive engineering sector evolves, the use of adhesive bonding applications has been continuously increasing [1] [2] [3]. As a result, there is a constant pursuit for safer, more efficient, and environmentally friendly vehicles. A toughened and high-performance adhesive can provide exceptional strength while facilitating the production of lightweight structures, thereby improving the safety and efficiency of vehicles [4]. Within the automotive industry, polyurethane adhesives have become increasingly popular due to their outstanding properties and powerful adhesion capabilities. This preference can be attributed to the excellent characteristics exhibited by these adhesives specially at higher strain rates. They have broad use in bonding dissimilar materials for structural aims, frequently experiencing environments that are vulnerable to material deterioration and bond attenuation, involving factors like dampness, vibrations, and temperature differences, among other variables [5] [6]. Studies, such as the one conducted by Tan et al. [7] has shown that increasing temperature and humidity can result in the weakening of these adhesive joints.

Considering that polyurethanes are currently being utilized in the automotive industry, it is necessary to complement the conventional challenges associated with the use of these adhesives, such as design limitations resulting from crashes at high strain rates,

environmental parameters, as well as understanding that passenger safety must be a top priority. As a result, it is of great importance to characterize the performance of bonded connections under high loading rates and impact conditions, especially since adhesives are polymers and therefore exhibit a viscoelastic and viscoplastic behaviour [8]. Therefore, it is crucial to understand the variations in their mechanical properties when exposed to varying strain rates and temperatures since they are highly susceptible to such parameters [9] [10] [11]. However, to fully comprehend changes in mechanical properties, such as fracture energy, it is important to study their sensitivity to strain rate, as they are strain rate dependent. The loading rate and strain rate are distinct concepts, as although they are related, they pertain to different aspects of material behaviour. Loading/displacement rate denotes the velocity at which an external force/displacement is exerted upon a material, whereas strain rate is a measure of the rapidity with which a material undergoes deformation in reaction to an applied stress, therefore, it is also crucial to comprehend the strain rate variation along the bondline of a joint subjected to a constant test speed. In several studies, the effect of test speed on adhesive fracture energy has been explored, however, very few works have examined the strain rate sensitivity of fracture energy.

Viana et al. [12] investigated the effect of loading rate on a crash-resistant epoxy under varying temperature conditions. The results indicate that for quasi-static conditions, the energy absorbed by the specimens decreased as temperature increased. This decline could be attributed to the decrease in adhesive yield stress with increasing temperature. A similar trend was observed in the research conducted by Jia et al. [13] [14] while studying ductile polyurethane adhesives. In both cases, there was a correlation between an increase in loading rate and a decrease in critical fracture energy. Nevertheless, when evaluating mode I fractures under quasi-static conditions, the critical energy release rate declined as

the temperature decreased. Conversely, for greater loading rates, the mode II fracture energy (G_{IIc}) exhibited a reduction as the temperature rose. Ribas et al. [15] also investigated the effect of loading rate and temperature on a two-part polyurethane adhesive under mixed mode I+II loading conditions. The study found that both loading rate and temperature had a comparable effect on both mode I and mode II parts of the mixed mode fracture test, although mode I appeared to have a greater overall sensitivity to these effects as also shown by Lopes et al. [16].

Comprehending the behaviour of the mechanical properties of both the adhesive and the substrate enables the development of strain rate dependent models that can be used to validate improved joint designs able to withstand dynamic loads during impact [2] [17]. This topic has been studied in some depth in this field; however, most of the published studies about strain rate effects on adhesive fracture toughness fail to adequately specify how the authors calculate the strain rate and its variation ahead of the crack tip in a fracture test [18] [19] [20] [21]. Others refer to the effect of test speed, rather than the strain rate [9] [22] [23] [24]. In some cases, the nominal strain rate is calculated by multiplying the test speed by the thickness of the adhesive [13] which doesn't show the real strain rate that the adhesive layer experiences.

Marzi et al. [25] and Karac et al. [26] carried out strain rate studies on crash-optimized structural adhesive and a rubber-toughened epoxy adhesive, respectively, using the TDCB (tapered double cantilever beam) test. According to Marzi et al. [25], high speed loading in mode I does not result in significant variations in strain rate during crack propagation. They also developed a numerical relationship between crosshead speed and average strain rate based on their results. In another study, Karac et al. [26] established a relationship between an approximate strain rate at the crack tip and test velocity based on an elastic-foundation analytical beam. Regarding mode II tests, Marzi [27] conducted a

study on an epoxy-based adhesive, in which an analysis of strain rate was performed using tapered end-notched flexure (TENF) tests. The author defined shear strain rate as the local velocity divided by the adhesive thickness. Leffer et al. [28] discovered that, during an ENF test, the shear deformation rate at the crack tip varies significantly from the start of the test until failure occurs, for a constant crosshead displacement, also for an engineering epoxy adhesive. Jia et al. [29] conducted numerical investigations involving polyurethane adhesives subjected to high strain rates, revealing a consistent alteration of strain rates in accordance with varying impact conditions. To undertake this investigation, the authors put forth a method based on weighted average strain rates for establishing the adhesive effective strain rate within the context of numerical simulation under high strain rate circumstances. The model underwent calibration and validation against empirical data obtained from tests involving DCB, ENF, and thick adherend shear tests (TAST). This study highlighted a good agreement between experimental outcomes and numerical predictions, thus authenticating the efficacy of the strain rate determination approach. Using a numerical approach, Nunes et al. [30] evaluated strain rate not only for the crack length itself but also during crack propagation, both for DCB and ENF tests, on a one-part crash-resistant epoxy adhesive. The authors found that strain rate before failure changed along the bondline for constant test speeds and that those changes were substantially lower to those observed during DCB tests. It was also found that a varying displacement rate affects strain rate by the same magnitude.

Considering the presented literature review, it is found that the existing literature tends to focus mainly on the effects of test speed rather than strain rate, whereas for design and numerical simulations, the strain rate sensitivity of the fracture energy is the key. The few studies conducted on the strain rate assessment of bonded joints, are mainly limited to numerical evaluations and mainly for epoxy adhesives. On the other hand, they don’t

consider the combined effects of temperature and loading rate on the strain rate that an adhesive experience in a fracture test. It should be noted that the considered numerical methods fail to provide a correct strain rate analysis for very flexible adhesives such as polyurethanes. Taking these points into account, the primary objective of this study is to address this research gap and answer the posed questions while experimentally investigating the fracture behaviour of two polyurethane adhesives at varying loading rates and temperatures. This was achieved through performing DCB testing at two distinct test speeds (quasi-static at 0.2 mm/min and a high loading rate at 200 mm/min) and two distinct temperatures (low temperature at -30°C and ambient temperature at 23°C).

2. Experimental details

The present section details the manufacturing process and testing procedures used to carry out the DCB tests and the strain rate analysis. The R curves were obtained at varying loading rates and temperatures, including strain rate values. The strain rate values were obtained using digital image correlation analysis. Any subsequent mention with the nomenclature QS and ISR are relative to the quasi-static condition (0.2 mm/min) and intermediate strain rate (200 mm/min), respectively. The term ISR is assigned to the loading rate of 200 mm/min, as this speed is not deemed as high as the rates to which the adhesive parts will be exposed in their respective applications. For the purposes of simplicity when referring to test temperatures, the terms LT and RT will be utilised to signify low temperature (-30 ºC) and room temperature (23 ºC) respectively. The experimental details are explained in the following sections.

2.1. Materials

For the experimental procedure, DCB specimens were fabricated using high strength steel (PM300) substrates. Two different ductile two-component polyurethane-based adhesives, named adhesive A and adhesive C, with mechanical properties modified for industrial use were investigated. Table 1 gives the physical and mechanical properties of each adhesive.

Table 1 - Physical and mechanical properties of the polyurethane adhesive A and adhesive C at room temperature [31].

	Adhesive A	**Adhesive C**
Glass transition temperature T_g (°C)	-5	-45
Maximum tensile strength (**MPa**)	3.4 ± 0.09	15
Maximum tensile strain (**%**)	33.4 ± 1.34	100
Young's modulus (**MPa**)	20.3 ± 1.23	350

2.2. Specimen geometry and manufacturing procedure

Figure 1 illustrates the specimen geometry. For each adhesive, a distinct thickness was applied based on the manufacturer's recommendations. Adhesive A was utilized with a bondline of 4 mm thickness, while the adhesive thickness for adhesive C was considered as 2 mm.

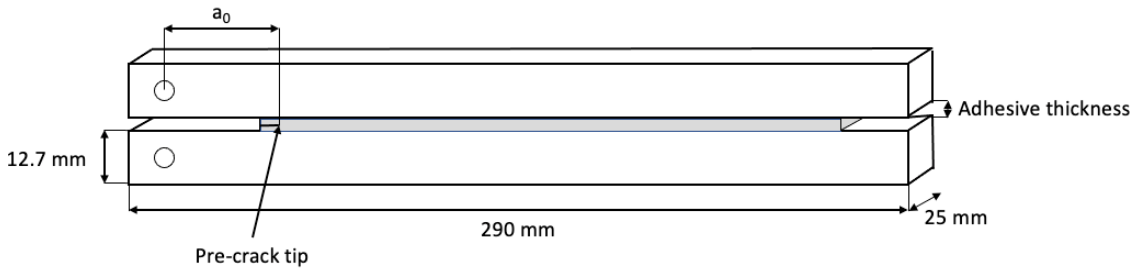


Figure 1 - DCB specimen geometry.

Before applying the adhesive, it is essential to prepare the surface to promote adhesion between the substrate and the adhesive. Initially, the surface of the substrate was sandblasted to eliminate any iron oxides, enabling a more adhesive-friendly surface, and avoiding interfacial failure [32] [33] [34]. Afterwards, the surface was degreased using acetone and primed to improve the adhesion of the adhesive to the surface.

After 24 hours the specimens were placed on a standard mould for producing DCB joints. The specimens were enclosed by a top and bottom plate with holes for the guide pins, which held them in position during the adhesive application process. Due to the low viscosity of the adhesive and the thickness of the bondline, it was necessary to use 3D printed parts to the sides. This allows for enough adhesive to be retained within the joint during the curing cycle. The initial crack length, a_0, was 45 mm and was introduced by positioning a razor blade with the thickness of 0.1 mm in the middle of the adhesive layer. Adhesive A necessitates an initial stage of 24 hours at room temperature followed by a post-curing process, which involves an additional 4 hours duration at 80ºC. Adhesive C, on the other hand, does not require any post-cure procedure, only a curing stage of 7 days at room temperature.

To conduct the strain rate analysis, it is essential to prepare the DCBs so that the image and data processing software GOM can record and measure the substrate displacement between two points on the specimen during test. Thus, a white paint layer was applied to the surface of the specimen, followed by a speckled black paint layer as illustrated in Figure 2.

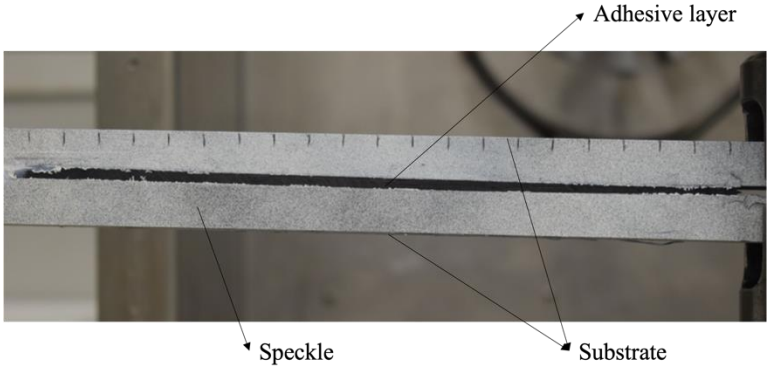


Figure 2 - DCB specimen with speckle for DIC analysis of strain rate.

2.3. Test plan

All tests were conducted on an Instron 8801 servo-hydraulic testing machine, fitted with a load cell with the capacity of ±100 kN. To carry out the experiments at -30 ºC, a thermal chamber was used, and nitrogen was injected in the chamber for cooling. Both adhesives underwent identical testing parameters at an ambient temperature of 23°C. The specimens were tested under quasi static and a high loading rate condition. Table 2 summarizes the tests conditions considered in this study.

Table 2 - Test conditions considered for different adhesives and thicknesses.

Adhesive and adhesive thickness	Room temperature 23°C		Low temperature -30°C
	0.2 mm/min	200 mm/min	200 mm/min
Adhesive A, thickness = 4 mm	√	√	√
Adhesive A, thickness = 0.5 mm	---	√	---
Adhesive C, thickness = 2 mm	√	√	√

Load and displacement data were recorded by the machine used and, subsequently, using the data reduction approach, the R curves were obtained and the critical energy release rate was determined for each condition. To analyse the strain rate a DIC (digital image correlation) setup was employed as explained in the following section.

2.3.1. DIC setup and image processing

In this study, the strain rate variation in relation to the crack size was conducted experimentally using DIC approach. To achieve optimal alignment between the test specimen and the camera, a laser-beam technique was employed to maintain perpendicularity between the DCB and the camera. Figure 3 illustrates the final system incorporating a 3D printed component that positions the laser at a right angle to the specimen.

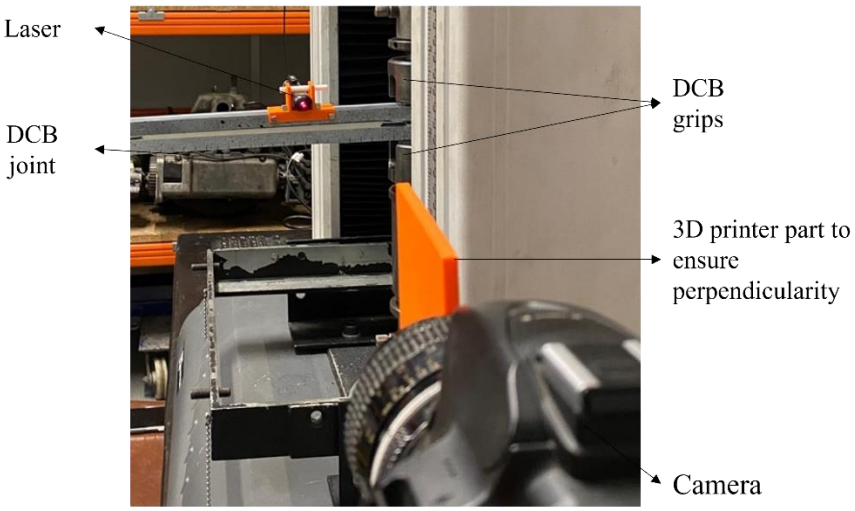


Figure 3 - Laser beam approach to ensure perpendicularity between the DCB joint and the camera.

The digital camera records the displacement of the specimen during testing, and the frames are then extracted and post-processed. Using DIC, it was feasible to measure the displacement of the specimens, near the interface, along the adhesive layer and then calculate the true and engineering strain rates for different points of the joint and over the test time. To acquire displacement data, the recorded images were analysed using GOM Correlate software. Two points were designated, one on each substrate, as reference points, to extract displacement during testing. Firstly, the speckle used was verified to ensure it was of good quality so that these points could be traced in all test frames. The software then tracked the displacement between these points over time.

As this data is extracted, the strain and strain rate were calculated using the formulas presented in Section 4.2.

3. Data reduction approach

Data reduction methods rely on monitoring crack length during propagation [35]. However, this is not a simple and viable option since there is potential for significant errors in calculating fracture energies, therefore, the compliance-based beam method

(CBBM) as a more suitable alternative was used in this study. For the tested adhesives, a fracture process zone (FPZ) is formed ahead of the main crack tip due to the nucleation of several micro-cracks across the adhesive thickness and also due to the damage and plasticity that the adhesive experiences in this zone. An extensive FPZ ahead of the crack tip can render it difficult to determine the exact location of the crack tip. Due to these effects, if the data reduction approach does not take these FPZ effects into account, the estimated crack size along the test will be more than slightly shifted, and the estimated crack tip will be much ahead of the actual crack [35]. Moreover, in highly ductile materials, a substantial amount of energy gets dissipated within the FPZ, thereby influencing the measured toughness [35] [36]. Traditional methods do not include this feature, but CBBM accounts for it. CBBM is a data reduction methodology derived from linear elastic fracture mechanics. It obviates the need for a crack length measurement during testing because the equivalent crack length is inferred solely by evaluating the specimen compliance. Considering this method, mode I fracture energy is given by

$$G_I = \frac{6\mathrm{P}^2}{B^2 h}\left(\frac{2{a_{eq}}^2}{h^2 E_f} + \frac{1}{5G}\right) \quad (1)$$

where P corresponds to the load, B is the specimen width, h is the thickness of the substrates, G is the shear modulus of the substrates, a_{eq} is the length of the crack equivalent and E_f corresponds to the corrected flexural modulus required as this method does not account for stress concentrations and substrate rotation near the crack tip [35].

4. Results and Discussion

In this section, representative load-displacement curves are shown for all tested conditions, alongside their corresponding critical fracture energy values. Furthermore, an evaluation of strain rate is proffered for each condition, including an assessment of the influence of adhesive thickness on strain rate and mode I fracture energy.

The aim of analysing the strain rate in this section is to provide answers to previously raised questions in the introduction section. This includes exploring the impact of test speed on the strain rate and determining whether increasing the load rate by a factor results in an equivalent increase in strain rate. Furthermore, this analysis aims to capture the variation in strain rate when the test is conducted at a constant load rate, particularly at higher load speeds, examine the relationship between temperature and changes in strain rate, and determine the feasibility of assuming a consistent strain rate throughout the bondline near the crack tip.

4.1. Experimental results

Figure 4 present typical load displacement curves of the DCB specimens tested at different loading rates and temperatures. For both adhesives A and C as the loading rate and temperature increase the maximum load that the specimen can sustain, as well as the maximum displacement increase as well.

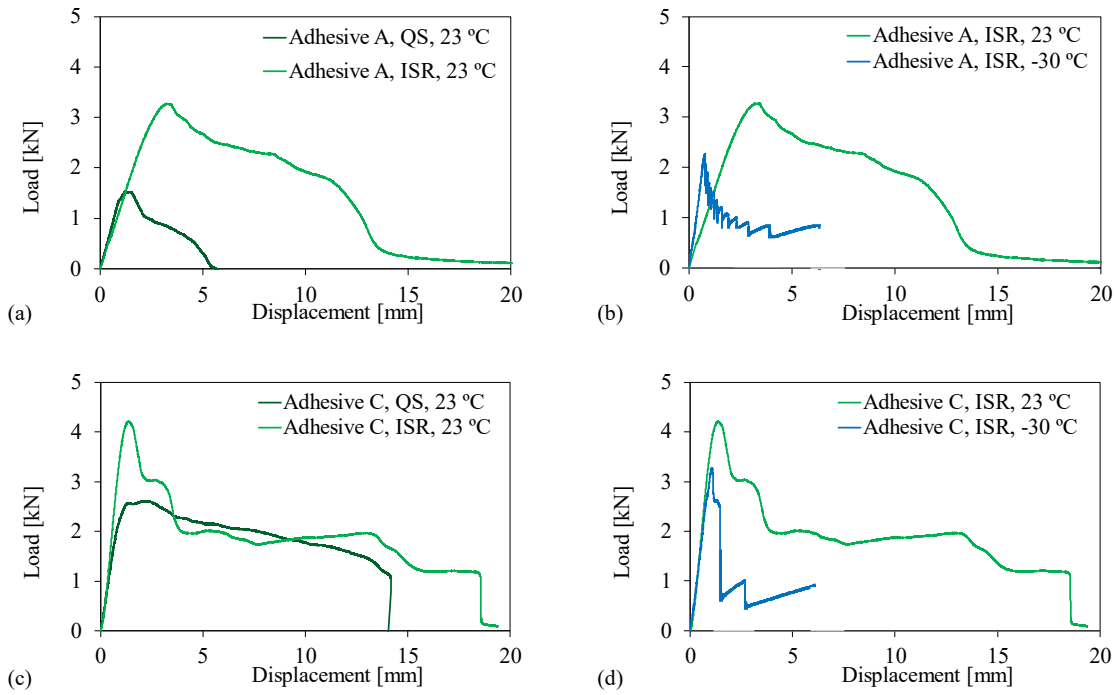


Figure 4 - Load-displacement curves of adhesive A: (a) Different loading rates at room temperature, adhesive A (b) Different temperatures at 200 mm/min, adhesive A (c) Different loading rates at room temperature, adhesive C (d) Different temperatures at 200 mm/min, adhesive C.

It can be observed that at low temperatures, both adhesives exhibit a more saw-like curve, a behaviour also noted by Perez et al. [31]. While adhesive A behaves stiffer and more brittle at low temperature as compared to the results of room temperature, this is not the case for adhesive C. It is widely acknowledged that low temperatures have an adverse effect on adhesives ductility [37]. As a polymer chain shifts from a rubbery (above its glass transition temperature, T_g) to a glassy state (below the T_g), its molecular mobility decreases, resulting in a more compact chain and a steeper slope in load-displacement curves. Remarkably, the polymer may still maintain a robust load-bearing capacity during this transition. However, adhesive C retains its stiffness at low temperature with some ductility since the considered low temperature, -30 ºC, is still above its T_g, while for adhesive A this temperature is well below its T_g (-5 ºC).

Also in Figure 4, for the specimens tested at 23 ºC, after reaching the peak of maximum load it is possible to observe a sudden and significant drop in load for adhesive C. Due to the flexible nature of these adhesives and the thick bondlines, when tested at temperatures above their T_g, the polymer chains become more mobile, resulting in the adhesive being more ductile and flexible. Furthermore, these types of adhesives usually present a large fracture process zone ahead of the crack tip. According to literature, if the adhesive is plastically deformable, then a plastic zone forms ahead of the crack tip, causing a damaged area [38]. Kinloch and Shaw [39] have demonstrated that adhesive fracture toughness is dependent on the size of the plastic zone, and that the constraining effects from the two adhesives determine the size of the plastic zone. Banea et al. [40] found that

the increase in adhesive fracture toughness is explained by the fact that as the adhesive layer increases, it can produce larger plastic zones prior to fracture. In this manner, the plasticity extends throughout the thickness of the adhesive and the energy dissipated is proportional to the adhesive thickness. Therefore, due to the large plastic zone that develops ahead of the crack tip and also the higher stress levels at some points close to the interfaces, multiple-site cracks are observed propagating simultaneously during DCB testing. As mentioned, within the extensive plastic zone, the uneven distribution of stress can become notably prominent, particularly in regions with more pronounced plastic deformation. Additionally, the stress distribution in this area is influenced by the stress constraints imposed by the substrate. It's important to note that stress levels near the interface increases. These areas with higher stress concentrations become points of weakness in the FPZ. If the stress exceeds the material's strength at these localized regions, cracks initiate and create a multiple-site cracking zone. After crack coalescence, the slope of the curve remains more stable since the adhesive requires a bit more energy for the evolution of the plastic zone and also creating new cracks. After a complete failure, there remains a low level of load-bearing capacity shown in the load-displacement curve, as there are still some adhesive bonds to rupture (see Figure 5).

During testing, firstly, there is a clear deformation ahead of the crack tip, as though the adhesive is being stretched, prior to crack propagation. Then, the crack begins to propagate and shortly thereafter, a new crack emerges in the FPZ, as illustrated in Figure 6. Eventually, these two sections join, and the fracture process zone becomes indistinguishable until this cycle repeats.

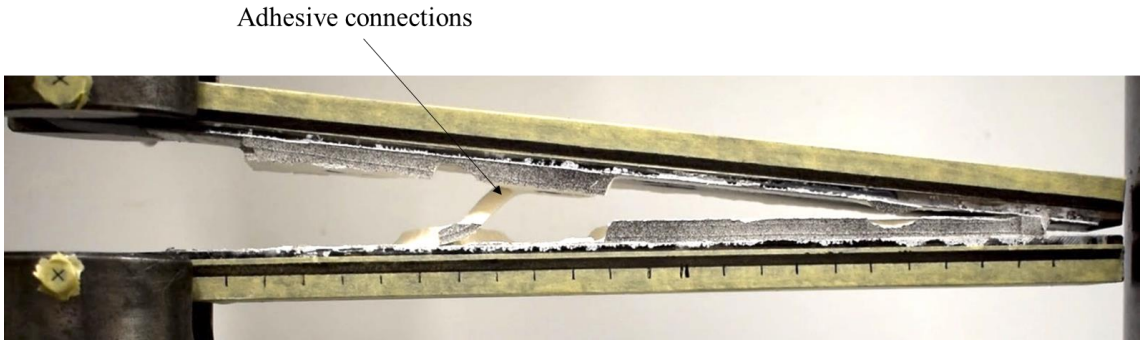


Figure 5 - Adhesive A specimen being tested under 200 mm/min loading rate at 23 ºC.

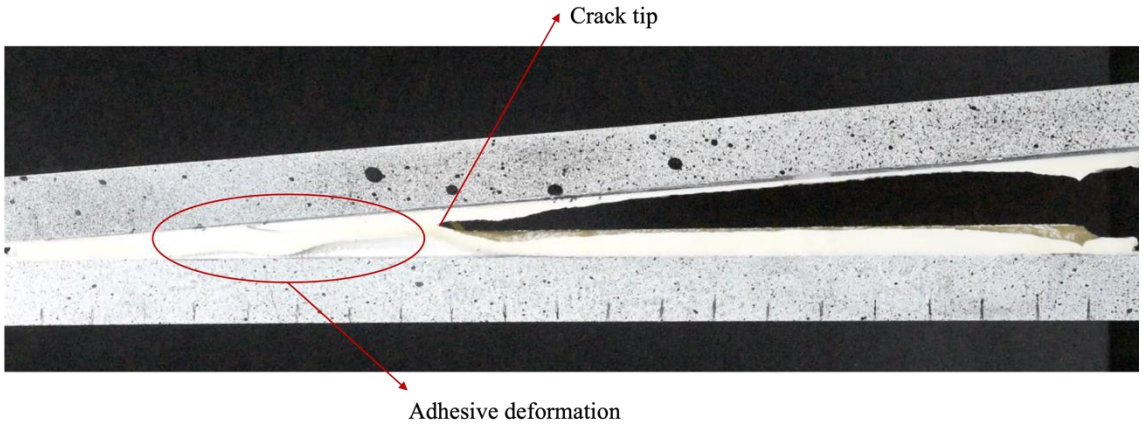


Figure 6 - Crack propagation during a DCB test at 23 ºC, 200 mm/min, adhesive A.

Figure 7 illustrates some of the specimens tested at room temperature under 200 mm/min loading rate. In all DCBs manufactured with adhesive A and tested at room temperature, it was verified that the crack propagated within the adhesive layer but near the interface, instead of propagating more towards the middle of the adhesive layer, as observed for adhesive C (see Figure 7). In low temperature results, as can be observed in Figure 8, the fracture surfaces for both adhesives revealed a different pattern as the ones observed at room temperature. At low temperature, the roughness of the surface changed specially for adhesive C that revealed some adhesive cluster in a spherical shape, which seem to have detached from one of the substrates, thus removing the primer in some points indicating the risk of debonding or interfacial failure between primer and the substrate at this temperature. On the other side, for adhesive A, the crack propagated towards the middle

of the adhesive layer for joints tested at -30 ºC. The presence of voids and other defects were discovered on the fracture surface near the end of the joints for adhesive A and C but this does not impact the determined fracture energy since these voids are located at the joint's end, where the corresponding zone in the R curve is typically excluded from fracture energy assessment.

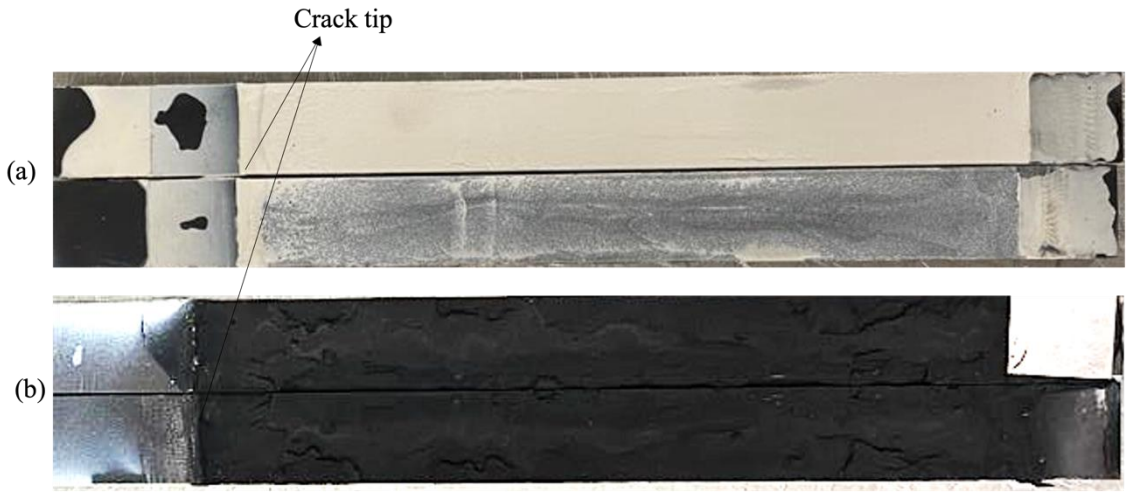


Figure 7 - Fracture surface of the specimens tested at room temperature, 23 ºC, in quasi-static condition: (a) Adhesive A (b) Adhesive C.

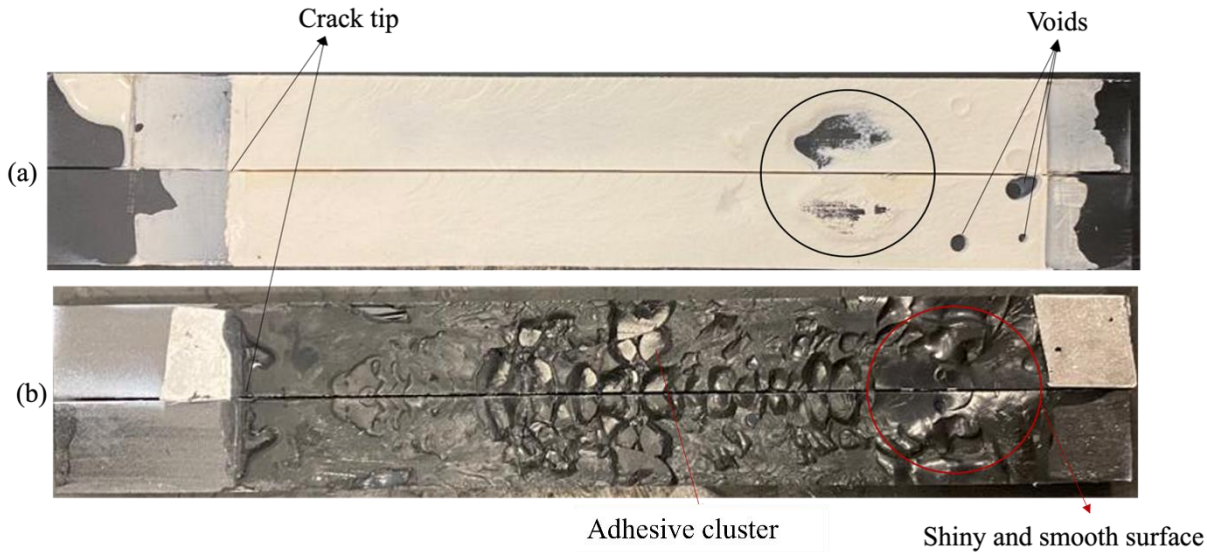


Figure 8 - Fracture surfaces of the specimens tested at low temperature, -30 ºC: (a) Adhesive A (b) Adhesive C.

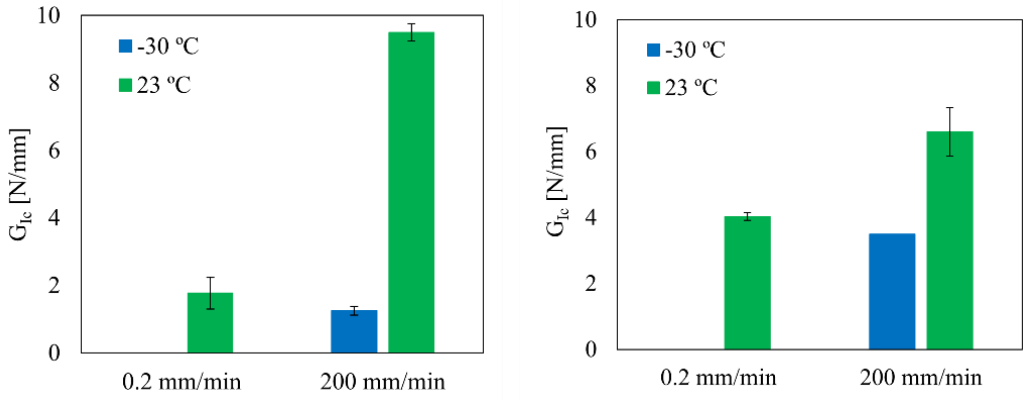


Figure 9 - Critical fracture energy values: (a) Adhesive A (b) Adhesive C.

According to the results shown in Figure 9 specimens tested under quasi-static conditions exhibited less resistance to crack propagation when compared to those tested at 200 mm/min at the same temperature. This is due to the fact that at quasi-static conditions, the ability of the bond to absorb energy is lower than at higher strains [13]. Hayashi et al. [41] also discovered that the combination of elevated temperatures and loading rates resulted in an increase in fracture toughness for structural acrylic adhesives.

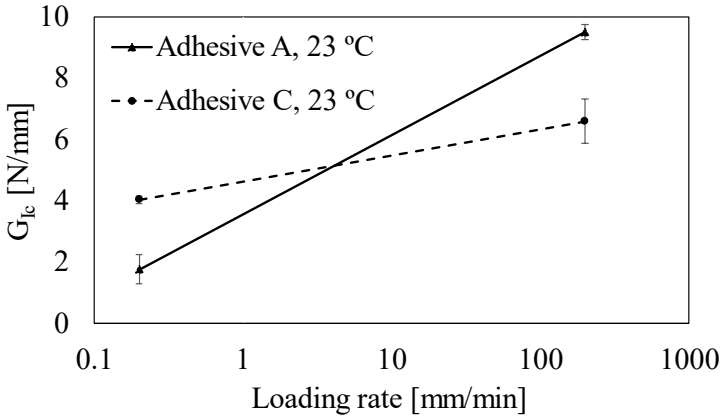


Figure 10 - Loading rate effect in mode I fracture energy at room temperature.

When comparing the results of both adhesives at 23 ºC under different loading rates (Figure 10), it becomes evident that adhesive A displays a greater susceptibility to loading rate than adhesive C. This difference could be attributed to the chemical composition of

each adhesive, but also due to the fracture process zone size. As mentioned previously, this study examined two distinct polyurethane adhesives with varying bondline thicknesses. Prior research indicates that the FPZ changes in relation to adhesive thickness, leading to differing joint fracture behaviour [40]. Taking into account the experimental results, adhesive A is expected to have a greater FPZ than adhesive C, which suggests that fracture process zone is also sensitive to strain rate.

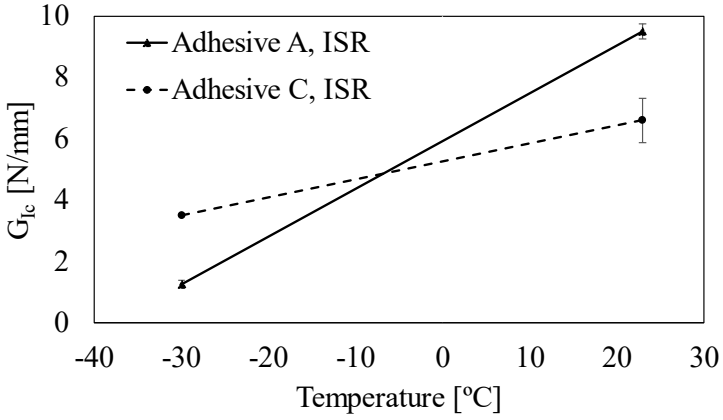


Figure 11 - Temperature effect in mode I fracture energy.

For the same loading rate, it is shown in Figure 11 that adhesive A is significantly more temperature-sensitive than adhesive C. One explanation for this significant difference is attributed to the T_g of the two adhesives. As stated in Table 1, adhesive A has a T_g of -5 ºC, compared to -45 ºC for adhesive C. Another possible reason for this phenomenon could be the stoichiometric ratio that determines the optimal balance between polyol and isocyanate in the formulation of polyurethane adhesives. Since the polyol is responsible for the soft segments that impart flexibility to the adhesive and the isocyanate is responsible for the hard segments that impart thermal resistance, having a larger isocyanate to polyol ratio for adhesive C leads to the formation of more urethane groups and a higher crosslinking density, ultimately resulting in an improved strength and a higher thermal stability compared to adhesive A [42]. Despite the difference of isocyanate

index, both adhesives exhibited a decrease in their fracture energies as the temperature decreased. Previous studies have demonstrated consistent findings. Melcher [43] investigated the mode I fracture toughness of a modified-epoxy adhesive joint in composites at liquid nitrogen temperature. The mode I fracture toughness of the adhesive was nearly 50% lower than at room temperature, and the failure mode changed from interfacial failure at room temperature to a mixed interfacial-cohesive failure at low temperature (-196 ºC). Nam et al. [44] also studied the mode I fracture toughness of a polyurethane adhesive at liquid nitrogen temperature. The adhesive became brittle, and the fracture toughness significantly decreased compared with the room temperature results.

4.2. Strain rate analysis

As discussed earlier, the strain rate at the crack tip may vary as the crack propagates. At the beginning of the test, when the load is applied, the strain rate near the crack tip may be relatively high at crack initiation in a mode I fracture test. Nevertheless, as a crack develops and the adhesive deforms, the strain rate will change. Material properties, test conditions, and specimen geometry can also influence the strain rate at the crack tip. For this reason, it is important to take into account these factors when designing and interpreting DCB test results for the assessment of fracture energy of adhesives.

Thus, one of the primary goals of this study is to assess changes in the strain rate as the crack propagates along the DCB specimens. Additionally, the presented results help to understand how the strain rate changes with test speed and how temperature affects the strain rate range experienced by the crack tip in a DCB test at constant test speed.

This examination necessitates the accurate definition of the strain rate for a specific specimen configuration. The standard definition of engineering strain rate in a material that undergoes dynamic loading is expressed using the following equation:

$$\dot{\varepsilon} = \frac{d\varepsilon}{dt} = \frac{d}{dt}\left(\frac{L(t)-L0}{dt}\right) = \frac{v(t)}{L0} \quad \textbf{(2)}$$

where ε and $\dot{\varepsilon}$ represents the strain and strain rate, respectively, t is time in seconds in this study, $L0$ is the initial adhesive thickness, $L(t)$ is the adhesive thickness at time t, and $v(t)$ is the velocity. Accordingly, the strain rate is defined as the velocity at which the paired points on the two sides of the adhesive layer move away from each other divided by the initial adhesive thickness. However, it should be kept in mind that this velocity is dependent on time and distance from the loading point. Therefore, even though the test speed is 0.2 or 200 mm/min at the loading point, it varies with distance. This equation is used in DCB tests to evaluate the adhesive layer's strain rate in mode I. However, this equation provides an engineering strain rate, while the true strain rate is the parameter used in numerical simulations. The true strain rate can differ significantly from its engineering value, particularly with more flexible adhesives and with thick bondlines like what is considered in the current study. This study presents all graphs in relation to true strain rate for both adhesives and compare them with the engineering strain rate for adhesive A, in order to compare the behaviour of both strain rate curves under different testing conditions. This measure considers the actual change in deformation occurring within the adhesive layer during its deformation. The true strain was calculated using the following expression:

$$\dot{\varepsilon}_{true} = \frac{\ln\left(\frac{L_t}{L_{t-1}}\right)}{\Delta t} \quad (3)$$

where L_t corresponds to the thickness value at moment t, L_{t-1} is the adhesive thickness of the increment before t, and Δt corresponds to the interval of time between both increments.

The data concerning the strain rate analysis conducted for all the tested conditions is presented in the subsequent figures. The graphs illustrate the variation in strain and strain rate over time at various points of overlap, so that it is possible to understand how these parameters vary along the bond line. For both adhesives, crack size was obtained during each test recurring to CBBM data reduction approach. An additional analysis of the position of the crack tip was performed using DIC for a more accurate position of the crack tip.

As the distance between substrates increases over time, there is a noticeable increase in strain for each point of the overlap. Figure 12 and Figure 13 present the data for the two adhesives at the same testing conditions (quasi-static at 23 ºC). It is evident that adhesive A exhibits a strain and strain rate values that are pretty similar to the ones obtained for adhesive C. The true strain rate values of the test conducted at 0.2 mm/min varies between 0.02 and 0.03 s^{-1} for adhesive A, while for adhesive C varies between 0.02 and 0.04 s^{-1}. For adhesive A, the true and engineering strain rates have more or less similar ranges, the latter varying between 0.027 and 0.035 s^{-1}.

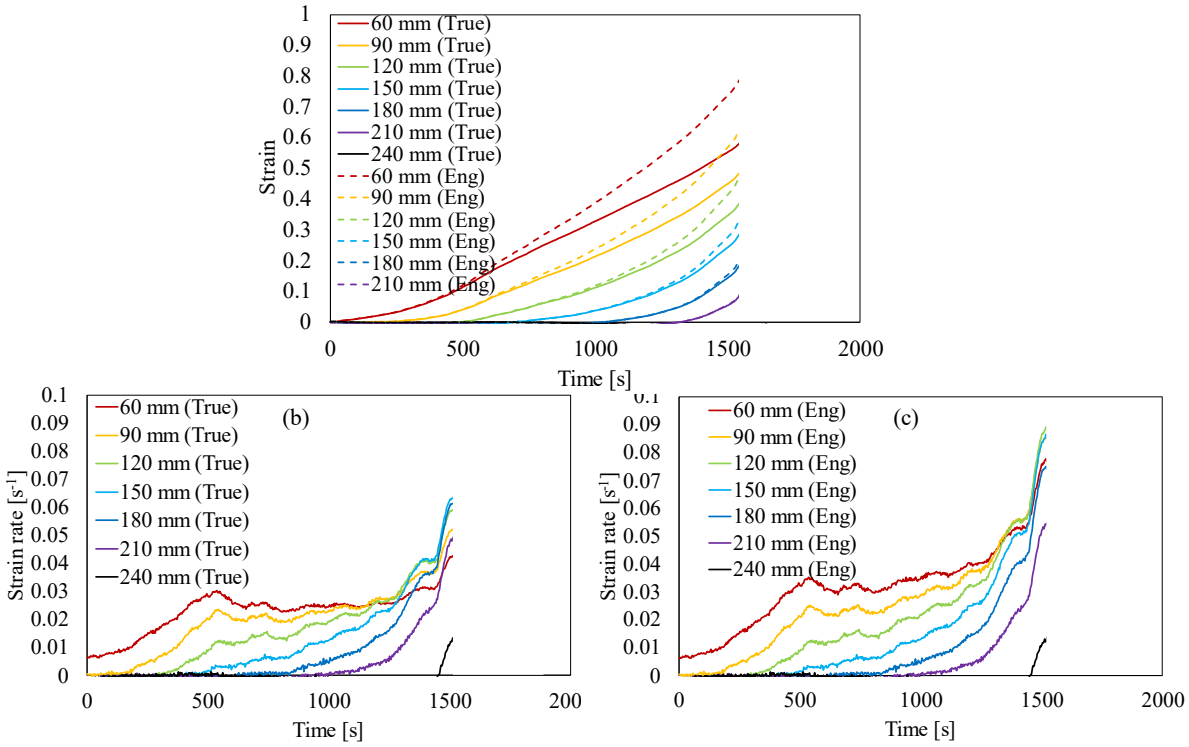


Figure 12 – True and engineering strains (a) and strain rates (b, c) as a function of time for different distances of the DCB edge, along the overlap (adhesive A under quasi-static condition at 23 ºC)

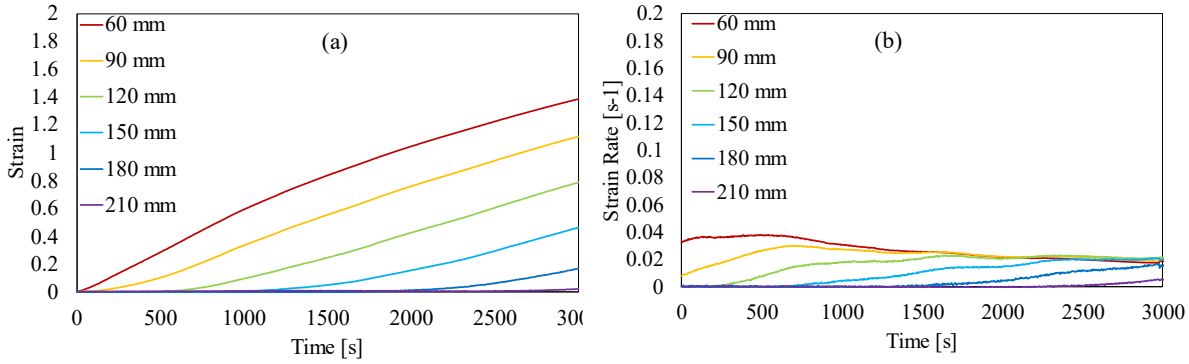


Figure 13 – True strain (a) and strain rate (b) as a function of time for different distances of the DCB edge, along the overlap (adhesive C under quasi-static condition at 23 ºC).

In Figure 14, the crack size as a function of times is plotted for both adhesives. For adhesive A, the required strain for failure is lower than that of adhesive C. The greater damage progression in adhesive A compared to adhesive C leads to a shorter crack propagation time under identical conditions. Moreover, considering that the FPZ of adhesive A is greater than that of adhesive C, this could mean that, at the end of the test,

the FPZ encompasses the rest of the adhesive layer, so that the adhesive can't withstand the strain it is subjected to and the crack propagates abruptly.

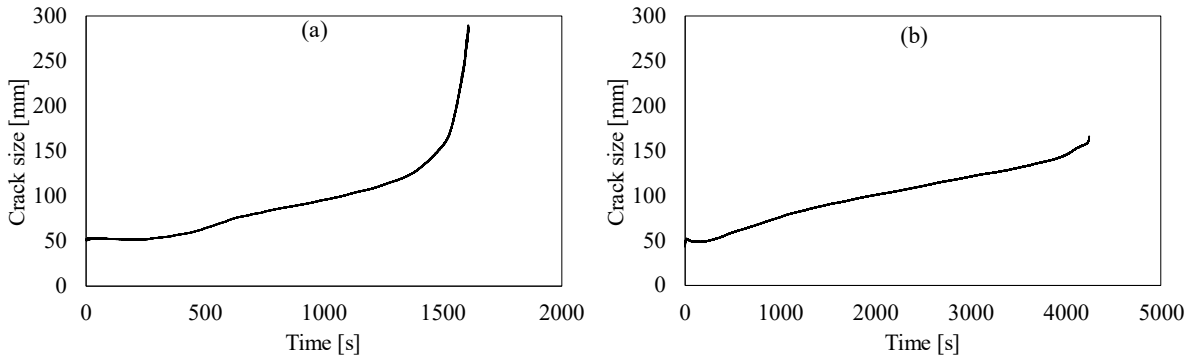


Figure 14 – Crack size as a function of time, 0.2 mm/min at 23 ºC: (a) adhesive A (b) adhesive C.

Based on the findings presented in Figure 15 and Figure 16, it becomes evident that as the test speed increases, the strain rate at crack tip exhibits a broader range of variation in a DCB test. For adhesive C, the strain rate values ranged between 20 and 55 s^{-1} at the crack tip and for adhesive A, they ranged between 15 and 26 s^{-1}. Figure 17 illustrates the progression of the crack over time for specimens exposed to a loading rate of 200 mm/min at 23 ºC. The trend of adhesive A in Figure 14 is now similarly observed for both adhesives.

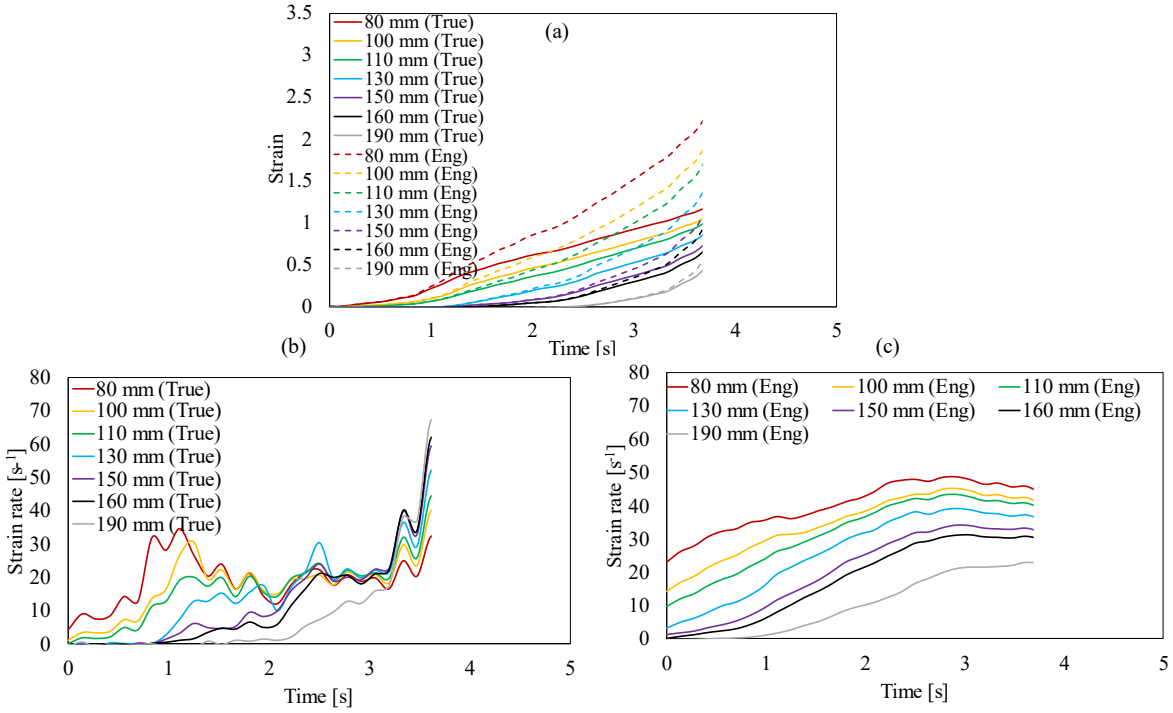


Figure 15 - True and engineering strains (a) and strain rates (b, c) as a function of time for different distances of the DCB edge, along the overlap, (Adhesive A under 200 mm/min at 23 ºC).

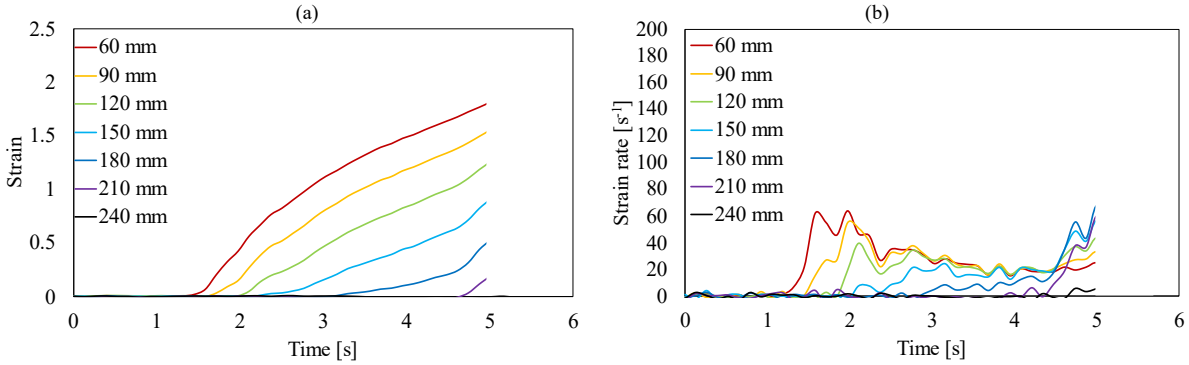


Figure 16 - True strain (a) and strain rate (b) as a function of time for different distances of the DCB edge, along the overlap (adhesive C under 200 mm/min at 23 ºC).

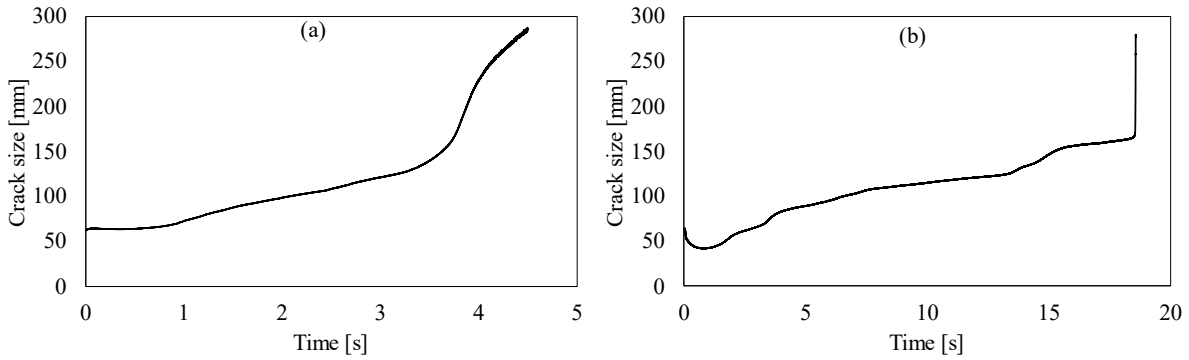


Figure 17 - Crack size as a function of time, 200 mm/min at 23 ºC: (a) adhesive A (b) adhesive C.

For low temperatures, the strain values at failure decrease due to the brittle behavior of the adhesive. This behaviour causes the crack to extend rapidly, shortening the test time significantly. When an adhesive is submitted to this type of conditions, i.e. low temperature and higher strain rates, the energy stores in a small area at the crack tip because of the low ductility of the adhesive, and is released when it reaches a critical value, therefore, the process of energy release occurs through abrupt crack propagation [31]. Analysis of Figure 18 shows that the strain rate on the crack tip varies between 14 and 26 s^{-1}, whereas for the same test speed at 23ºC the strain rate varies between 11 and 30 s^{-1} (see Figure 15), indicating a reduction in the strain rate range. As brittle polymers behave differently to ductile adhesives with more mobile polymer chains [45] [46], they do not exhibit the same strain rate dependent behaviour under these conditions. Therefore, the sensitivity to strain rate decreases with decreasing the temperature.

In Figure 19, adhesive C exhibits a strain rate at the crack tip that consistently remains at approximately 21 s^{-1}, indicating a low level of variation and consequently, reduced sensitivity. In brittle conditions, stress serves as the key parameter that determines the point/time at which the crack begins to propagate. Hence, the initial "zero" segment corresponds to the values at which the crack has not yet propagated, in additional, failure does not occur until a strain of 5-10%.

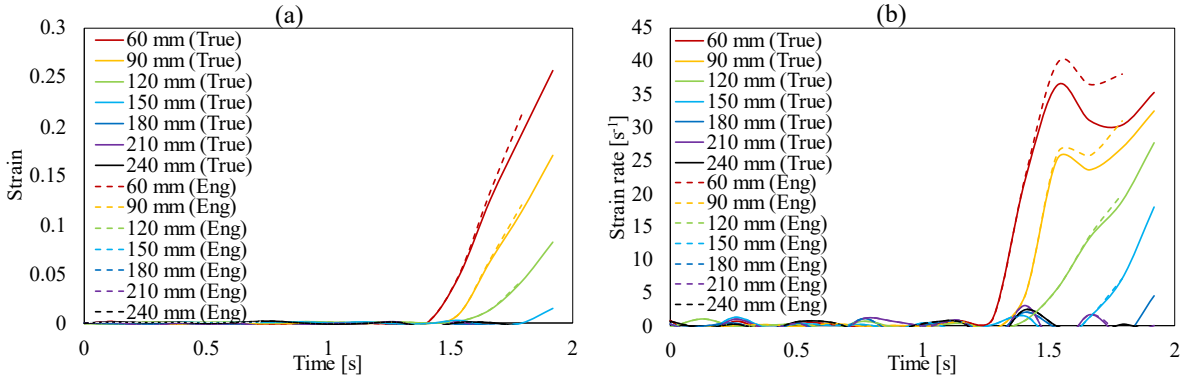


Figure 18 - True and engineering strain (a) and strain rate (b) as a function of time for different distances of the DCB edge, along the overlap, Adhesive A under 200 mm/min at -30 ºC.

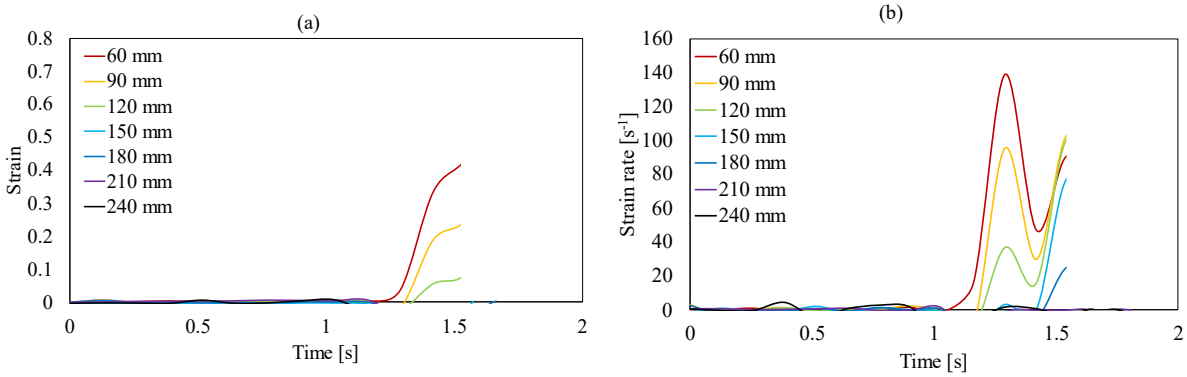


Figure 19 - True strain (a) and strain rate (b) as function of time for different distances of the DCB edge, along the overlap, Adhesive C under the test speed of 200 mm/min at -30 ºC.

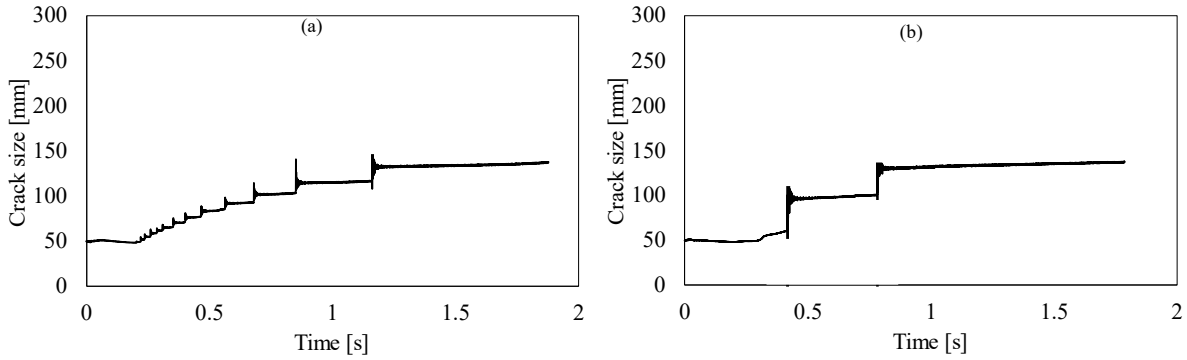


Figure 20 - Crack size as a function of time, 200 mm/min at -30 ºC: (a) adhesive A (b) adhesive C.

During the initial phase of testing at low temperatures, for most of the testing duration, both strain and strain rate values remain minimal. This is primarily due to the machine taking nearly 1 second to apply the load. Consequently, once displacement commenced, the specimens failed within approximately one second, rendering only the time of the actual displacement. Also, as at low temperatures the joint failed suddenly, it is not possible to observe a stable crack propagation along the entire bondline.

Figure 20 displays the propagation of a crack over time in a more brittle state. Both tests, which exhibited a sudden propagation of the crack for this state, had similar testing times and behavior.

After analysing both the true strain rate and the engineering strain rate for all tested conditions of adhesive A, it is clear that they differ significantly in cases of greater flexibility. A notable example is the comparison of the curves for specimens tested at 200 mm/min at room and low temperatures. At low temperature, adhesive A the engineering and true strain rate values exhibit less variation when compared to the values obtained from room temperature tests. Furthermore, there is a greater disparity in values observed when comparing tests carried out at higher loading rates but at the same test temperature.

In Figure 21, the values of fracture energy of both adhesives are shown as a function of the true strain rate variation during the test. A trend line is established to aid in predicting the fluctuation of strain rate values across test speeds ranging from quasi static to high strain rate. However, it cannot provide an accurate reflection of these values, as further testing is required at various loading rates to determine whether the behaviour is linear or not.

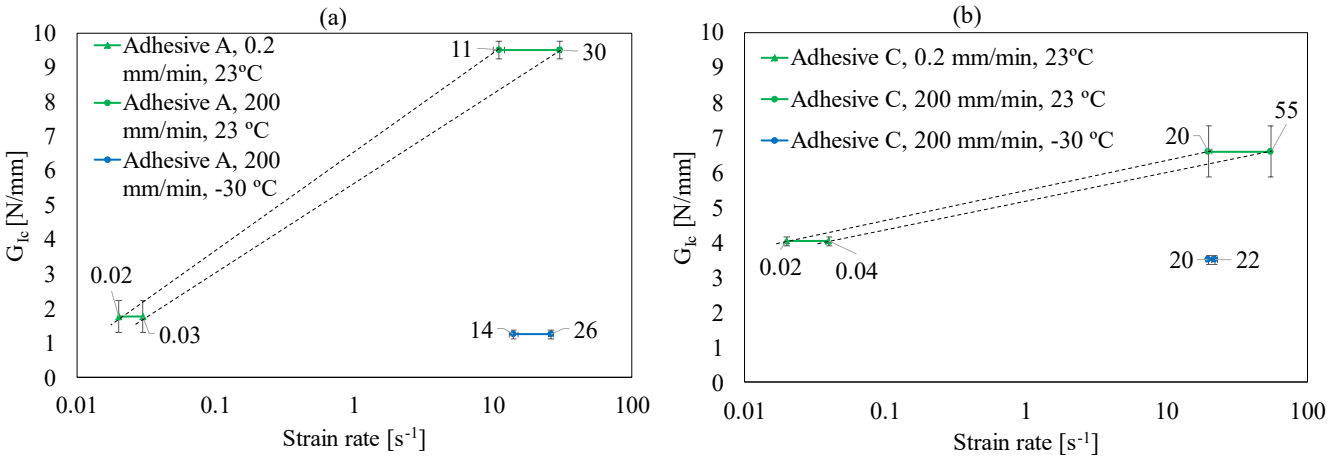


Figure 21 - Fracture energy as a function of true strain rate (a) adhesive A (b) adhesive C.

This analysis provides insight into the requirement for maintaining a consistent strain rate during testing for higher test speeds. As can be seen from Figure 21 the strain rate variation for a specific condition increases with the loading rate, implying that the strain rate variation is not negligible for higher test speeds. Consequently, a broader range of strain rate is achievable for higher strain rates, enabling the attainment of similar fracture energies. Another noticeable point is that for adhesive A and C loaded at 200 mm/min, the low temperature condition reduced the variation of strain rate.

4.3. Effect of adhesive thickness on strain rate

While for brittle and semi brittle adhesives with a small FPZ, T-stress has a critical impact on the G_{IC} obtained from DCBs with different adhesive thicknesses [47], however, as mentioned in Section 4.1, Banea et al. [40] revealed for adhesives with a higher level of ductility, the size of the plastic zone, where the energy is dissipated, is a function of the adhesive thickness. On the other hand, it is known that strain rate affects the fracture energy of the tested adhesive. Therefore, as part of the current research, a study was conducted to investigate the impact of adhesive thickness on the fracture energy and strain rate range for adhesive A, under 200 mm/min displacement rate conducted at 23 ºC.

In was found that during the initial stage of the test, both the specimen with 4 mm adhesive thickness and the specimen with 0.5 mm have consistent and similar crack propagation rates. However, towards the end of the test just before complete failure, there is a sudden and significant increase in crack size for the specimen with a thicker bondline. The cause of this may be attributed to the sudden reduction in load and the coalescence of the crack. The reduction in thickness by a factor of 8 led to an increase in strain rate for the same test speed, although not to the same extent, as it illustrated in Figure 23. For the thicker

bondline, the strain rate values along the overlap range between 11 and 30 s^{-1}, whereas for the 0.5 mm adhesive layer, they range between 40 and 120 s^{-1}.

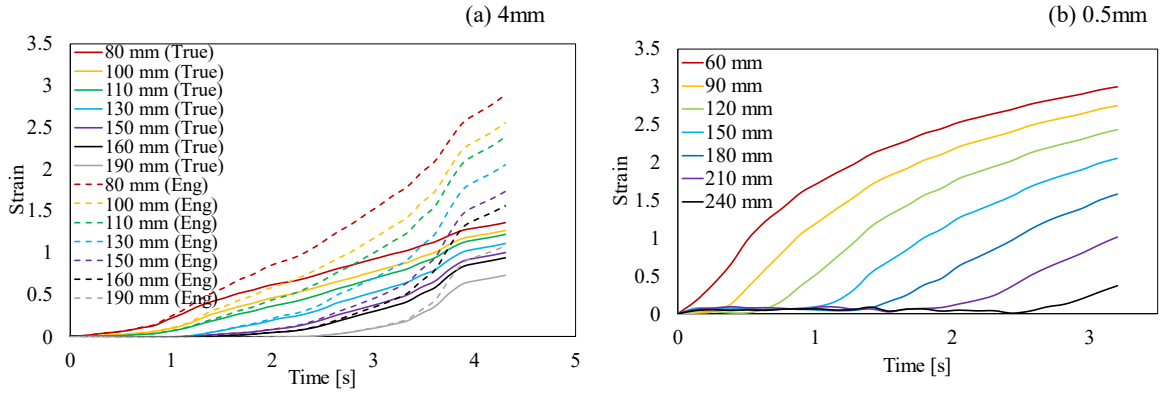


Figure 22 - Effect of thickness on strain for adhesive A at 200 mm/min test speed at 23 ºC, for different distances of the DCB edge, along the overlap: (a) 4mm adhesive thickness, and (b) 0.5 mm adhesive thickness.

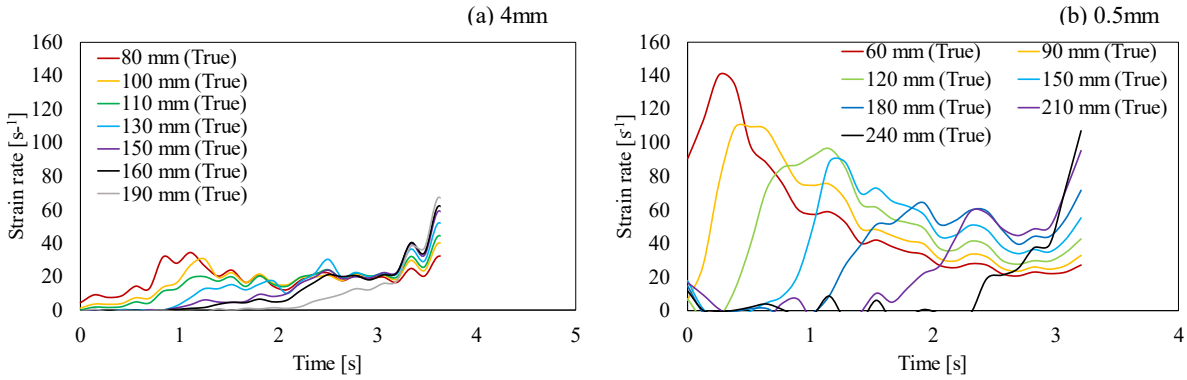


Figure 23 - Effect of thickness on strain rate for adhesive A at 200 mm/min test speed at 23 ºC, for different distances of the DCB edge, along the overlap: (a) 4mm adhesive thickness, and (b) 0.5 mm adhesive thickness.

Based on the presented results, it can be stated that increasing the thickness results in a reduction of the strain rate range, which means that thinner bondlines can induce a more significant error in the fracture energy results when compared to thicker bondlines. However, this relationship is not directly proportional to the magnitude of the thickness increase. Specifically, an eight-fold increase in adhesive thickness does not equate to an eight-fold increase in strain rate; in fact, it leads to a four-fold increase of strain rate.

Furthermore, it can be stated that the fracture energy, G_{IC}, diminishes as the joint thickness decreases. This is due to the fact that although the strain rate increases for thinner bondlines, this increment cannot counteract the reduction of the fracture process zone size on the 0.5 mm joint.

5. Conclusions

The research into the effects of loading rate and temperature on the mode I fracture behaviour of these polyurethane adhesives has provided valuable insight into the mechanical properties and behaviour of adhesives under different loading conditions and service temperatures. But most importantly, it has facilitated and helped to deepen the understanding of how the strain rate fluctuates along the overlap throughout the test and over time, for various testing situations and thicknesses.

Therefore, the study examined the critical fracture energy and strain rate for mode I of two polyurethane adhesives under two loading rates (0.2 mm/min, 200 mm/min) and two temperatures (-30°C, 23°C).

Based on the findings, the following conclusions were drawn:

- Adhesive A is more sensitive to loading rate and temperature fluctuations than adhesive C;
- Adhesive A exhibited a larger fracture process zone than adhesive C, indicating that a greater fracture process zone is more sensitive to strain rate;
- For tests performed under a constant loading rate, increasing the test speed between two tests does not result in a variation of the strain rate values in the same magnitude;
- The best performance between all the conditions was verified for adhesive A under 200 mm/min at 23 ºC, revealing a G_{Ic} of 9.5 N/mm;

- Even when maintaining a constant loading rate during testing, there are fluctuations in the strain rate, indicating that it does not remain consistent throughout the testing process; This study provided insight into the need to maintain consistent strain rate control during testing, particularly for tests performed at higher strain rates. The variation in strain rate for a particular condition rose with the loading rate, suggesting that the strain rate variation is significant, especially for high test speeds. When the specimen is subjected at low temperature the strain rate does not suffer significant fluctuations;
- True and engineering strain rate will differ more under situations where the adhesive becomes more flexible. Low temperature results revealed the best agreement between both strain rates;
- The reduction in thickness did not reveal a proportionality as expected in strain rate values. Furthermore, thinner bondlines are more likely to incite a significant error in fracture energy results than thicker bondlines due to a reduction of the strain rate range on thicker bondlines. Despite the strain rate values increasing in thinner bondlines, the size of the fracture process zone will decrease, resulting in a reduction of the adhesive's fracture energy.

References

[1] Da Silva, L. F., & Adams, R. D. (2007). Joint strength predictions for adhesive joints to be used over a wide temperature range. International Journal of Adhesion and Adhesives, 27(5), 362-379.

[2] Machado, J. J. M., Marques, E. A. S., & da Silva, L. F. (2018). Adhesives and adhesive joints under impact loadings: An overview. The Journal of adhesion, 94(6), 421-452

[3] Viana, G. M. S. O., Costa, M., Banea, M. D., & Da Silva, L. F. M. (2017). A review on the temperature and moisture degradation of adhesive joints. Proceedings of the Institution of Mechanical Engineers, Part L: Journal of Materials: Design and Applications, 231(5), 488-501.

[4] Banea, M. D., da Silva, L. F., Carbas, R., & Campilho, R. D. (2017). Effect of material on the mechanical behaviour of adhesive joints for the automotive industry. Journal of Adhesion Science and Technology, 31(6), 663-676.

[5] Abdel-Monsef, S., Renart, J., Carreras, L., Maimí, P., & Turon, A. (2020). Effect of environmental conditioning on pure mode I fracture behaviour of adhesively bonded joints. Theoretical and Applied Fracture Mechanics, 110, 102826.

[6] Abdel-Monsef, S., Renart, J., Carreras, L., Turon, A., & Maimí, P. (2021). Effect of environment conditioning on mode II fracture behaviour of adhesively bonded joints. Theoretical and Applied Fracture Mechanics, 112, 102912.

[7] Tan, W., Na, J. X., & Zhou, Z. F. (2023). Effect of temperature and humidity on the creep and aging behavior of adhesive joints under static loads. The Journal of Adhesion, 99(4), 672-690.

[8] Nunes, P. D. P., Marques, E. A. S., Carbas, R. J. C., Akhavan-Safar, A., & Da Silva, L. F. M. (2021). DCB tests at constant strain rate using crash-resistant epoxy adhesives: A numerical and experimental approach. Proceedings of the Institution of Mechanical Engineers, Part D: Journal of Automobile Engineering, 235(13), 3234-3242.

[9] Machado, J. J. M., Hayashi, A., Nunes, P. D. P., Marques, E. A. S., Carbas, R. J. C., Sato, C., & Da Silva, L. F. M. (2019). Strain rate dependence of a crash resistant adhesive as a function of temperature for the automotive industry. Proceedings of the Institution of Mechanical Engineers, Part L: Journal of Materials: Design and Applications, 233(11), 2189-2203.

[10] S. Hartshorn, Structured adhesives: chemistry and technology, New York: Plenum Press, 1986.

[11] Wake, W. C. (1978). Theories of adhesion and uses of adhesives: a review. Polymer, 19(3), 291-308.

[12] Viana, G., Machado, J., Carbas, R., Costa, M., Da Silva, L. F. M., Vaz, M., & Banea, M. D. (2018). Strain rate dependence of adhesive joints for the automotive industry at low and high temperatures. Journal of adhesion science and Technology, 32(19), 2162-2179.

[13] Jia, Z., Yuan, G., Hui, D., Feng, X., & Zou, Y. (2019). Effect of high loading rate and low temperature on mode I fracture toughness of ductile polyurethane adhesive. Journal of Adhesion Science and Technology, 33(1), 79-92.

[14] Jia, Z., Yuan, G., Hui, D., Feng, X., & Zou, Y. (2018). Effect of high strain rate and low temperature on mode II fracture toughness of ductile adhesive. International Journal of Adhesion and Adhesives, 86, 105-112.

[15] Ribas, M. J., Akhavan-Safar, A., Pigray, N., Carbas, R. J., Marques, E. A., Borges, C. S., ... & da Silva, L. F. (2023). From High Strain Rates to Elevated Temperatures: Investigating Mixed-Mode Fracture Behaviour in a Polyurethane Adhesive. Polymers, 15(12), 2675.

[16] e Castro Lopes, F. V. B., Akhavan-Safar, A., Carbas, R. J. C., Marque, E. A. S., Goyal, R., Jennings, J., & da Silva, L. F. M. (2023). The role of loading mode on the property degradation of adhesives at high temperatures. Fatigue & Fracture of Engineering Materials & Structures, 46(5), 1848-1863.

[17] Sekiguchi, Y., Hayashi, A., & Sato, C. (2020). Analytical determination of adhesive layer deformation for adhesively bonded double cantilever beam test considering elastic–plastic deformation. The Journal of Adhesion, 96(7), 647-664.

[18] Bascom, W. D., Ting, R. Y., Moulton, R. J., Riew, C. K., & Siebert, A. R. (1981). The fracture of an epoxy polymer containing elastomeric modifiers. Journal of Materials Science, 16, 2657-2664.

[19] Bitner, J. L., Rushford, J. L., Rose, W. S., Hunston, D. L., & Riew, C. K. (1981). Viscoelastic fracture of structural adhesives. The Journal of Adhesion, 13(1), 3-28.

[20] Hunston, D. L., & Bullman, G. W. (1985). Viscoelastic fracture behaviour for different rubber-modified epoxy adhesive formulations. International journal of adhesion and adhesives, 5(2), 69-74.

[21] Lataillade, J. L., Grapotte, D., & Cayssials, F. (1994). The impact resistance of CTBN-modified epoxy adhesive joints. Le Journal de Physique IV, 4(C8), C8-771.

[22] Biel, A. (2005). Constitutive behaviour and fracture toughness of an adhesive layer (Doctoral dissertation, Chalmers tekniska högskola).

[23] Makhecha, D. P., Kapania, R. K., Johnson, E. R., Dillard, D. A., Jacob, G. C., & Starbuck, J. M. (2009). Rate-dependent cohesive zone modeling of unstable crack growth in an epoxy adhesive. Mechanics of Advanced Materials and Structures, 16(1), 12-19.

[24] Raghavan, D., He, J., Hunston, D., & Hoffman, D. (2002). Strain rate dependence of fracture in a rubber-toughened epoxy system. The Journal of Adhesion, 78(8), 723-739.

[25] Marzi, S., Hesebeck, O., Brede, M., & Kleiner, F. (2009). A rate-dependent cohesive zone model for adhesively bonded joints loaded in mode I. Journal of adhesion science and technology, 23(6), 881-898.

[26] Karac, A., Blackman, B. R. K., Cooper, V., Kinloch, A. J., Sanchez, S. R., Teo, W. S., & Ivankovic, A. (2011). Modelling the fracture behaviour of adhesively-bonded joints as a function of test rate. Engineering Fracture Mechanics, 78(6), 973-989.

[27] Marzi, S. (2012). Measuring the critical energy release rate in mode II of tough, structural adhesive joints using the tapered end-notched flexure (TENF) test. The European Physical Journal Special Topics, 206(1), 35-40.

[28] Leffler, K., Alfredsson, K. S., & Stigh, U. (2007). Shear behaviour of adhesive layers. International Journal of Solids and Structures, 44(2), 530-545.

[29] Jia, Z., Yuan, G., Feng, X., & Zou, Y. (2019). Numerical study on the mechanical behavior of a polyurethane adhesive under high strain rate. Composites Part B: Engineering, 158, 131-140.

[30] Nunes, P. D., Borges, C. S., Marques, E. A., Carbas, R. J., Akhavan-Safar, A., Antunes, D. P., ... & da Silva, L. F. (2020). Numerical assessment of strain rate in an adhesive layer throughout double cantilever beam and end notch flexure tests. Proceedings of the Institution of Mechanical Engineers, Part E: Journal of Process Mechanical Engineering, 234(5), 415-425.

[31] Perez, M., Akhavan-Safar, A., Carbas, R. J., Marques, E. A., Wenig, S., & da Silva, L. F. (2022). Loading rate and temperature interaction effects on the mode I fracture response of a ductile polyurethane adhesive used in the automotive industry. Materials, 15(24), 8948.

[32] Wang, F., Bu, H., Ma, W., Zhang, P., & Zhan, X. (2023). Influence of the different surface treatments on fracture property of CFRP adhesive joint. Journal of Adhesion Science and Technology, 37(6), 961-975.

[33] Houjou, K., Sekiguchi, Y., Shimamoto, K., Akiyama, H., & Sato, C. (2023). Energy release rate and crack propagation rate behaviour of moisture-deteriorated epoxy adhesives through the double cantilever beam method. The Journal of Adhesion, 99(6), 1016-1030.

[34] Wang, W., & Xian, G. (2023). Effects of steel surface treatment with silanized carbon nanotubes on the bonding properties between steel and epoxy adhesive. The Journal of Adhesion, 99(2), 297-319.

[35] De Moura, M. F. S. F., Campilho, R. D. S. G., & Gonçalves, J. P. M. (2008). Crack equivalent concept applied to the fracture characterization of bonded joints under pure mode I loading. Composites science and technology, 68(10-11), 2224-2230.

[36] Da Silva, L. F. M. (2008). Modeling of adhesively bonded joints (pp. 3-22). A. Öchsner (Ed.). Berlin: Springer.

[37] Viana, G., Costa, M., Banea, M. D., & Da Silva, L. F. M. (2017). Behaviour of environmentally degraded epoxy adhesives as a function of temperature. The Journal of Adhesion, 93(1-2), 95-112.

[38] Papini, M., Fernlund, G., & Spelt, J. K. (1994). The effect of geometry on the fracture of adhesive joints. International Journal of Adhesion and Adhesives, 14(1), 5-13.

[39] Kin Loch, A. J., & Shaw, S. J. (1981). The fracture resistance of a toughened epoxy adhesive. The Journal of Adhesion, 12(1), 59-77.

[40] Banea, M. D., da Silva, L. F. M., & Campilho, R. D. (2015). The effect of adhesive thickness on the mechanical behavior of a structural polyurethane adhesive. The Journal of Adhesion, 91(5), 331-346.

[41] Hayashi, A., Sekiguchi, Y., & Sato, C. (2022). Effect of temperature and loading rate on the mode I fracture energy of structural acrylic adhesives. Journal of Advanced Joining Processes, 5, 100079.

[42] Chattopadhyay, D. K., & Webster, D. C. (2009). Thermal stability and flame retardancy of polyurethanes. Progress in Polymer Science, 34(10), 1068-1133.

[43] Melcher, R. J., & Johnson, W. S. (2007). Mode I fracture toughness of an adhesively bonded composite–composite joint in a cryogenic environment. Composites Science and Technology, 67(3-4), 501-506.

[44] Nam, S., Yu, Y. H., Choi, I., & Bang, C. S. (2014). Fracture toughness improvement of polyurethane adhesive joints with chopped glass fibers at cryogenic temperatures. Composite Structures, 107, 522-527.

[45] Bauwens, J. C. (1972). Relation between the compression yield stress and the mechanical loss peak of bisphenol-A-polycarbonate in the β transition range. Journal of Materials Science, 7, 577-584.

[46] Ree, T., & Eyring, H. (1955). Theory of non-newtonian flow. i. solid plastic system. Journal of Applied Physics, 26(7), 793-800.

[47] Akhavan-Safar, A., Ayatollahi, M. R., Moazzami, M., & Da Silva, L. F. M. (2018). The role of T-stress and stress triaxiality combined with the geometry on tensile fracture energy of brittle adhesives. International Journal of Adhesion and Adhesives, 87, 12-21.

[48] Tan, W., Na, J. X., & Zhou, Z. F. (2023). Effect of temperature and humidity on the creep and aging behavior of adhesive joints under static loads. The Journal of Adhesion, 99(4), 672-690.

[49] Omairey, S., Jayasree, N., & Kazilas, M. (2021). Defects and uncertainties of adhesively bonded composite joints. SN Applied Sciences, 3(9), 769.

[50] Bezemer, A. A., Guyt, C. B., & Vlot, A. (1998). New impact specimen for adhesives: optimization of high-speed-loaded adhesive joints. International journal of adhesion and adhesives, 18(4), 255-260.